Hindawi Publishing Corporation
Journal of Nanomaterials
Volume 2014, Article ID 617405, 42 pages
http://dx.doi.org/10.1155/2014/617405

Review Article

Removal of Hazardous Pollutants from Wastewaters: Applications of TiO_2-SiO_2 Mixed Oxide Materials

Shivatharsiny Rasalingam, Rui Peng, and Ranjit T. Koodali

Department of Chemistry, University of South Dakota, Vermillion, SD 57069, USA

Correspondence should be addressed to Ranjit T. Koodali; ranjit.koodali@usd.edu

Received 6 February 2014; Accepted 26 March 2014; Published 16 June 2014

Academic Editor: Fan Dong

The direct release of untreated wastewaters from various industries and households results in the release of toxic pollutants to the aquatic environment. Advanced oxidation processes (AOP) have gained wide attention owing to the prospect of complete mineralization of nonbiodegradable organic substances to environmentally innocuous products by chemical oxidation. In particular, heterogeneous photocatalysis has been demonstrated to have tremendous promise in water purification and treatment of several pollutant materials that include naturally occurring toxins, pesticides, and other deleterious contaminants. In this work, we have reviewed the different removal techniques that have been employed for water purification. In particular, the application of TiO_2-SiO_2 binary mixed oxide materials for wastewater treatment is explained herein, and it is evident from the literature survey that these mixed oxide materials have enhanced abilities to remove a wide variety of pollutants.

1. Introduction

The energy demand is expected to be greater than 25 TW by the year 2050. This increase is expected to pose undue burden on natural resources and create challenges for sustaining our environment and quality of human life. In addition to energy, the demand for clean water is also expected to rise rapidly due to increasing global population. In addition, with the expeditious pace of industrialization, the disposal of industrial effluents poses threats to the environment and is becoming the biggest concern for the sustainable development of human society. Wastewater reclamation and recycling are essential goals to protect the global ecosystem and improve the quality of the environment. Several methods have been utilized for the removal of pollutants from contaminated water sources [1–9]. Among them, advanced oxidation processes (AOP) have emerged to be promising, efficient, economic, and reliable for the removal of pollutants from aquatic environments [4, 9, 10]. Among the various AOP methods, heterogeneous photocatalysis, using titanium dioxide (TiO_2) based photocatalysts, has emerged as a viable process for degrading a wide variety of pollutants [11–13].

Although TiO_2 has several important properties, such as ease of synthesis, excellent photostability, nontoxicity, and valence bands that are located at high positive potentials, there are several drawbacks that impair the performance of TiO_2 in photocatalytic processes. The absorbance of TiO_2 is limited to the UV region, and, thus, only a small fraction of the solar spectrum is utilized. The fast recombination of the photoinduced electron-hole pairs impedes the efficiency of the overall photocatalysis reaction. In addition, the relatively low surface area of TiO_2 limits the number of adsorptive sites of the target pollutant molecule. To overcome these aforementioned challenges, researchers have developed TiO_2 based mixed oxide materials that can provide large number of adsorptive sites by dispersion of TiO_2 species into a porous support with large surface area. Silica has been widely employed as a robust and stable mesoporous support for immobilizing photoactive TiO_2 species. The TiO_2-SiO_2 mixed oxide photocatalysts have shown significantly enhanced activities compared to pure TiO_2 for a number of photocatalytic reactions for environmental remediation. The improved photocatalytic performance over TiO_2-SiO_2 mixed oxide materials can be accredited to the presence of

highly dispersed TiO_2 species in the SiO_2 support, the better adsorption of the pollutant, and the presence of Ti-O-Si bonds that favor the activation of the organic pollutant [14].

In this review, we will first discuss the different types of aqueous pollutants followed by a discussion of selected removal techniques and their basic principles. Then, a brief overview of the synthesis methods of titania-silica (TiO_2-SiO_2) mixed oxides is presented. This is followed by an extensive description of available characterization techniques of periodic and aperiodic titania-silica catalysts. Following this, the heterogeneous photocatalytic degradation of several pollutants, in particular, organic materials in aqueous phase, is discussed. Finally, the factors that influence the degradation reactions are critically reviewed.

1.1. Aquatic Pollution. Clean water is the most important and indispensable resource that maintains the demands for the daily activities of every aspect of human society, such as drinking, cleansing, industrial manufacture, and farm irrigation. However, the squandering of clean water at discretion and careless handling of wastewater to aquatic systems from households and industries severely contaminate the quality of natural aquatic environments. In general, the sources that result in water pollution can be classified as point and nonpoint sources [15]. The former one contains pollutants that are discharged from industries, septic materials, animal feedlots, mines and oil industries, and so forth into water sources [16]. The latter one includes runoffs from agriculture, sediment, animal wastes, and so forth [17]. Nonpoint sources, due to their irregularity, are more difficult to be tracked compared to point sources [18]. However, according to the Environmental Protection Agency (EPA), nonpoint sources are claimed to be the major cause of aqueous pollutants. The existence of these pollutants in water systems can cause serious environmental issues and pose threat to public hygiene and health. For instance, the contamination of groundwater by pesticides can endanger aquatic ecosystems. As the fertilizer is discharged into water sources, it can boost the multiplication of algae, which interrupts the oxygen level and upsets the ecological balance in the water system. Moreover, close contact or drinking of the contaminated water can cause skin rashes and other severe diseases like typhoid fever and stomach illness in humans. Waste inorganic and/or organic chemicals, in particular heavy metal ions, in the water may be ingested by fish and may also cause infection in humans, who catch and consume it. In the following section, the most commonly occurring hazardous pollutants along with their effects will be discussed.

1.2. Hazardous Pollutants. The most commonly observed hazardous wastes that threaten the global aquatic system can be divided into four groups according to the classification by the EPA: (i) hazardous wastes from nonspecific industrial processes, (ii) hazardous wastes from specific industrial sources, (iii) commercial chemical products, and (iv) toxic wastes. The EPA estimates that the above-mentioned pollutants have been increasingly detected during the past few decades in rivers, lakes, and oceans. In the following part, we will discuss the some important inorganic and organic wastes in water.

1.2.1. Inorganic Wastes

Anionic Wastes. Phosphates (PO_4^{3-}) and nitrates (NO_3^-) are the most prevalent pollutants in contaminated surface water [19, 20]. Phosphorus (P) and nitrogen (N) are indispensable elements used in fertilizers for agriculture. Application of extensive amounts of P and N containing fertilizers on arable lands causes extensive accumulation of the phosphate (PO_4^{3-}) and nitrate (NO_3^-) in the soil. Due to the use of manual irrigation and/or natural rainfall, phosphates and nitrates can leach into ground and surface water sources, such as rivers and lakes. In addition to the P and N containing fertilizers, the manure from livestock is also a major source of phosphate and nitrate contaminants in water systems.

The contamination of water by nitrates poses a threat to the health of humans and other animals. Nitrate is found to be extremely toxic at high concentrations in water. It has been postulated to be the origin of methemoglobinemia in infants and it can cause toxic effects on livestock. Although phosphorus is not as toxic as nitrate in water, it can stimulate the growth of algae in water along with nitrate pollutants. Their excessive discharge to the surface water sources can lead to severe eutrophication in surface water sources. Eutrophication is the most widespread water contamination in global aquatic systems and it brings about numerous negative aftermaths to the environment and ecosystem. The most commonly observed consequence of eutrophication is that it causes the multiplication of algae and aquatic weeds, which give bad odor and taste of water in the aquatic systems, and prevents the use of such polluted systems as sources for clean water for industry, agriculture, and humans. In addition, eutrophication can induce the growth of phytoplankton and zooplankton in various aquatic environments. Besides, eutrophication is considered to be the cause for the disappearance of coral reefs and the extinction of several fish species.

Cyanides are another important class of anionic pollutants. Cyanides, which can be generated from either anthropogenic or natural sources, commonly exist in the form of cyanide salts, such as sodium cyanide and potassium cyanide, or in gaseous phase as hydrogen cyanide. Cyanides can be discharged into aquatic system from carelessly treated industry sewage, coal gasification, electroplating operations, and incomplete combustion of fuels. Cyanides cause severe threat to human life as the cyanide anion (CN^-) is recognized to be highly toxic. The ingestion and/or inhalation of cyanide anion (CN^-) by humans can lead to low vitamin B_{12} levels in the human body and can be lethal.

Cationic Wastes. The most commonly seen inorganic cationic wastes in aquatic systems are heavy metal ions, such as lead (Pb^{2+}) [21], arsenic ($As^{3+/5+}$) [22], mercury (Hg^{2+}) [23], chromium (Cr^{6+}) [24], nickel (Ni^{2+}) [25], barium (Ba^{2+}), cadmium (Cd^{2+}) [26], cobalt (Co^{3+}) [27], selenium (Se^{2+}) [28], and vanadium (V^{5+}) [25]. These above-mentioned heavy metal ions can be introduced into aquatic system via diverse

means [29]. For example, large amounts of heavy metal ions are produced from natural processes, such as weathering, volcano activities, and crustal movement. As in the modern society, the major sources of heavy metal pollutants are from human/industry activities, for instance, printed board and semiconductor manufacturing, metal finishing and plating, industrial dyeing processes, and so forth. Many heavy metal ions, for example, Fe^{3+}, Zn^{2+}, Cu^{2+}, Mn^{2+}, Co^{3+}, Ni^{2+}, and so forth, are actually essential trace elements (required in less than 100 mg per day) to maintain the daily metabolism of the human body. However, these heavy metal ions exhibit fatal toxicity and can poison humans and animals under excessive exposure and close contact. The indication of heavy metal poisoning in humans can be divided into acute and chronic symptoms. Acute symptoms include fatigue, hallucinations, headache, nausea, numbness, and abdominal pain. Chronic symptoms contain anxiety, dyslexia, lack of concentration, migraines, and so forth. Therefore, the removal of heavy metal ion pollutants from aquatic system is indispensable.

1.2.2. Organic Wastes. Organic pollutants are toxic molecular compounds and can cause significant diseases in humans, when exposed to high concentration levels. These organic compounds originate from a variety of industrial products such as detergents, petroleum hydrocarbons, plastics, organic solvents, pesticides, and dyes, and they can be found in diverse environments. In addition, these organic pollutants are a threat to wildlife and human, due to long-term deleterious effect and chemical complexity. In particular, thousands of persistent organic pollutants (POPs) are a family of chemicals consisting of a diverse group of organic substances, which are toxic, bioaccumulative, and prone to long range of transport [30–33]. It was reported elsewhere that POPs mainly differ in the level of chlorine substitutions and persist in the environment with long lives particularly in soils, sediments, and air [34]. They are released into the environment via municipal and industrial wastes, landfill effluents, agricultural practices, and so forth and undergo various reactions that validate their prevalence. There are a wide number of pollutants listed under the toxic and hazardous categories and some of the main types are detailed here.

Aliphatic organic compounds are mainly runoffs from the surface and are particularly seen in urban areas. In addition, the petroleum oils and the byproducts from the combustion of oil also are mostly aliphatic compounds. A variety of aliphatic organic compounds, that include alkenes, alkynes, dichlorodifluoromethane, 1,2-dichloroethane, 2-propanol, and tetramethylammonium ions, have been reported as toxic pollutants from aquatic environment mainly from surface runoffs. Polycyclic aromatic hydrocarbons (PAH) are another type of organic substances released to the environment from the incomplete combustion of organic substances including wood, carbon, and oil. They are neutral, nonpolar organic molecules consisting of two or more fused benzene rings and reported as a priority pollutant by the EPA [35]. The extensive use of polychlorinated biphenyls (PCBs) in numerous industrial processes, electrical transformers, capacitors, carbonless copy paper, and plastics increases their penetration into the environment.

Surfactants are among the most versatile group of organic compounds utilized in industrial, household, personal care, and health products [36]. Owing to their existence in anionic, cationic, nonionic, and amphoteric forms, they have the ability to alter the physicochemical state of the natural habitat. At high concentrations, they can form complexes in water and cause harmful effects to microorganisms. Pesticides are another type of organics found in diverse chemical structures and are used for various agricultural and nonagricultural applications such as herbicides, insecticides, fungicides, and germicides. Dyes are colored substances that have strong affinity for the substrate to which it is being applied. Dyes are applied to numerous substrates such as textiles, leather, plastic, and paper. Dyes can be classified under different categories according to their application method, chemical structure, usage, or the type of chromophore present in them [37].

Phenol and phenolic compounds byproducts formed from many industrial processes, such as the manufacturing of herbicides, plastics, polymer precursors, photographic developers, dyes, drugs, and pulp and paper industry [38]. In addition, incomplete mineralization of the phenolic compounds ends up with natural organic byproducts that include humic substances, lignins, and tannins, which are prevalent in our environment. The toxicity of phenols and phenol derivatives is mainly attributed to the ease of donation of free electrons, forming phenoxy radicals and intermediates. These phenoxy radicals can penetrate the cell and damage membranes of endoplasmic reticulum, mitochondria, and nucleus and also their components like enzymes and nucleic acids. Furthermore, exposure to phenol may damage the skin through its reaction with amino acids in the epidermis [39].

2. Removal Techniques

Continuous increase of pollutants in water bodies has necessitated the need to develop cost-effective methods for their removal. Destroying the pollutants to benign chemicals and/or removing these pollutants from contaminated water is imperative for a green environment. There are numerous treatment processes that have been applied for pollutant removal from wastewater, such as electrochemical oxidation [40], biodegradation [41, 42] membrane process [43], coagulation [44, 45], adsorption [46–49], precipitation [50], sonochemical degradation [51, 52], micellar enhanced ultrafiltration, and AOP [4, 9, 10]. Though these methods are considered as efficient methods for pollutant removal, each method has its own benefits and drawbacks. In this section, we will explain some of the most common methods that are frequently used for pollutant removal and their basic principles.

2.1. Electrochemical Oxidation. Electrochemical oxidation is an efficient and economic method, suitable when the wastewater contains nonbiodegradable organic pollutants. This method poses several advantages since it does not require

auxiliary chemicals, high pressures, or high temperatures. In addition, owing to its versatility and cost-effectiveness, electrochemical techniques have gained great attention for the removal of pollutants. The process of electrochemical oxidation mechanism is mainly based on the generation of the hydroxyl radicals at the electrode surface.

Two different types of mechanisms have been elaborated for electrochemical oxidation, such as direct and indirect oxidation methods [53]. In direct electrochemical oxidation, the degradation of organic compound occurs directly over the anode material, where the hydroxyl radical ($^{\bullet}OH$) or the reactive oxygen species react with the organic compound. The pollutants are first adsorbed at the surface of the anode and are then degraded by an anodic electron transfer reaction as given by

$$M + H_2O \longrightarrow M\left(^{\bullet}OH\right) + H^+ + e^- \quad (1)$$

In the indirect electrochemical oxidation, the organics are treated in the bulk solution by oxidants, such as $^{\bullet}OH$, Cl_2, hypochlorite (ClO^-), peroxodisulfate ($S_2O_8{}^{2-}$), and ozone (O_3), which are electrochemically generated at the electrode surface. Even though high removal efficiencies are achieved by both the direct and indirect electrochemical oxidation processes, their effectiveness strongly depends on the treatment conditions including pH, current density, types and concentration of pollutants, supporting electrolyte, flow rate, electrode preparation method, and nature of the electrode materials. Several electrode materials that include Pt, PbO_2, Ti-SnO_2, Ti/Pt, Ti/Pt–Ir, Ti/PbO_2, Ti/PdO–Co_3O_4, Ti/RhO_x–TiO_2, Ti coated oxides of Ru/Ir/Ta, IrO_2, Ti/RuO_2, SnO_2, PbO_2, and so forth, and boron doped diamond (BDD) [6, 54–73] have been listed as efficient electrodes for the degradation of organics by electrochemical oxidation. Apart from these anode materials, graphite anodes are also considered as efficient materials for anodic oxidation of several organic pollutants [6, 62]. Particularly, the high oxygen overpotential, high electrocatalytic activity, chemical stability, long lifetime, and cost-effectiveness have been credited for the high efficiency of these graphite electrodes. In a recent publication, Govindaraj et al. investigated the electrochemical oxidation of bisphenol A (BPA) from aqueous solution using graphite electrodes [6]. The effect of the supporting electrolyte (type and concentration), initial pH, and applied current density on the performance was discussed in their work. The oxidation of polyhydroxybenzenes was conducted using a single-compartment electrochemical flow cell as illustrated in Figure 1 [56]. Diamond-based material was used as the anode and stainless steel was used as the cathode.

The effectiveness of this electrode was evaluated by monitoring the concentration of BPA. Chemical oxygen demand (COD) removal of 78.3% was obtained, when 0.05 M NaCl was used as the electrolyte at an initial pH of 5 and a current density of 12 mA/cm^2. In a different study, the effect of different types of supporting electrolytes in the degradation of phenol using BDD electrode was studied by Alencar de Souza and coworkers [70]. The electrochemical performance was examined by measuring COD and the concentrations of all phenolic compounds formed during the electrolysis process. The oxidation kinetic constants using different electrolytes were found to be in the following order: $k_{Na_2SO_4} \approx k_{Na_2CO_3} > k_{H_2SO_4} > k_{H_3PO_4}$. However, the addition of chloride ion to the electrolyte solution caused a major change in the reaction kinetics, and the rate constants were found to be in the following order: $k_{H_2SO_4} > k_{Na_2SO_4} > k_{Na_2CO_3}$. The difference in the reaction kinetics was explained by the oxidation mediated by the chloride ions, which was formed at low pH values. Though the concentration of chloride ions helped to rapidly increase the reaction rate, increment in the supporting electrolyte concentration also assisted to improve the reaction kinetics. Apart from the above-mentioned studies, there are several reports describing the utilization of BDD for oxidation of several organics such as salicylic acid [68], nitrophenol [73], nitrobenzene [72], and tetracycline [66]. A brief review regarding the application of BDD for incineration of synthetic dyes towards environmental application [67] and another review article by Martínez-Huitle and Ferro providing clarity for the electrochemical oxidation of organic pollutants are available [53].

2.2. Biological Process. In the 1990s, biological processes were used for the removal of heavy metal due to the reactive ability of microorganisms with a variety of pollutants that include organic and inorganic species. It was recognized that the microorganisms influence the mobility of the metal by modifying the chemical and physical characteristics of the metals [93]. Recently, Lu et al. investigated a novel biological filter with bacterial strain of *P. putida* immobilized in Ca-alginate granules for removal of formaldehyde in the gas phase [94]. The effects of inlet concentration, empty bed residence time, and nutrient feeding rate on the performance of the system were examined in their study. It was found that the removal efficiency of the dripping biofilter system increased from 68.6% to 93.5%, when the inlet formaldehyde concentration was in the range of 0.2 to 1.34 mg/m^3. Among the various technologies, such as adsorption [95], chemisorption, photocatalytic oxidation [96], and botanical filtration [97], that have been tried for the removal of formaldehyde, the complete removal is still a challenging problem due to low kinetics, byproduct formation, and low efficiency using any of the above-mentioned methods. However, biological degradation technology with high removal efficiency has been successfully applied in industries for effluents and waste gas treatments. Even though biological processes have been used for several applications that include heavy metal ion removal and indoor air purification, its application has not been intensely investigated for numerous reasons. Thus, researchers have combined biological process with other techniques such as chemical processes [98, 99], photocatalysis [100], and AOP [74, 101, 102].

Combined biological and chemical degradation methods were carried out to evaluate the effectiveness of mature municipal landfill leachate in laboratory scale by Di Iaconi and coworkers. The biological treatment was followed by chemical oxidation for further removal of COD [98]. Higher removal efficiency was obtained due to the use of chemical treatment. In another study, a combined AOP and biological process was carried out to remove pesticides in aqueous

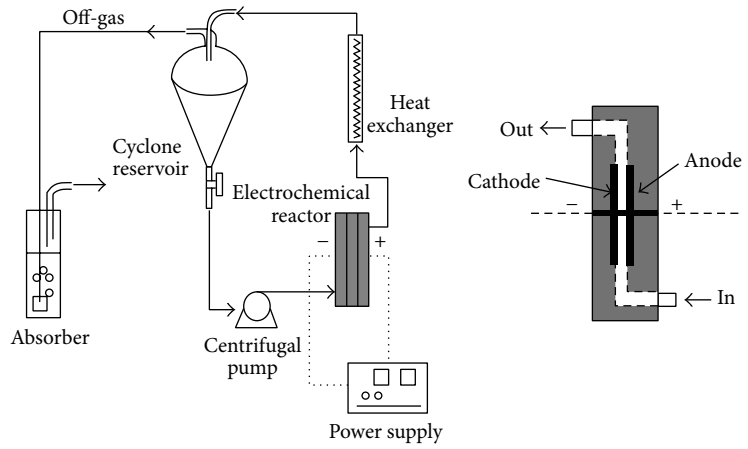

Figure 1: The pilot plant arrangement and illustration of electrochemical cell (reprinted with permission from [56]).

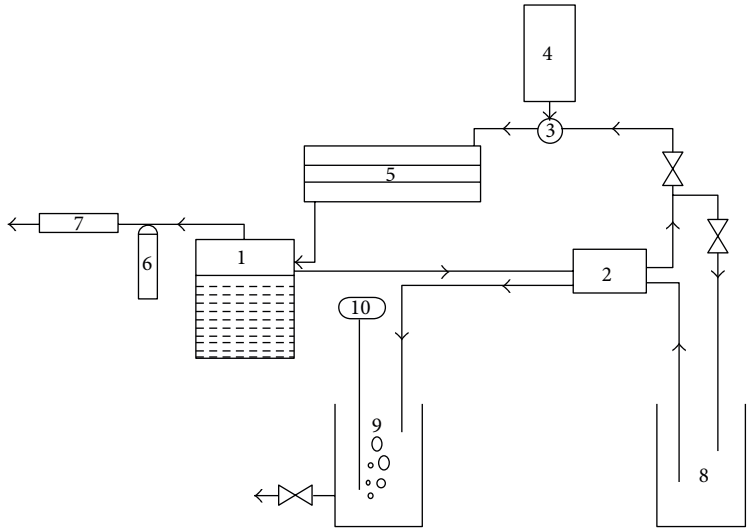

Figure 2: Experimental setup for combined chemical and biological degradation: (1) chemical oxidation tank, (2) peristaltic pump, (3) diffuser valve, (4) ozone generator, (5) UV emitting device, (6) excess KI trap, (7) ozone destruction device, (8) neutralizer, (9) biological treatment tank, and (10) air sparger (reprinted with permission from [74]).

solution [74]. The experimental setup for their study is illustrated in Figure 2. The chemical oxidation process was carried out in the tank labeled as 1. The UV emitting device (labeled as 5) consists of a stainless steel tube with a coaxial mercury vapor lamp. Ozone was produced from air by an ozone generator and was continuously fed into the oxidation tank. Finally, the pH of the system was adjusted to 7, and then the pollutant was fed to the biological treatment tank labeled as 9.

It was found that O_3 and O_3/UV oxidation treatment was able to achieve 90 and 100% removal of the pesticide deltamethrin, in a period of 210 min. Utilization of ozone with UV irradiation was found to enhance the degradation of pesticides. It has been well documented elsewhere that the rate of pesticide removal mainly depends on both the chemical nature of the pesticides being treated [103] and the treatment conditions [104]. In a different study, a sequential UV and biological degradation of a mixture of 4-chlorophenol, 2,4-dichlorophenol, 2,4,6-trichlorophenol, and pentachlorophenol were tested with an initial concentration of 50 mg/L [105]. Under their reaction conditions, pentachlorophenol degraded faster compared with other phenolic compounds and 4-chlorophenol degraded the slowest. A combined biological and chemical procedure was also used as an ecologically and economically favorable remediation technique for 2,4,6-trinitrotoluene (TNT) reduction in contaminated ground and surface water [106, 107]. It was observed that the anaerobic transformation process resulted in a faster reduction of TNT due to significant change in the redox potential of the solutions under both aerobic and anaerobic conditions. Biodegradation of organic pollutants by halophilic bacteria was carried out by Le Borgne and coworkers [108].

In a very recent study, wastewater from a pharmaceutical formulation facility in Israel was treated with a biological activated-sludge system followed by ozonation [101].

This work was aimed at reducing the concentrations of carbamazepine (CBZ) and venlafaxine (VLX), before their discharge into the municipal wastewater treatment plant, and they achieved efficient removal of the drugs by this collective method. The byproducts identified from the incomplete oxidation of ozonation were likely to be more biodegradable than the parent compounds; thus, a postozonation biological treatment was endorsed for the efficient removal of these toxic pharmaceuticals from the wastewater. A recent review has discussed the chemical and biological treatment technologies for leather tannery chemicals and wastewaters [109]. It was concluded from the review that there has not been a full scale application of emerging technologies using AOP to remove xenobiotics present in tannery wastewater, and, thus, there is an opportunity for researchers to explore this aspect. In addition, adsorption process has been widely used as an efficient technique for the removal of a variety of toxic pollutants and this is discussed in Section 2.3.

2.3. Adsorption. Adsorption is an effective and well-known process and has been widely explored as an alternate technique compared with the other waste removal methods due to the lower cost, flexibility and simplicity of design, and ease of operation. Moreover, adsorption does not result in production of any harmful substances. Discharge of several types of pollutants that include household wastes, phenolic wastes [46], dyes [110–112], pesticides [113], herbicides, and metal ions [114, 115] into the water body causes health issues not only for humans but also for aquatic life.

Dyes have been identified as a major contaminant in wastewater. Many industries, such as textile, leather, paper, plastics, food, and cosmetics, use several dyes as coloring materials [49]. Most of these dyes are very toxic, and when released into the environment, they can be transported over long distances in water sources resulting in their widespread dispersal. More than a million tonnes of dyes and coloring materials are produced annually, and the drinking water quality is greatly affected by the unsafe release of these dyes into the water body [44, 45]. In addition, the presence of even very small amounts (<1 ppm) of dyes, in particular the synthetic dyes, in water is undesirable. Therefore, the presence of dyes in wastewater is a major concern for toxicological and esthetical reasons.

Adsorption is a method that is capable of removing nondegradable waste pollutants. There are several adsorbents that include clay minerals [46, 116], activated carbon [82, 117], coal [111], wood, fly ash [118, 119], and biomaterials [108, 120–122] that have been listed for the removal of industrial wastes. However, due to the lack of effective adsorbate-adsorbent interactions, some of the above-mentioned materials are found to be noneffective for the adsorption of pollutants. Consequently, oxide materials, which are considered as an important class of adsorbents, have been explored for adsorption. In this regard, silica gels [123], zeolites [116, 124], Al_2O_3 [110], SiO_2 [81, 125, 126], and TiO_2 [14, 127] have been studied as adsorbents for removal of color effluents. The materials used and the factors influencing the adsorption will be extensively discussed in this section.

First, a brief discussion about the principle and equations related to some of the adsorption isotherms is made. Generally, the equilibrium adsorption capacity q_e (mol/g) is estimated by using

$$q_e = \frac{(C_o - C_e)\,V}{m}, \tag{2}$$

where C_o is the initial concentration of the pollutant (analyte); C_e is the equilibrium concentration of the pollutant (analyte); V is the volume of the analyte solution; m is the adsorbent mass.

A wide variety of equilibrium isotherm models that include Langmuir, Freundlich, Dubinin-Radushkevich, Temkin, Flory-Huggins, and Hill isotherms that have been classified under two parameter isotherms, and Redlich-Peterson, Sips, Toth, Koble-Corrigan, Khan, and Radke-Prausnitz isotherms grouped under three parameter categories [114, 128–130] are available. Among these, Langmuir, Freundlich, and Redlich-Peterson isotherms are the most commonly used models in adsorption studies and are detailed here.

The Langmuir isotherm has been applied to a variety of pollutant sorption processes, which involve homogeneous surfaces and negligible interaction between the adsorbed molecules. In addition, monolayer adsorption on the adsorptive site is the main assumption, in the Langmuir adsorption process, and the saturated monolayer adsorption capacity can be obtained using the following formula [128]:

$$q_e = \frac{q_m K_L C_e}{1 + K_L C_e}, \tag{3}$$

where q_e is the amount adsorbed per unit mass of adsorbent; q_m is the saturated monolayer sorption capacity; K_L is the sorption equilibrium constant (Langmuir constant); C_e is the equilibrium concentration of the solution. The above Langmuir isotherm equation can be arranged in four different linear forms which are named as Langmuir-1, Langmuir-2, Langmuir-3, and Langmuir-4. Among these, Langmuir-1 and Langmuir-2 are widely used to find the adsorption capacity [130]. The relevant equations are as follows:

$$\begin{aligned}
&\frac{C_e}{q_e} = \left(\frac{1}{q_m}\right) C_e + \frac{1}{K_L q_m} \quad \text{Langmuir-1,}\\
&\frac{1}{q_e} = \left(\frac{1}{K_L q_m}\right) \frac{1}{C_e} + \frac{1}{q_m} \quad \text{Langmuir-2,}\\
&q_e = q_m - \left(\frac{1}{K_L}\right) \frac{q_e}{C_e} \quad \text{Langmuir-3,}\\
&\frac{q_e}{C_e} = K_L q_m - K_L q_e \quad \text{Langmuir-4.}
\end{aligned} \tag{4}$$

Freundlich expressed an empirical equation, known as the Freundlich adsorption isotherm, in 1906. The relationship between the concentration of the solute in equilibrium, C_e, and the amount adsorbed, q_e, is a constant, K_F, and is expressed as follows:

$$q_e = K_F C_e^{\,1/n}. \tag{5}$$

The constants $1/n$ and K_F are calculated using the linearized form by taking the logarithm of the Freundlich isotherm as shown in the following equation:

$$\log q_e = \log K_F + \frac{1}{n} \log C_e. \quad (6)$$

The Freundlich isotherm can be applied for nonideal adsorption as well as multilayer adsorption processes.

The Redlich-Peterson equation is another popular model and has three different parameters commonly named as A, B, and g. The combination of the Langmuir and Freundlich models is given by the Redlich-Peterson isotherm, and the mechanism does not obey the monolayer adsorption. Several authors suggest that this model is appropriate for the sorption of metal ions over wide range of concentrations. At high concentration, the Redlich-Peterson approaches the Freundlich isotherm, and, at lower concentration, it follows the Langmuir model. The Redlich-Peterson model is given by the following equation:

$$q_e = \frac{AC_e}{1 + BC_e^g}. \quad (7)$$

By using the subsequent linearized form of the above equation, the constants A, B, and g can be obtained:

$$\frac{C_e}{q_e} = C_e^g \frac{B}{A} + \frac{1}{A}. \quad (8)$$

A large number of materials have been employed as adsorbents for removal of pollutants and they include natural materials, such as clays, coal, fly ash, zeolites and other siliceous materials, biomaterials, agricultural and industrial solid wastes, activated carbon, oxides, and mixed oxide materials.

Natural materials are well known as adsorbents from the beginning of recorded human development. In particular, clays have been utilized as an adsorbent and as an ion-exchange material for the removal of ions and organics due to their low cost, natural abundance, high adsorption capacity, and ion-exchangeable property [49, 131–134]. In the past decades, clay minerals such as bentonite, diatomite, and kaolin have garnered increasing interest due to their ability to adsorb both inorganic and organic materials. In particular, the adsorption of methylene blue (MB) dye molecule has been extensively studied over different clay minerals [131, 133, 135–138]. Apart from these clay minerals, zeolites and siliceous materials, such as silica, glass fibers, and perlite, deserve specific attention for wastewater treatment, as a result of their high availability and stability.

Fly ash is another type of natural material, which is relatively abundant and inexpensive and is currently being explored as an adsorbent for the removal of various organic pollutants that are present in wastewater, such as phenolic compounds, pesticides, and dyes. It has been documented elsewhere that these contaminants can be effectively removed by using fly ash as an adsorbent [49, 118, 119, 139]. In addition, the efficiency of fly ash is improved by converting the fly ash into zeolites [140] and mesoporous materials, such as MCM-41 and MCM-42 [141].

Biomaterials are another type of natural materials, which are mainly used for adsorption and degradation for water treatment applications. A few publications have discussed the adsorption of hazardous and toxic pollutants using biological materials [142–144]. The use of biomass for water treatment is gaining attention due to their availability in large quantities at low cost, in particular, for the removal of heavy metals [93, 142, 143], dyes [145–148], and phenols [149]. Srinivasan and Viraraghavan have examined various biosorbents including fungi, bacteria, algae, chitosan, and peat for decolorizing dye wastewaters and the mechanism(s) involved. In addition, the effects of various factors that influence dye wastewater decolorization and also the methods for increasing the biosorption capacity of the adsorbents are critically examined in this review [5]. The removal efficiency of pollutants by these biomaterials was enhanced by the attachment of polymers [150].

Activated carbon is another important, efficient, and commercially available material that consists of a wide variety of pores in it. Even though the adsorption process proceeds through a sequence of diffusion steps from the bulk phase into the mesopores followed by diffusion into the micropores, the major adsorption sites on activated carbon were reported to be located in the micropores [151, 152]. The studies on the adsorption of dyes using activated carbon and its derivatives have been widely discussed, and the ability of intake on the activated carbon was found to be increased, when adsorbates with relatively higher molar mass and lower water solubility were used [2, 151, 153, 154]. Annadurai and coworkers utilized activated carbon for the adsorption of rhodamine 6G (R6G) molecule [117]. The effects of particle size, temperature, and solution pH on the adsorption were examined in their study, and a maximum dye adsorption of 44.7 mg/g was obtained under their operating condition (temperature of 60°C, pH of 7, and particle size of 0.5 mm). It was observed that increasing the temperature and decreasing the particle size influenced the amount adsorbed, whereas little impact was noticed from changes in the solution pH towards adsorption. In addition, it has been noted that the intraparticle diffusion of dye molecules within the adsorbents was the rate limiting step in the adsorption process.

In a recent literature, Prola et al. used multiwalled carbon nanotubes (MWCNT) and powder activated carbon (PAC) for the adsorption of direct blue 53 dye from aqueous solution [155]. The isotherm model was best fit with the Sips isotherm model and the maximum adsorption capacities were found to be 409.4 and 135.2 mg/g for MWCNT and PAC, respectively. In addition to the dye molecules, adsorption of metal ions was also achieved by using activated carbon as an adsorbent. Adsorption of copper ions [156, 157] and chromium ions [158], from aqueous solutions by activated carbon, has been documented in recent publications. Furthermore, the influence of surface chemistry of activated carbon on the removal of nitrate ions from water was analyzed by Ota and coworkers [159]. Additionally, the removal of surfactants was also carried out over the activated carbon surface [36, 160]. Apart from the applications of pure activated carbons, modification methods and effects of activated carbon for water treatment have been extensively clarified in some

review articles suggesting the importance of activated carbon for the uptake of pollutants from the water environment [161, 162]. Even though the above-mentioned natural materials and activated carbon have been used as adsorbents, owing to the lack of effective adsorbate-adsorbent interactions, a number of the above-mentioned materials are found to be inactive for the adsorption of organics in the polluted water. Thus, only moderate adsorption capacity can be achieved by using some of these adsorbents.

Oxides constitute an important class of adsorbents, and, in this regard, zeolites [163], silica gels [123, 164], SiO_2 [92, 165], Al_2O_3 [110], and TiO_2 [166–170] have been established as effective adsorbents for the removal of several water pollutants. Microporous aluminosilicate materials (zeolites) are three-dimensional structures with negatively charged lattice. Owing to their high ion-exchange capability, relatively high surface area, and low cost, zeolite materials are good adsorbents and their usefulness has been reviewed by Ghobarkar et al. [171]. Another naturally abundant oxide material, silica, has earned much attention for pollutant removal due to the presence of silanol groups [172, 173]. In addition to high surface area and mechanical stability, the porous nature of silica makes it attractive for decontamination applications. However, due to its low resistivity towards the alkaline media, the application of silica is limited below pH level of 8 [173]. Furthermore, the acidic silanol groups provide strong and irreversible adsorption, in comparison with other surface functional groups. Even though the silica materials have this limitation, their high adsorption capacity for the removal of pollutants compared with other oxide materials, TiO_2, Al_2O_3 [14], and ZrO_2 [174] makes them attractive. Although adsorption is viewed as a promising water treatment method for industrial applications, it does not degrade the pollutant since the adsorption process merely removes pollutants from the aqueous phase and transfers them onto a solid matrix [175]. Thus, AOP have emerged as efficient methods for the mineralization of organic pollutants.

2.4. Advanced Oxidation Processes (AOP). AOP is an oxidation technique, which typically uses ambient conditions (room temperature and atmospheric pressure). Several AOP techniques such as ozonation, H_2O_2 photolysis, Fenton process, photo-Fenton process, and heterogeneous photocatalysis have been explored for the elimination of pollutants, particularly from water sources. These AOP techniques destroy the pollutants by chemical oxidation or reduction. In particular, AOP relies on the production of hydroxyl radicals ($^{\bullet}OH$), which are short-lived, extremely highly reactive species and attack most organic molecules with rate constants of $10^{-6} - 10^{-9}\,M^{-1}\,s^{-1}$. Moreover, the versatility of AOP is enhanced by different possible ways for the production of hydroxyl radicals. It is beyond the scope of this review to provide a review of all the AOP techniques in depth and the methods and materials used. Instead, we will cover the basic principles of selected AOP methods and their applications. Our focus is directed towards the use of TiO_2-SiO_2 materials for pollutant removal, in this review.

2.4.1. Ozonation. Ozone is unstable in water and the chemical properties of ozone rely on the experimental conditions. The molecular ozone can react as a dipole, electrophile, or nucleophile due to the two different resonance structures. In addition, depending on the pH, temperature, and concentration of organic and inorganic compounds in water, the half-life of ozone varies from a few seconds up to a few minutes. Ozone is a powerful oxidant and it can oxidize a large number of organic and inorganic materials. Ozone reacts either directly or indirectly with aqueous compounds. In the direct reaction, the molecular ozone directly reacts with the compounds, whereas the $^{\bullet}OH$ radicals resulting from the decomposition of ozone (expressed in the following equations [12–15]) react with the compounds in the indirect reactions [176]:

$$^{-}OH + O_3 \longrightarrow O_2^{-} + HO_2 \quad (9)$$

$$O_2^{-} + O_3 \longrightarrow O_3^{-} + O_2 \quad (10)$$

$$O_3^{-} + H^{+} \longleftrightarrow HO_3 \quad (11)$$

$$HO_3 \longrightarrow {}^{\bullet}OH + O_2 \quad (12)$$

The direct reactions are very slow and solute selective, whereas the indirect radical reactions are fast and nonselective. Additionally, the direct reactions are dominant in acidic solutions, while the indirect reactions occur mostly at basic pH values. It was reported elsewhere that catalytic ozonation significantly enhanced the rate of oxidation more than noncatalytic ozonation [177], and, thus, catalytic ozonation has received much attention in wastewater treatment for removal of pollutants, such as phenolic compounds [177, 178]. Turhan and Uzman have reported the removal of phenol from water using ozone [179]. Ozonation of phenol gave catechol, hydroquinone, *p*-benzoquinone, *o*-benzoquinone, maleic acid, and oxalic acid as the ring cleavage intermediate products and it was noticed that some of the intermediates such as catechol, hydroquinone, and *p*-benzoquinone can be destroyed completely using ozone to CO_2 and H_2O. However, destruction requires long ozonation time and high dosage of ozone. It was reported by Hoigné and coworkers that the hydroxyl radicals are the active species in the decomposition of organics. Furthermore, they have reported that the amount of $^{\bullet}OH$ radicals determined the ozonation efficiency and the effect of these $^{\bullet}OH$ radicals in the reaction kinetics during ozonation was examined by utilizing $^{\bullet}OH$ radical scavengers. However, studies towards the direct determination of the amount of $^{\bullet}OH$ radical produced during the ozonation process are scarce [180].

Einaga and coworkers carried out catalytic oxidation of benzene with ozone over several support materials, such as Al_2O_3, SiO_2, TiO_2, and ZrO_2, and they found that the surface area of the catalysts is one of the important factors that affect the reaction. In addition, they carried out oxidation of benzene with ozone over several Mn ion-exchanged zeolite catalysts, such as Mn-Y, Mn-b, Mn-MOR, and Mn-ZSM-5 to investigate the effect of catalyst support on the reaction [181]. Mn-Y catalyst exhibited high activity for complete oxidation of benzene and formed CO_x without release of any organic

byproducts under moderate conditions. However, formic acid was formed with supported manganese oxide catalysts, Mn/SiO_2 and Mn/SiO_2-Al_2O_3 [182]. Recently, Einaga et al. have reported the effect of catalyst composition and preparation conditions on catalytic properties of Mn-based oxides for benzene oxidation with ozone. In their studies, they have compared the catalytic properties of several Mn oxides, from the standpoint of activity, product distribution, and efficiency of ozone utilization [183]. Even though chemical oxidation with ozone is considered as one of the effective techniques for treatment of wastewater, in some cases, ozone is used in combination with other treatments, particularly with biological treatment, to improve the degradation rate of pollutants [74, 101, 102, 104, 184, 185].

2.4.2. UV/H_2O_2 Treatment. H_2O_2 treatment in AOP also involves the formation of $^{\bullet}OH$ radicals generated by the photolysis of H_2O_2 in the presence of UV irradiation and is very effective for the degradation of most of the organic pollutants. Owing to the higher molar absorption coefficient of the peroxide anion, the photolysis rate has been found to be pH dependent and increases at high pH values [186–188]. It was documented elsewhere [186] that the generated $^{\bullet}OH$ radicals react with the organic substrate by three different mechanisms as listed below:

$$\text{Hydrogen abstraction } HO^{\bullet} + RX \longrightarrow R^{\bullet} + H_2O \quad (13)$$

$$\text{Electrophilic addition } HO^{\bullet} + RX \longrightarrow HORX \quad (14)$$

$$\text{Electron transfer } HO^{\bullet} + RX \longrightarrow XR^{\bullet} + HO^{-} \quad (15)$$

Owing to the commercial availability, thermal stability, infinite solubility in water, storage, and ease of formation of hydroxyl radical, the use of hydrogen peroxide as an oxidant has received significant attention for water purification. However, the rate of formation of hydroxyl radicals influences the oxidation of organic contaminants and this has been noted as the main disadvantage of the UV/H_2O_2 treatment process. Several studies have utilized the UV/H_2O_2 process for degrading organic compounds in aqueous media. Cater et al. used UV/H_2O_2 treatment to remove methyl *tert*-butyl ether (MTBE), a pollutant commonly found in gasoline contaminated in groundwater [187]. In their study, they have examined the effectiveness of UV/H_2O_2 treatment in the oxidation of MTBE. The degradation of MTBE was found to obey pseudo-first-order kinetics and showed good efficiency with the figure-of-merit electrical energy per order (E_{EO}) in the range of 0.2–7.5 kWh/m^3/order. In another study, removal of naproxen, a nonsteroidal anti-inflammatory drug, was carried out by UV/H_2O_2 process by Felis et al. [189]. A 93% removal of naproxen was achieved after 3 min. of treatment with UV/H_2O_2 at pH = 6. In addition, they have obtained lower rate, when naproxen was subjected to aerobic or anaerobic treatment prior to the UV/H_2O_2 treatment. Wu et al. achieved a 100% removal of dimethyl sulfoxide (DMSO) when used with H_2O_2/UV treatment after 3 hours of degradation at pH = 3 [190]. In this study, the DMSO concentration was kept at 1,000 mg/L, and the H_2O_2 concentration was kept the same as that of DMSO with 5.5 mW/cm^2 UV irradiation intensity at a temperature of 25°C. In contrast, a lower decomposition (83%) was attained at a pH of 10, at the same temperature and the same period of time. According to this study, an acidic medium is more effective for the degradation of DMSO.

There are a large number of organic pollutants, such as phenols and phenolic compounds, benzene and substituted benzene, salicylic acid, proline, pyridine, and dyes [191], that have been degraded or mineralized using UV/H_2O_2 treatment. However, this treatment method is not the focus of this study. In addition to the UV/H_2O_2 treatment for oxidation of pollutants, another process involves the use of O_3/UV. Even though H_2O_2 increases the generation of $^{\bullet}OH$ radicals in the ozone process, the cost of this process is too high due to the combination of two different processes, O_3/UV and O_3/H_2O_2. Shu and Chang utilized this combined process for the decoloration of textile dye C.I. Direct Black 22 [191, 192]. From their findings, it was noticed that the ozonation process took less time to remove the color than the H_2O_2/UV process. The H_2O_2/UV method removed 99% of total organic carbon (TOC) from the effluent. Consequently, a combination of both methods was proposed in order to achieve good efficiency. It has been noted that this combined method is mainly used for the removal of color effluents from wastewater due to its high efficiency for removal of both TOC and color [193].

2.4.3. Fenton Reaction. Fenton reaction is a homogeneous catalytic oxidation process that uses a mixture of hydrogen peroxide (H_2O_2) and ferrous ions. Due to its simplicity and the availability of chemicals, this oxidation is considered as an advanced technique for waste removal. In acidic environment, H_2O_2 and Fe^{2+} ions in the contaminated solution produce hydroxyl radicals expressed as follows:

$$H_2O_2 + Fe^{2+} \longrightarrow Fe^{3+} + OH^{-} + HO^{\bullet} \quad (16)$$

The decomposition of H_2O_2 is initiated by the ferrous ion and results in the formation of hydroxyl radical ($HO^{\bullet}$). These hydroxyl radicals, which are powerful oxidizing agents, then attack substrates and chemically decompose them. However, these hydroxyl radicals can be scavenged by reaction with Fe^{2+} and/or H_2O_2, by the following equations:

$$HO^{\bullet} + Fe^{2+} \longrightarrow OH^{-} + Fe^{3+} \quad (17)$$

$$HO^{\bullet} + H_2O_2 \longrightarrow H_2O + HO_2^{\bullet} \quad (18)$$

In addition, Fe^{3+}, which is formed during the reaction, regenerates Fe^{2+} ions by reacting with H_2O_2 as per the following equations:

$$Fe^{3+} + H_2O_2 \longleftrightarrow Fe - OOH^{2+} + H^{+} \quad (19)$$

$$Fe - OOH^{2+} \longrightarrow HO_2^{\bullet} \quad (20)$$

$$Fe^{2+} + HO_2^{\bullet} \longrightarrow Fe^{3+} + HO_2^{-} \quad (21)$$

$$Fe^{3+} + HO_2^{\bullet} \longrightarrow Fe^{2+} + H^{+} + O_2 \quad (22)$$

An extended Fenton reaction, named photo-Fenton reaction, takes advantage of UV irradiation for the formation of hydroxyl radicals in addition to the above-mentioned equations and is described by (23) and (24). Under these irradiation conditions, Fe^{2+} is regenerated by the photolysis of the Fe^{3+} ions/complex. Consider

$$H_2O_2 + UV \longrightarrow HO^{\bullet} + HO^{\bullet} \quad (23)$$

$$Fe^{3+} + H_2O + UV \longrightarrow HO^{\bullet} + Fe^{2+} + H^{+} \quad (24)$$

There are several reports that have examined the applications of Fenton and photo-Fenton reactions. For example, Gutowska et al. studied the degradation mechanism of Reactive Orange 113 in aqueous solution by using H_2O_2/Fe^{2+} [194]. In another report, a comparative study of Fenton and photo-Fenton oxidative decolorization was carried out against Reactive Black 5 (RB5). The pH, H_2O_2, and Fe^{2+} dosage, dye concentration, and initial concentration ratios between $[Fe^{2+}]:[H_2O_2]:[RB5]$ were varied in their study. The optimal ratios were found to be $[H_2O_2]/[RB5]$ of 4.9 : 1 and $[H_2O_2]/[Fe^{2+}]$ of 9.6 : 1, with pH of 3. Even though both the Fenton and photo-Fenton reactions effectively decolorized the RB5 dye with 97.5 and 98% efficiency, the TOC removal rates were found to be significantly different. A significant removal (46.4%) was obtained with photo-Fenton reaction, whereas only 21.6% TOC removal was observed with the Fenton reaction. This result indicates that UV irradiation plays an important role in the mineralization of the RB5 dye. Elmolla and Chaudhuri degraded antibiotics amoxicillin, ampicillin, and cloxacillin in aqueous solution by the photo-Fenton process and examined the effects of UV irradiation, $H_2O_2/(COD)$ and H_2O_2/Fe^{2+} ratios, pH, and the initial concentration of antibiotics. They obtained complete degradation within 2 min., under the following optimal conditions: H_2O_2/COD molar ratio of 1.5, H_2O_2/Fe^{2+} molar ratio of 20, and pH of 3 [195]. Even though there are several reports that acknowledge the applicability of the Fenton and photo-Fenton oxidation for a variety of organics, large-scale industrial operations seem to be lacking; however, pilot plant studies show promise.

2.4.4. Heterogeneous Photocatalysis. Heterogeneous photocatalysis is a process, which embraces a large variety of reactions such as oxidation, dehydrogenation, metal deposition, organic synthesis, water splitting, photoreduction, hydrogen transfer, isotopic exchange, disinfection, anticancer therapy, water detoxification, and gaseous pollutant removal [196, 197]. Heterogeneous photocatalysis is considered as an effective AOP technique, particularly for air and water purification treatment. Heterogeneous photocatalysis can be carried out in gas or liquid phases, and the overall process can be explained by five different reactions: (i) transfer of the reactants in the fluid phase to the surface, (ii) adsorption of at least one of the reactants, (iii) reaction in the adsorbed phase, (iv) desorption of the product(s), and (v) removal of the products from the interface region [75]. Commonly, the heterogeneous photocatalysts are semiconductors, such as titanium dioxide (TiO_2), which can produce electron-hole pairs by the illumination with photons whose energy is equal to or greater than the bandgap of the semiconductor as shown by

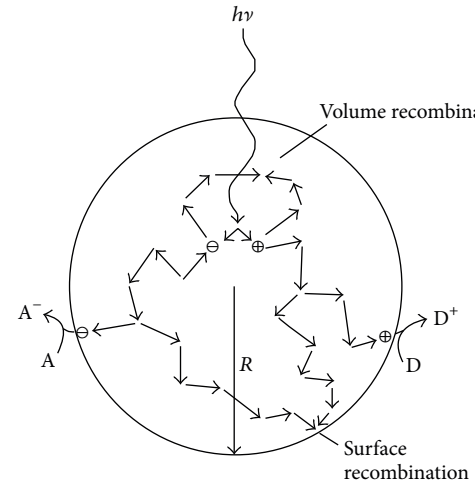

Figure 3: Recombination of electrons and holes within a semiconductor particle in the presence of acceptor (A) and donor (D) (reprinted with permission from [75]).

$$TiO_2 \xrightarrow{h\nu} e^{-}_{CB} + h^{+}_{VB} \quad (25)$$

The electron-hole pairs then dissociate into free photoelectrons in the conduction band and holes in the valence band are produced [75, 196, 198, 199]. The photoefficiency can be reduced by the surface or volume recombination of the electron-hole pairs either in the bulk or at the surface as depicted in Figure 3. Thus, recombination is undesirable and is detrimental to the photocatalytic activity.

In this photocatalysis process, the contaminant molecule gradually breaks down by its reaction with highly reactive oxidative species (ROS), such as $HO^{\bullet}$, $O_2^{\bullet -}$, and $HOO^{\bullet}$, which can be generated during the illumination process by the following equations [197, 200–203]:

$$h^{+}_{VB} + OH^{-}_{ads} \longrightarrow HO^{\bullet}{}_{ads} \quad (26)$$

$$h^{+}_{VB} + H_2O \longrightarrow HO^{\bullet} + H^{+} \quad (27)$$

$$2HO^{\bullet} \longrightarrow H_2O_2 \quad (28)$$

$$2H^{+} + O_2 + 2e^{-} \longrightarrow H_2O_2 \quad (29)$$

$$2H_2O + 2h^{+}_{VB} \longrightarrow H_2O_2 + 2H^{+} \quad (30)$$

$$H_2O_2 \xrightarrow{h\nu} 2HO^{\bullet} \quad (31)$$

$$e^{-}_{CB} + O_{2(ads)} \longrightarrow O_2^{\bullet -} \quad (32)$$

$$O_2{}^{-} + 2H^{+} + e^{-}_{CB} \longrightarrow H_2O_2 \quad (33)$$

$$O_2^{\bullet -} + H_2O_2 \longrightarrow HO^{\bullet} + HO^{-} + O_2 \quad (34)$$

$$O_2^{\bullet-} + H^+ \longrightarrow HOO^{\bullet} \quad (35)$$

$$O_2^{\bullet-} + h^+_{VB} \longrightarrow O_2 \quad (36)$$

$$O_2^{\bullet-} + HOO^{\bullet} + H^+ \longrightarrow O_2 + H_2O_2 \quad (37)$$

Among all these ROS, it has been widely noted that hydroxyl radicals are the most potent and important species responsible for the degradation of pollutants. Table 1 shows a comparison of the various removal techniques.

Frank and Bard have reported the heterogeneous photocatalytic oxidation of cyanide and sulfite in the presence of several semiconductors that include TiO_2, ZnO, CdS, Fe_2O_3, and WO_3, in aqueous medium under sunlight [204]. It was noticed that TiO_2, ZnO, and CdS showed good activity for cyanide oxidation, and no oxidation was seen using Fe_2O_3 and WO_3. In addition, the rates of the photocatalytic oxidation were found to be greater for sulfite than cyanide. Among these oxides, titanium dioxide (TiO_2) is an effective semiconductor material that has been explored for numerous applications including adsorption [168, 169], heterogeneous photocatalysis for splitting of water [205, 206], solar cell applications [207], and degradation of pollutants.

The removal of inorganic anions that include cyanide [208–210], nitrite [211], and sulfite [204] has been studied in the presence of TiO_2. In addition, the degradation of variety of pollutants that include several dye molecules [11, 13, 212–216], phenol and phenol derivatives [12, 46, 217, 218], and salicylic acid [219, 220] has also been researched.

Even though TiO_2 has been utilized as a photocatalyst for the degradation of a number of pollutants, its efficiency towards degradation is partly limited owing to its poor adsorptive property. In order to improve the efficiency of titania, researchers have prepared mixed oxide materials that can provide greater number of adsorptive sites; furthermore, by generating highly porous structures with large surface areas, effective dispersion of titania can also be achieved [221, 222]. Among the various mixed oxides, titania-silica has met the expectations of several researchers, due to the high surface area and the hydrophobic nature of silica [14].

3. Titania-Silica (TiO_2-SiO_2) Mixed Oxides

As discussed in the previous section, the presence of various inorganic and organic hazardous pollutants in the aquatic system poses a huge threat to public hygiene and human health. Hence, effective and economic means of remediating the polluted water sources need to be developed. Several conventional methods for removal of hazardous materials from wastewater, such as physical adsorption, condensation, biofiltration, and catalytic destruction [7], show varying degree of efficiencies in wastewater treatment. However, these above-mentioned traditional wastewater treatment techniques face several drawbacks or limitations: (i) physical adsorption method only immobilizes the pollutants onto solid adsorbent instead of degrading them into harmless materials, (ii) the condensation and/or biofiltration methods show relatively low efficiency and only a limited number of pollutants can be treated in this manner, and (iii) catalytic destruction processes are normally carried out under harsh conditions, such as extremely high temperatures (sometimes as high as 900°C). Therefore, an improved technique that presents high remediation efficiency that can be carried out under moderate conditions is desired. AOP, which are applicable at ambient temperature and pressure conditions, are recognized to be an ideal technique for environmental remediation. Extensive research interest has been devoted into heterogeneous photocatalysis and promising results have been obtained for the removal of highly toxic and nonbiodegradable pollutants that are commonly found in industrial wastewaters.

The following sections will briefly provide an overview of the synthesis of TiO_2-SiO_2 mixed oxides and an extensive discussion about the applications of TiO_2-SiO_2 mixed oxide materials towards the degradation of aquatic pollutants will also be carried out. A variety of synthetic methods have been reported for the preparation of periodic mesoporous materials, which are materials with uniform, regular, and well-arranged pores, and aperiodic TiO_2-SiO_2 mixed oxide materials that have randomly arranged pores. Thus, some of the main preparation methods followed by the structural characterization of titania-silica are presented here. Finally, the photocatalytic activity of these TiO_2-SiO_2 materials will be elaborated in great depth. Consequently, the factors that influence the photocatalytic activity such as the structural properties of the photocatalysts, pollution type and concentration, and pH will also be reviewed.

3.1. Periodic TiO_2-SiO_2 Mixed Oxide Materials. Among numerous semiconductor materials, there has been considerable interest in the use of TiO_2 as a photocatalyst to degrade a variety of pollutants in water [196, 223–225]. However, the photocatalytic performance of TiO_2 is significantly constrained by the fast recombination of the photogenerated electron-hole pair. In addition, its large bandgap energy (3.2 eV in anatase), low adsorption efficiency, surface area, and porosity restrict the widespread application of TiO_2 photocatalysts.

In order to promote AOP in practical applications, TiO_2 based photocatalysts with large specific surface area and porosity that is conducive to adsorption of aquatic pollutants need to be developed. A common strategy is to incorporate TiO_2 into periodic mesoporous support materials such as SiO_2. Periodic mesoporous SiO_2 materials possess high surface area, tunable pore size, and large pore volume that facilitate good dispersion of TiO_2 and adsorption of pollutant molecules as well.

In recent years, TiO_2 has been incorporated into highly ordered mesoporous siliceous materials such as SBA-15, MCM-41, and MCM-48. These periodic mesoporous siliceous supports with very high surface area and long-range ordered array of mesopores are recognized to be robust and stable supports for immobilizing TiO_2 species. In addition, the large surface area of mesoporous SiO_2 enables the high dispersion of TiO_2 species. With the above-mentioned merits, TiO_2 containing periodic mesoporous materials are expected to achieve markedly enhanced efficiencies for the

Table 1: Different removal techniques and its advantage(s) and disadvantage(s).

Removal techniques	Advantage(s)	Disadvantage(s)
Electrochemical oxidation	Does not require auxiliary chemicals, high pressures, or high temperatures.	Low selectivity and low reaction rates.
Biological process	Ecologically favorable process.	High capital and operational cost. Handling and disposing the secondary sludge pose problems.
Adsorption	Cost-effective method. Easy availability and operation. Most profitable process and more efficient than the conventional methods (i.e., precipitation, solvent extraction, membrane filtration, etc.).	Merely removes the pollutants from one phase (aqueous) to another (solid matrix). Expensive process for regeneration especially if the pollutants are strongly bound to the adsorbents.
Advanced oxidation processes (AOP)		
(i) Ozonation	Powerful oxidation technique oxidizes a large number of organic and inorganic materials.	More complex technology and requires high capital/operational cost. High electric consumption.
(ii) UV	An effective method that typically does not leave any byproducts which are harmful to the environment.	Less effective if the wastewater has high amounts of particulates which can absorb UV light.
(iii) UV/H_2O_2	An effective technique in the oxidation and mineralization of most organic pollutants. Ease of formation of $^{\bullet}OH$ radicals.	Less effective, when the wastewater has high absorbance. High operational cost.
(iv) $O_3/UV/H_2O_2$	Most effective process due to the fast generation of $^{\bullet}OH$ radicals. Can treat a wide variety of contaminants.	Needs to compete with high turbidity, solid particles, and heavy metal ions in the aqueous stream. High operational cost.
(v) Fenton reaction	Simple process. Easy availability of chemicals.	Production of sludge iron waste and handling the waste pose logistical problems.
(vi) Photo-Fenton reaction	Reduction of sludge iron waste compared to original Fenton reaction. Effective and fast degradation.	Needs a controlled pH medium for better performance.
(vii) Heterogeneous photocatalysis	Long-term stability at high temperature. Resistance to attrition. Low-cost and environmentally benign treatment technology.	Could form byproducts that can be harmful to the environment. Requires efficient catalysts that can absorb in the visible region.

photocatalytic degradation of aqueous wastes in comparison with nonsupported TiO_2.

In this section, the commonly conducted synthetic methods for the preparation of TiO_2 containing periodic SiO_2 mesoporous materials will be discussed. In addition, typical characterization techniques along with examples in which TiO_2 containing periodic SiO_2 mesoporous materials are used as photocatalysts for degradation of aqueous pollutants will also be covered.

3.1.1. Ti-SBA-15. SBA-15 is an important mesoporous material that is prepared by the using of triblock copolymers as structure directing agents. Because of its relatively large pore size (>6 nm) and thick pore walls, it has been used as a support to disperse TiO_2.

Synthesis. The synthetic methods for the incorporation of TiO_2 into SBA-15 mesoporous materials are mainly based on sol-gel reactions that include the hydrolysis, condensation, and precipitation of both titania and silica sols. A variety of synthetic procedures have been designed and developed. Several experimental variables that include solvent, pH, temperature, nature of silica and titania precursor, and surfactant type have been varied with a purpose of obtaining TiO_2 species in different phases and/or immobilizing them in different locations in SBA-15 support. These are discussed in the following section.

(1) *Coprecipitation Method.* In this synthetic route, the titania and silica precursors are introduced to the synthesis pot and they undergo hydrolysis simultaneously. In a typical synthesis, desirable amounts of silica precursor, for instance, tetraethyl orthosilicate (TEOS) or trimethyl orthosilicate (TMOS) along with titania precursor, such as tetraethyl orthotitanate, tetraisopropyl orthotitanate, or tetrabutyl orthotitanate, are added to a solution containing a triblock copolymer such as Pluronic P-123 (poly(ethylene-oxide)$_{20}$-poly(propylene-oxide)$_{70}$-poly(ethylene-oxide)$_{20}$). After sufficient stirring, the suspension is transferred to a Teflon-lined autoclave and subjected to hydrothermal

reaction at temperatures ranging from 100 to 250°C for as long as 24 h. Compared to the synthesis procedures under ambient conditions, the use of higher temperature and pressure in the hydrothermal synthesis ensures the complete hydrolysis of both the silica and titania precursors as well as the successful formation of the hexagonal phased SBA-15 material. In addition, the hydrothermal synthesis also results in the homogeneous distribution of the titania species in the SBA-15 siliceous support and often leads to the establishment of Ti-O-Si heterolinkages that are reported to be highly active in various photocatalytic reactions. After the hydrothermal reaction, a washing procedure is necessary to remove any unreacted precursors. Eventually, the materials are calcined in order to eliminate the surfactant.

(2) *Postimpregnation Method*. Compared to coprecipitation, the postimpregnation method has been studied more frequently. The merits of utilizing the postimpregnation synthetic method for the preparation of titania incorporated SBA-15 can be summarized as follows. First, the hexagonal phase of SBA-15 is more robust to withstand the conditions utilized for the coprecipitation method. Second, by postimpregnation method, titania species can be grafted onto the pore wall or surface of the mesopores of the SBA-15 mesoporous materials rather than to the framework positions. The anchored titania species on the pore walls have a greater probability to interact with reactant molecules that infiltrate the pores of SBA-15. In addition, via the postimpregnation method, a relatively large amount of titania can be loaded in the preformed SBA-15 mesoporous support. Therefore, more available active sites can be generated with higher loadings of titania.

The synthesis of SBA-15 mesoporous materials has been established and well documented [226]. In a typical synthesis route, an appropriate amount of triblock copolymer Pluronic P-123 (poly(ethylene-oxide)$_{20}$-poly(propylene-oxide)$_{70}$-poly(ethylene-oxide)$_{20}$) is added and dissolved in a mixture solution of water and hydrochloric acid. After the addition of silica precursor, for instance, tetraethyl orthosilicate (TEOS), the mixed solution is transferred to Teflon-lined autoclave and subjected to hydrothermal synthesis. The solid product then undergoes filtration, washing, and drying steps and is finally calcined in air to decompose the triblock copolymer to obtain SBA-15. During the postimpregnation synthesis, a variety of titania precursors can be immobilized into the preformed SBA-15 hexagonal structured mesoporous material. A certain amount of preformed SBA-15 is sonicated in isopropanol and this is followed by the addition of the required amount of titania precursor with stirring. Water is then added slowly to the resulting mixture to initiate the hydrolysis of the titania precursor. After the completion of the hydrolysis of titania precursor, the solid is recovered by centrifugation and calcined in the presence of air to give Ti-SBA-15.

3.1.2. Ti-MCM-41 and Ti-MCM-48. MCM-41 and MCM-48 belong to the M41S series of mesoporous materials that were originally developed by Mobil research scientists. These mesoporous materials have been widely employed as supports to disperse TiO_2.

Synthesis. Compared to Ti-SBA-15, the syntheses of titania incorporated into MCM-41 and MCM-48 periodic mesoporous materials require careful control of experimental conditions. The relatively small pore diameters (1.8 to 2.5 nm) and thin pore walls (1.2 to 2 nm) in MCM-41 and MCM-48 make the synthesis of these materials a little challenging. The successful formation of the hexagonal phased mesopores of MCM-41 and the cubic phased mesopores of MCM-48 is extremely sensitive to experimental conditions such as reaction temperature, time, surfactant concentration, precursor concentration, pH, and solvent used in the reaction. The syntheses of titania loaded MCM-41 and MCM-48 mesoporous materials are also based on sol-gel chemistry and can be mainly divided into two categories including coprecipitation and postimpregnation method.

(1) *Coprecipitation Method*. The coprecipitation method of synthesis of Ti-MCM-41 and Ti-MCM-48 is performed similar to Ti-SBA-15. However, instead of using triblock copolymer Pluronic 123, the structure directing agent used in the MCM-41 and MCM-48 synthesis is a cationic surfactant such as cetyltrimethyl ammonium bromide (CTAB). In a typical synthesis, a certain amount of CTAB is dissolved in a solution of water and alcohol. The synthesis gel contains titania and silica precursor, cationic surfactant, ethanol, and aqueous ammonia. Under basic conditions (pH > 8), the silica species exist as polyanions. The cooperative interaction between the silicate anionic species (I^-) and the cationic surfactant (S^+) induces a phase separation. With time, the silicate moieties undergo polymerization which decreases their charge density. Concurrently, the surfactant molecules undergo rearrangement to match the charge density at the surfactant-inorganic interface. The final mesophase formed is based on the structure having the lowest interface free energy or chemical potential. Meanwhile, the titania precursor undergoes hydrolysis and condensation to form either Ti-O-Ti or Ti-O-Si linkages. The gel is then transferred to a Teflon-lined autoclave and is typically held at 110°C to carry out the hydrothermal synthesis for as long as 48 h. After filtration, washing, and calcination to remove the surfactant, titania incorporated in MCM-41 or MCM-48 is obtained.

(2) *Postimpregnation Method*. Apart from the coprecipitation method, postimpregnation method is widely conducted for the synthesis of titania modified MCM-41 and MCM-48 mesoporous materials. The postimpregnation method is favored in the preparation of Ti-MCM-41 and Ti-MCM-48 photocatalysts for the ease of synthesis and the preservation of highly ordered hexagonal (MCM-41) or cubic (MCM-48) mesoporous structures. The method is similar to that discussed previously for Ti-SBA-15.

3.1.3. Structural Characterizations. The important techniques to characterize the titania containing mesoporous materials are discussed in this section.

Powder X-Ray Diffraction (XRD). Powder X-ray diffraction (XRD) is an informative technique to verify the periodic nature of the mesoporous structures in SBA-15, MCM-41, and MCM-48 materials and, additionally, the crystallinity and phases of the embedded titania species may also be inferred from powder XRD studies.

Figure 4 shows the low-angle XRD patterns of a series of titania loaded SBA-15 mesoporous materials [76]. In all of the XRD patterns for the TiO_2/SBA-15 samples, it can be observed that, in the range of 2θ between 0.8° and 2°, three well-resolved peaks are observed. These are ascribed to the reflections due to d_{100}, d_{110}, and d_{200} and demonstrate the characteristic hexagonal space group *P6mm* in SBA-15 periodic mesoporous materials. With the addition of various amounts of titania, the intensity of the peaks due to intrinsic reflections in SBA-15 materials decreases subtly. This small decrease in the peak intensity in the titania loaded samples can be explained by the incorporation of titania in the mesopores of the SBA-15 that results in the less scattering contrast between the pores and pore walls. However, the relatively inappreciable change in the d_{100}, d_{110}, and d_{200} reflections indicates that the SBA-15 is a robust and stable support for immobilizing titania species.

Apart from the low-angle XRD, long-range XRD analysis was also carried out to investigate the nature of the titania species in the Ti-SBA-15 mesoporous materials. Figure 5 presents the wide-angle XRD patterns for a series of titania incorporated SBA-15 samples and a pure SBA-15 as reference [77]. It can be seen that the pure SBA-15 sample shows a broad peak at around $2\theta = 25°$. This peak is due to the presence of amorphous silica that is the predominant phase in SBA-15. In addition, at relatively low loadings of titania (from 7% to 22%), as shown in Figures 5(b) to 5(e), the XRD patterns only show a broad peak at $2\theta = 25°$ due to SBA-15. This phenomenon is most likely due to the high dispersion of the titania species in the large surface area SBA-15 mesoporous materials. Titania clusters are confined within the mesosized pores of SBA-15 and/or maybe amorphous in nature. However, with further increase of the titania loading (26% to 31%), peaks due to bulk TiO_2 can be perceived. This indicates that, in the materials at these two loadings, titania clusters have aggregated to form larger particles on the SBA-15 support.

Similar observations can also be found from the powder XRD analysis for titania incorporated into MCM-41 and MCM-48 mesoporous materials. Kasahara et al. performed powder XRD analysis for titania incorporated MCM-41 mesoporous materials [227]. Typical Bragg reflections of the MCM-41 mesoporous materials with *P6mm* hexagonal symmetry were observed from the low-angle XRD patterns in all samples. In the wide-angle XRD plot, a characteristic peak due to only amorphous silica located at $2\theta = 25°$ was found. This indicates the high dispersion of titania in the MCM-41 mesoporous support. Thus, low- and high-angle powder XRD experiments are useful in identifying the mesoporous and the titania phase (at high loadings).

Nitrogen Physisorption. In order to investigate the textural properties, such as surface area, pore volume, and pore size of titania incorporated into periodic mesoporous materials, nitrogen physisorption studies are carried out.

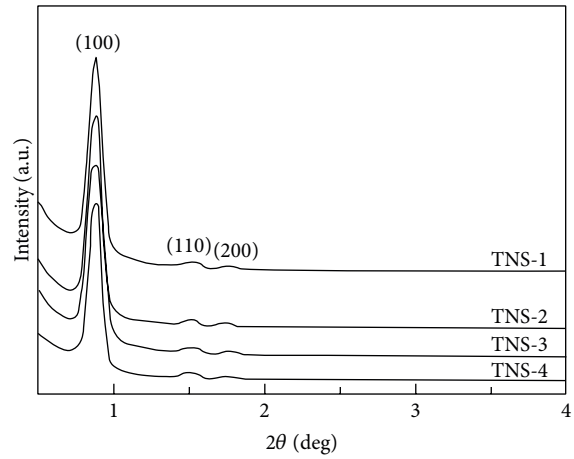

Figure 4: Small-angle XRD patterns of TiO_2/SBA-15 samples (reprinted with permission from [76]).

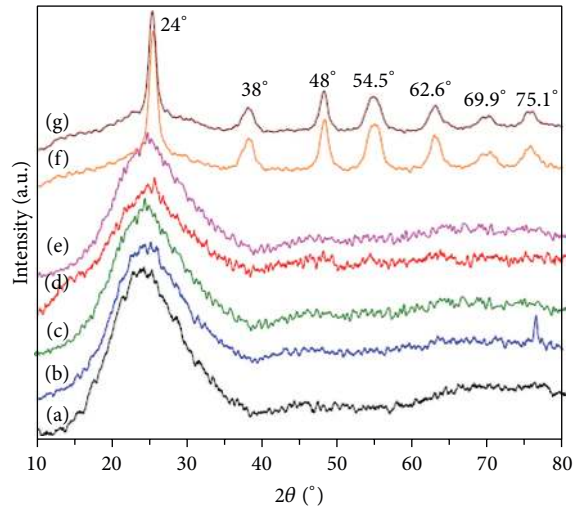

Figure 5: Wide-angle XRD patterns of TiO_2/SBA-15 mesoporous samples with different loadings of TiO_2: (a) bare SBA-15, (b) 7% TiO_2, (c) 12% TiO_2, (d) 18% TiO_2, (e) 22% TiO_2, (f) 26% TiO_2, and (g) 31% TiO_2 (reprinted with permission from [77]).

Figure 6(a) depicts the nitrogen adsorption-desorption isotherms for a series of titania containing MCM-41 mesoporous samples [78].

All the isotherms indicate type IV classification that is typical for mesoporous materials. In addition, a steep inflection that occurs at relative pressure values from 0.2 to 0.4 is an indication of the periodic array of the mesopores in the samples. Figure 6(b) presents the pore size distribution plots of the same batch of samples. The plots exhibit a very narrow pore size that is centered at around 28 Å indicating their uniformity.

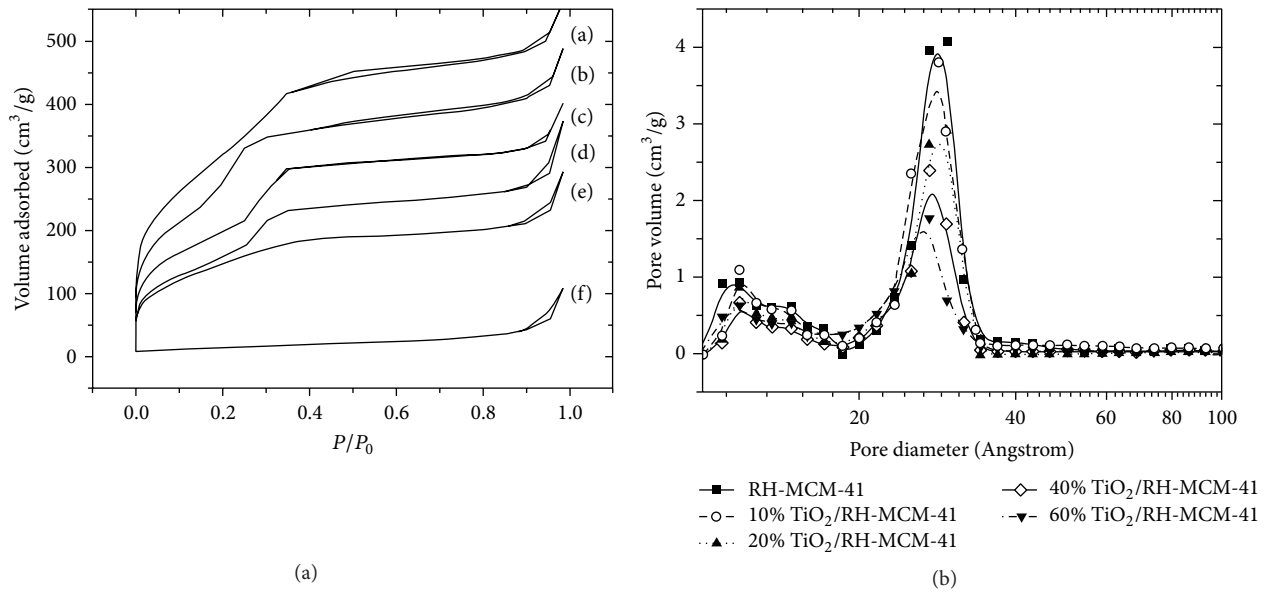

FIGURE 6: (a) N_2 adsorption-desorption isotherm: (a) RH-MCM-41, (b) 10% TiO_2/RH-MCM-41, (c) 20% TiO_2/RH-MCM-41, (d) 40% TiO_2/RH-MCM-41, (e) 60% TiO_2/RHMCM-41, and (f) bare TiO_2. (b) Pore size distribution in RH-MCM-41 and TiO_2/RH-MCM-4 (reprinted with permission from [78]).

Inductively Coupled Plasma-Atomic Emission Spectrometry (ICP-AES). Depending on the various synthetic and processing methods, the amount of the titania species in the final mesoporous materials may be different from the amount added or expected. This may be due to some unreacted titania precursor or due to loss of weakly adsorbed titanyl species during the washing process. It is important to estimate the actual amount of titania retained in the final mesoporous material. ICP-AES is a commonly adopted analytical technique to accurately determine the actual contents of titania species in the final titania loaded periodic mesoporous materials. Tian et al. performed the ICP-AES analysis for a series of titania loaded MCM-41 samples with variable Ti concentrations [228]. The results indicate that only about one-tenth of the titania content was preserved in the final materials compared with the initially introduced Ti precursors in the synthesis gel. Since there can be significant differences between the amount of titania actually retained in the mesopore matrix and the amount added, it is crucial to estimate the real titania loading in the sample and ICP-AES analysis is an important technique in this regard. It should be pointed out that atomic absorption spectroscopy (AAS) is less useful in comparison to ICP method for determination of titania since refractory materials such as titania are difficult to be quantified by the AAS method.

UV-Vis Diffuse Reflectance Spectroscopy (DRS). DRS is a sensitive tool in understanding the optical properties and the local environment and coordination of Ti^{4+} ions in titania containing periodic mesoporous materials. Also, one can estimate the bandgap and particle sizes of TiO_2 by the DRS method. Figure 7 shows the DRS of a set of Ti-SBA-15 samples that contain different Ti amounts [79]. It can be seen that

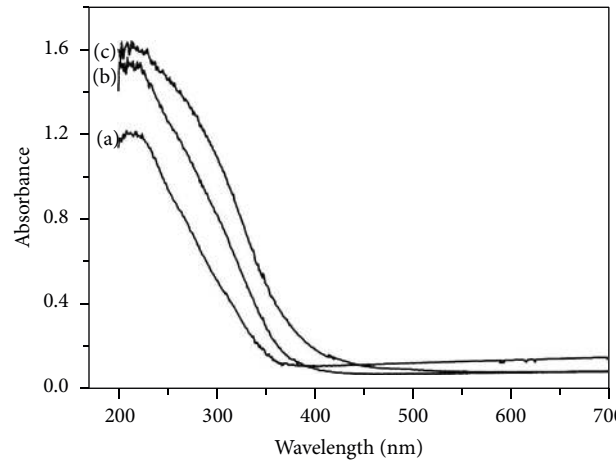

FIGURE 7: Diffuse reflectance UV-Vis spectra of Ti-SBA-(x) materials with varying titania loadings corresponding to (a) Ti-SBA-(6), (b) Ti-SBA-(9), and (c) Ti-SBA-(12) (reprinted with permission from [79]).

the Ti-SBA-15 samples exhibit absorption only in the UV region (<400 nm). Besides, the absorption onset shifts to higher wavelength with an increase of the titania content in the sample. This is due to the formation of the relative large clusters of titania at higher loadings. Apart from the absorption onset, there is an extra band near 214 nm in the sample with the least amount of TiO_2. This band is due to the ligand-to-metal charge-transfer (LMCT) from the O^{2-} to Ti^{4+} due to the presence of spatially isolated and tetrahedrally coordinated Ti^{4+} in the Ti-SBA-15 sample. With an increase of TiO_2 content in the sample, this band also displays a red

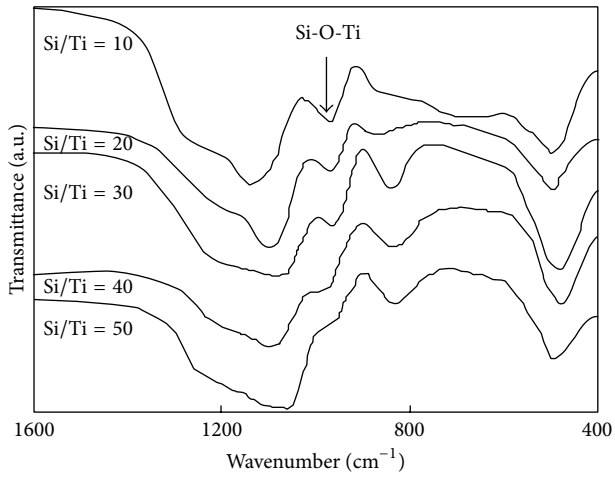

Figure 8: FT-IR spectra of Ti-MCM-41 with different Si/Ti ratios (reprinted with permission from [80]).

shift, which indicates that a portion of Ti^{4+} undergoes polymerization to form octahedrally coordinated Ti^{4+}. Hence, by conducting the DRS study, a better understanding of the optical properties and chemical environment of the titania species in the mesoporous materials can be obtained.

Fourier Transform-Infrared (FT-IR) Spectroscopy. FT-IR spectroscopy is widely applied to elucidate the surface environment of the titania containing periodic mesoporous materials. Figure 8 presents the FT-IR spectra of a series of Ti-MCM-41 samples with different Si/Ti ratios [80]. From the FT-IR spectra, an absorption peak appearing at 960 cm^{-1} is observed that may be assigned to the vibration of Ti-O-Si. With an increase of Ti content in the Ti-MCM-41 sample, the peak is observed to be more conspicuous. However, one should be careful in assigning this peak to Ti-O-Si since this vibration is also widely attributed to the presence of Si-O-H group. Thus, the use of FT-IR spectroscopy to infer the presence of Ti-O-Si bond is challenging. Other than this peak, three additional peaks at 440, 800, and 1060 cm^{-1} are due to the stretchings from the Si-O-Si support.

Raman Spectroscopy. The crystal phase of titania plays a critical role in photocatalytic reactions. Hence, Raman spectroscopy has been largely conducted to investigate the phase of titania in the periodic mesoporous materials. Figure 9 illustrates the Raman spectra of a series of Ti-SBA-15 samples [77]. In the samples with 26 and 31 wt.% of TiO_2 and pure TiO_2, Raman bands at 640, 520, 400, and 150 cm^{-1} with an additional shoulder at 200 cm^{-1} can be observed. The peaks at 640, 200, and 150 cm^{-1} can be assigned to E_g symmetric mode, the peak at 520 cm^{-1} is due to the combination of both B_{1g} and A_{1g} symmetry, and the peak at 400 cm^{-1} is due to B_{1g} symmetry. The Raman spectra indicate that titania exists in the anatase phase in these materials. For the Ti-SBA-15 samples with the TiO_2 loading lower than 22 wt.%, the peak intensities drop significantly indicating the presence of small sized and/or amorphous titania species. This is caused by the high dispersion of the titania species in the high surface area SBA-15 support at relatively low TiO_2 content.

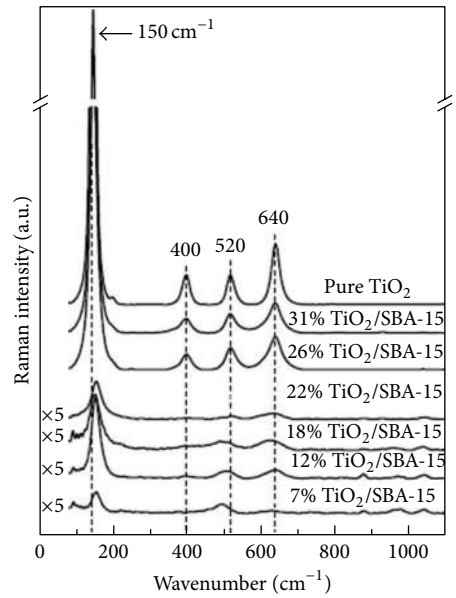

Figure 9: Raman spectra of TiO_2/SBA-15 mesoporous materials with different loadings of TiO_2 and pure TiO_2 samples (reprinted with permission from [77]).

X-Ray Photoelectron Spectroscopy (XPS). XPS is a useful technique to elucidate the oxidation states of the titania and silica species and to also identify the presence of Ti-O-Si linkages from the peak positions of the binding energies. Figure 10 shows the XPS spectra of O 1s core-level of TiO_2/SBA-15 mesoporous samples [77]. As can be seen, all of the samples show a clear peak at a binding energy of 532.8 eV. This peak can be assigned to oxygen in bulk silica (Si-O-Si). Apart from the peak appearing at the binding energy of 532.8 eV, an extra peak in the range of 530.0–530.6 eV can also be observed in all studied samples. This peak can be ascribed to the presence of

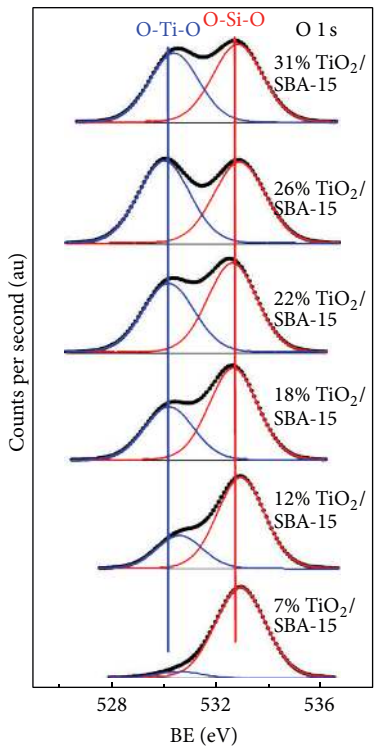

Figure 10: O 1s core-level spectra of TiO_2/SBA-15 mesoporous samples (reprinted with permission from [77]).

oxygen from Ti-O-Ti bonds. In addition, the intensity of the oxygen peak in the Ti-O-Ti species increases with the loading of titania in the samples.

Transmission Electron Microscope (TEM). TEM studies are widely conducted to illustrate the degree of the periodicity and morphologies of the mesoporous structures in various support materials, such as SBA-15, MCM-41, and MCM-48. Although powder XRD and nitrogen adsorption isotherms provide clues regarding the degree of periodicity of the pores, TEM studies can provide unequivocal evidence regarding the uniformity of the pores. Also, TEM can be used to identify the crystallinity and the phase of the titania species within the ordered mesoporous silica support. Figure 11 shows the TEM images of a representative Ti-SBA-15 mesoporous material [83]. Figures 11(a) and 11(b) indicate the highly periodic nature of the SBA-15 mesoporous materials indicating hexagonal phased pores in the materials after the incorporation of titania species. In order to elucidate the nature of titania species, high resolution transmission electron microscopy (HRTEM) and selected area electron diffraction (SAED) studies were carried and the results are shown in Figures 11(c) and 11(d). The d-spacings were determined to be 3.5122, 2.4000, 1.8947, and 1.7561 Å, which correspond to d_{101}, d_{103}, d_{200}, and d_{202} planes of anatase phase, respectively. Hence, the TEM results indicate that titania is in the form of anatase within the pores of SBA-15 periodic mesoporous materials.

Field Emission-Scanning Electron Microscope (FE-SEM). FE-SEM is an instructive instrument to understand the surface morphologies of the titania loaded periodic mesoporous materials. Figure 12 presents the SEM images of a sequence of titania incorporated SBA-15 materials with two different morphologies [83]. As can be clearly seen from the SEM images, the sample labelled Rod-SBA-15 exhibits uniform rod shaped materials and the length of the rods is fairly similar (~1 mm). However, the Normal-SBA-15 shows "wheat" like shape. After the incorporation of titania, both types of SBA-15 samples preserve their original morphologies. This indicates that SBA-15 is a very stable and robust support material for accommodating titania species.

3.1.4. Photocatalytic Reactions. In this section, we will discuss the photocatalytic reactions explored using titania incorporated into periodic mesoporous materials.

Photocatalytic Degradation of Dyes. Photocatalysis is an effective way to decompose dyes, which constitute an important class of pollutant. Among them, the degradation of MB dye has been explored extensively. During the photocatalytic processes, MB can be converted into gaseous CO_2 and inorganic ions such as SO_4^{2-}, NH_4^+, and NO_3^-. Yang et al. investigated the photocatalytic performance of the Ti-SBA-15 mesoporous materials for the degradation of MB [229]. The removal efficiency of MB was correlated with their adsorption on TiO_2/SBA-15 mesoporous materials. The dark adsorption study indicated that the uptake amount of MB increased with the surface area of TiO_2/SBA-15 materials. In addition, the sample with higher surface area presented better photocatalytic performance in the degradation of MB. It is well known that, besides the surface area of the catalyst, other factors, such as crystal phase, crystallite size, and crystallinity of the titania species, also impact the photocatalytic activity. However, the photocatalytic activity is a balance between the surface area and crystallinity. Thus, the TiO_2/SBA-15 sample with 30% loading of TiO_2 showed the highest photocatalytic activity among all samples due to the high surface area without sacrificing too much crystallinity of TiO_2. Similar observations can be seen from the works reported by Sahu et al. [226], Zhu et al. [79], and Acosta-Silva et al. [77], in which the anatase TiO_2 nanospecies were incorporated in SBA-15 mesoporous materials to realize the photocatalytic decomposition of MB. The photocatalytic activity of TiO_2-SBA-15 was shown to be significantly higher than that of pure TiO_2.

In addition to the structural properties of the photocatalysts, the experimental conditions also had a dramatic influence on the photocatalytic decolorization of MB. Suraja et al. investigated the effect of the reaction time, concentration of MB, and the pH environment over the photocatalysis process [8]. With time, the photocatalytic degradation rate of MB increased due to the larger exposure under the light source. Regarding the concentration of MB, the photocatalytic degradation capacity stayed more or less identical at relatively low (<25 mg/L) initial dye concentration. However, after the initial concentration of MB exceeded 25 mg/L, a sudden decrease in the activity was noticed. This can be explained by the fact that, at high concentrations of

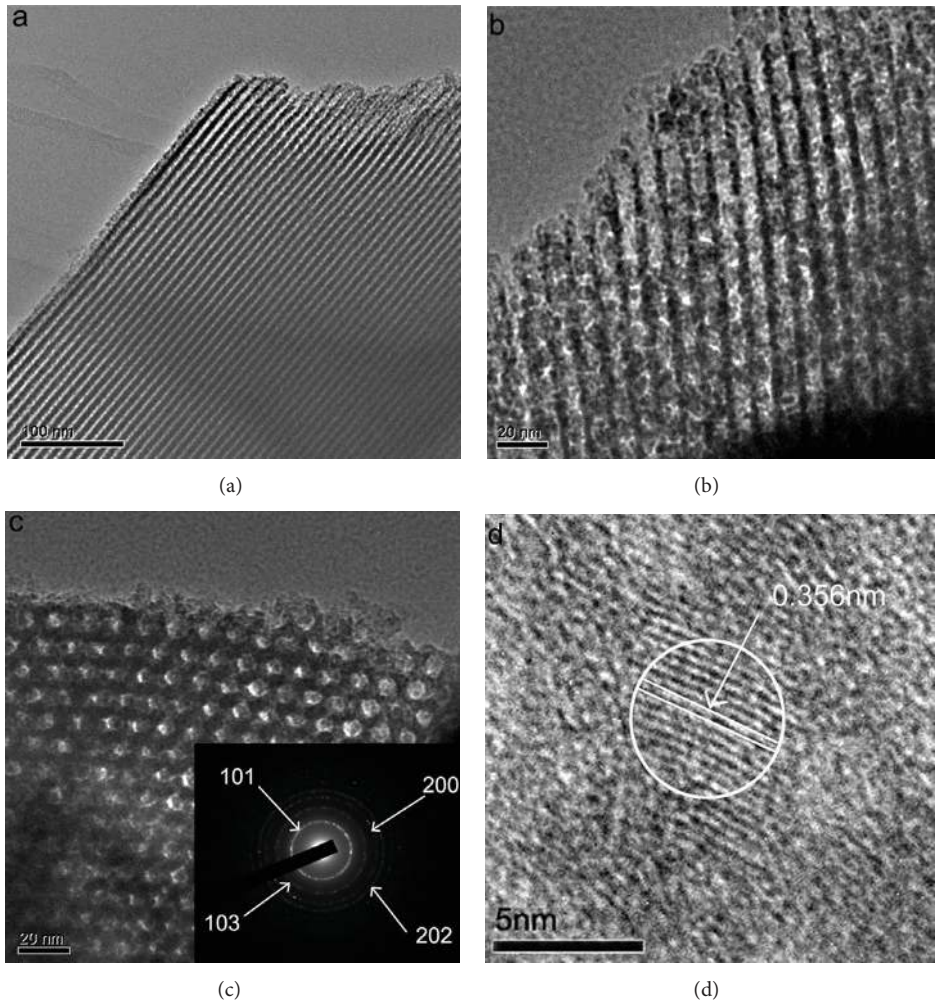

Figure 11: TEM images of (a) SBA-15 along [81] direction, ((b) and (c)) TiO_2/SBA-15 along [81, 82] direction (inset shows the SAED pattern), and (d) a typical HRTEM image of TiO_2 nanoparticle encapsulated in the channel of SBA-15 (reprinted with permission from [83]).

MB, irreversible adsorption of MB takes place. The lack of desorption of MB molecules from the surface prevents MB molecules in solution to adsorb at the surface and, thus, the degradation is low at high concentrations of MB. The pH of the solution in the photocatalytic reaction showed a significant impact on the MB degradation efficiency. Either acidic or basic conditions were proven to be detrimental for the MB degradation. The highest efficiency was achieved under neutral conditions.

Besides the hexagonal SBA-15 mesoporous materials, TiO_2 containing cubic MCM-48 mesoporous materials have also been studied for MB photodegradation. Liou and Lai developed TiO_2/MCM-48 composite materials and evaluated their performance for photocatalytic decomposition of MB [230]. Their results indicate that lower loadings of TiO_2 enhanced both adsorption of MB and photocatalytic activities. This was mainly due to the fact that, at high loadings, aggregation of TiO_2 caused clogging of the pores in MCM-48 and brought down their uptake of MB molecules. At lower TiO_2 contents, high dispersion of titania in the MCM-48 mesoporous materials enabled more efficient contact and reaction with MB molecules.

Rhodamine dyes (R6G and B (RhB)) are also commonly seen as pollutants in the aquatic environment and they can be decomposed by titania incorporated into periodic mesoporous materials. De Witte et al. tested the photocatalytic performance of titania loaded SBA-15 for the photodecomposition of R6G [231]. The TiO_2/SBA-15 sample with larger pore diameters presented superior photocatalytic activity compared to the rest of the samples. This can be explained by the fact that the larger pore sized material facilitated better diffusion of R6G molecules and ensured good contact with TiO_2. Beyers et al. also confirmed the observation that large pore sizes in TiO_2/SBA-15 sample are conducive for the photocatalytic degradation of R6G [232]. In addition, the location (inside or outside of the SBA-15 channels) of the TiO_2 species in the TiO_2/SBA-15 samples and its influence on the photocatalytic activity were studied as well. Tian

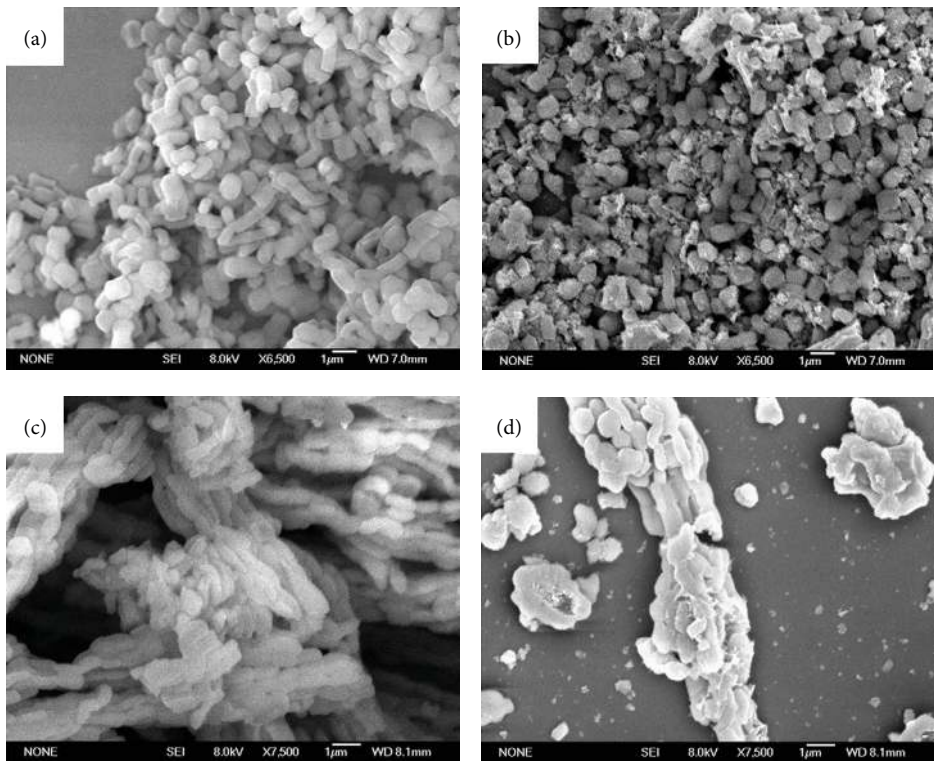

Figure 12: SEM images of (a) Rod-SBA-15, (b) TiO_2/Rod-SBA-15, (c) Normal-SBA-15, and (d) TiO_2/Normal-SBA-15 (reprinted with permission from [83]).

et al. examined the photocatalytic degradation of RhB by using titania loaded MCM-41 mesoporous materials [228]. It was suggested that the photocatalytic performance was based on both the loading and the position of the titania species. Compared with the pure TiO_2 sample, TiO_2/MCM-41 exhibited marked enhanced photocatalytic activity for RhB degradation.

Li et al. investigated the photocatalytic properties for methyl orange (MO) degradation over the TiO_2/SBA-15 mesoporous materials with different morphologies [83]. The rod-like SBA-15 supported sample presented higher photocatalytic activity than that of regular TiO_2/SBA-15. It was proposed that the rod-like SBA-15 mesoporous materials possessed smaller particle size and shorter channel than the regular SBA-15. In addition, the rod-like SBA-15 particles were arrayed in an ordered manner compared to the random distribution in the regular SBA-15 particles. All these properties in the rod-like SBA-15 materials facilitated the high dispersion of small particles of TiO_2. Hence, the TiO_2/SBA-15 with rod-like structure exhibited better photocatalytic activity for MO degradation.

Anandan conducted the photocatalytic degradation of MO by using titania incorporated MCM-41 mesoporous materials and the role of peroxomonosulphate (PMS), peroxodisulphate (PDS), and H_2O_2 as electron accepters was examined in the photocatalytic reaction [233]. Ti-MCM-41 photocatalysts presented dramatically higher activity for MO degradation compared with bare TiO_2. The enhanced efficiency can be ascribed to the large surface area of MCM-41 support that realized the high dispersion of TiO_2 photoactive species and facilitated the adsorption of MO. Among the electron accepters, PMS displayed the best performance in photodegradation of MO. It was proposed that the presence of PMS effectively brought down the photoinduced electron-hole recombination in TiO_2 and realized the enhanced formation of hydroxyl radicals ($OH^\bullet$) for the decomposition of MO. PDS showed lower activity due to its limited reactivity with only photogenerated electrons on TiO_2. H_2O_2 was found to be inert in the photocatalytic process for MO degradation due to its scavenging of hydroxyl radicals ($OH^\bullet$).

Ding et al. observed that Ti-SBA-15 exhibited enhanced photocatalytic activity for the degradation of indigo carmine (IC) than anatase titania [234]. The enhanced photocatalytic activity in Ti-SBA-15 sample was mostly due to its high porosity and specific surface area and presence of more accessible photooxidative sites. Jyothi et al. developed titania incorporated into hexagonal MCM-41 and cubic MCM-48 mesoporous materials as photocatalysts for the photodecoloration of IC [235]. It was found that the hexagonal Ti-MCM-41 sample showed higher activity for the photodegradation of IC than that over the Ti-MCM-48 sample. This was ascribed to the smaller pore size (2.3 nm) in the MCM-41 mesoporous materials that confined the titania species into relatively small sizes. In contrast, the larger pore size (4.1 nm) of the MCM-48 support resulted in the growth of relatively large titania species. Hence, the MCM-41 sample with smaller titania clusters possessed higher dispersion of titania, which resulted in better photocatalytic performance.

Bhattacharyya et al. applied Ti-MCM-41 materials for the photocatalytic decoloration of Orange II dye [236]. The optimal loading of titania was determined to be 50 wt.%, at which the best adsorption capacity for Orange II dye and appropriate crystallinity and particle size of TiO_2 can be reached. Tseng et al. evaluated the activity of TiO_2/SBA-15 for the photodecomposition of Acid Red 1 (AR1) dye [237]. The photocatalytic results indicated that TiO_2/SBA-15 was an effective catalyst for the photodegradation of AR1 and improved overall photocatalytic efficiency can be found over TiO_2/SBA-15 compared with pure TiO_2. The highest activity was achieved from the sample with 30 wt.% loading of TiO_2. The nanoscale sized TiO_2 clusters that were confined by the pores of SBA-15, the Ti-O-Si linkages, and the strong surface acidity of SBA-15 were considered to be the three main factors for an enhancement in the photocatalytic decolorization of AR1.

Photocatalytic Degradation of Phenolic Compounds. Phenols constitute another important class of pollutants. Alvaro et al. compared the photocatalytic activity of TiO_2/MCM-41 and TiO_2/SBA-15 for phenol degradation [238]. In the TiO_2/MCM-41 series of materials, the photocatalytic activity increased with increasing content of titania in the samples. However, in the SBA-15 based samples, the photocatalytic activity was maximum at an optimal concentration of titania and then decreased with an increase in titania loading. Comparing the phenol degradation efficiencies between TiO_2/MCM-41 and TiO_2/SBA-15 sample, it was observed that, in general, MCM-41 based samples showed higher activities than the SBA-15 based samples for the same loadings of titania. This can be attributed to the higher surface area of the MCM-41 support that enabled efficient dispersion of titania species when compared to SBA-15. Wang et al. assessed the phenol degradation efficiency by using TiO_2/SBA-15 mesoporous materials [76]. It was found that the photocatalytic efficiency improved with the loading of TiO_2 in the sample. The higher activity of the TiO_2/SBA-15 sample than that of commercial TiO_2 was attributed to the high specific surface area of the SBA-15 support that favored the diffusion of phenol as well as its good contact with the catalyst.

Adams et al. designed TiO_2/SBA-15 catalysts in different morphologies (thin film and powder form) to study their activity for the photodegradation of 2,4-dichlorophenol (2,4-DCP) [239]. Under identical experimental conditions, the thin films were able to degrade 2,4-DCP approximately half as fast as compared to the suspension form. The lower activity from the thin film sample was rationalized by its lower absorption of light compared to the powder sample. Despite inefficient photon capture, the thin film sample presented a promising prototype for the design for highly active photocatalysts. Orlov et al. tested the activity of a series of TiO_2/SBA-15 samples for *p*-chlorophenol photodegradation [240]. Among all of the catalysts, the one containing the highest concentration of spatially isolated, tetrahedrally coordinated Ti^{4+} ions showed the best activity for *p*-chlorophenol degradation. This can be explained by the generation of long-lived photoinduced electron-hole pairs in the tetrahedrally coordinated Ti^{4+} ions that enhanced the overall photocatalytic efficiency.

Do et al. developed a set of Ti-MCM-41 samples with variable TiO_2 loading for the photodegradation of 4-nitrophenol (4-NP) [80]. It was observed that, initially, the photocatalytic activity increased with an increase of the TiO_2 loading in the Ti-MCM-41 sample. The highest activity was achieved from the sample with Si/Ti ratio of 20. Further increase in the TiO_2 loading in the sample caused a drop in the activity. The decrease in the activity was attributed to the aggregation of TiO_2 in nonframework positions of the MCM-41 support.

Artkla assessed the photocatalytic degradation of polyphenols (gallic acid) by using TiO_2/MCM-41 catalysts [78]. Several parameters, such as the loading of TiO_2 and the pH, were investigated to establish a structure-activity relationship. It was observed that using MCM-41 as support for titania significantly enhanced the photocatalytic activity for gallic acid degradation. Increase of the TiO_2 loading (>10 wt.%) was found to be detrimental for the photocatalytic reaction. This was explained by the formation of bulk TiO_2 (anatase) that caused pore clogging and precluded efficient contact between reactants and active sites in the MCM-41 mesoporous materials.

Photocatalytic Removal of Inorganic and Minor Organic Wastes. Aguado et al. prepared titania incorporated MCM-41 and SBA-15 mesoporous materials for photooxidation of free cyanides and iron (III) cyanocomplexes [241]. The TiO_2/MCM-41 and TiO_2/SBA-15 samples presented higher activity than that of pure TiO_2 (anatase) for photooxidation of CN^-. TiO_2/SBA-15 was found to be almost as active as commercial Degussa P25, which exhibited the highest activity. TiO_2/SBA-15 was further adopted and studied for photooxidation of iron (III) cyanocomplexes. The efficient photocatalytic performance from TiO_2/SBA-15 can be rationalized by reduction of screening effect compared to bare titania particles, the prevention of the formation of $Fe(OH)_3$, and the presence of silica support that provided adsorption sites for the iron species resulting from the breakage and reaction of the complex. A similar observation can also be found from a work reported by López-Muñoz et al., who developed a series of TiO_2/SBA-15 for photooxidation of free cyanide and hexacyanoferrate (III) [242].

Artkla et al. assessed the activity for photocatalytic degradation of tetramethylammonium (TMA) ions over TiO_2/MCM-41 mesoporous materials [243]. TiO_2/MCM-41 presented enhanced activity for photodegradation of TMA compared to bare TiO_2 sample. Among all of the TiO_2/MCM-41 with various TiO_2 contents, the sample with 10 wt.% of TiO_2 exhibited the highest activity. In addition, the optimal photocatalytic efficiency was attained under neutral pH environment. Xu and Langford incorporated titania into MCM-41 mesoporous support to study the photocatalytic degradation of acetophenone [244]. It was established that the preparation method used for immobilizing titania species into MCM-41 support had a significant impact on the performance of the catalysts. The crystallinity of TiO_2 was an overriding factor that governed the photocatalytic activity of TiO_2/MCM-41 in

this study. The sample with more crystalline titania species showed higher activity.

3.2. Aperiodic TiO_2-SiO_2 Mixed Oxide Materials. Aperiodic titania-silica binary mixed oxides are commonly synthesized using the sol-gel method. Aperiodic mesoporous materials do not possess uniform and periodic arrangement of pores. Several reported methods of preparation that include coprecipitation, impregnation, hydrothermal, flame hydrolysis, and chemical vapor deposition (CVD) have been implemented to tune the structural features of the mixed oxides by optimizing the synthetic procedures. In a recent review article, we have successfully discussed the different synthetic methodologies to prepare TiO_2-SiO_2 mixed oxide materials [245]. To provide better transition and clarity to the readers, a brief discussion of the synthesis methods and the characterization techniques is elaborated herein.

3.2.1. Synthesis of Aperiodic TiO_2-SiO_2 Mixed Oxides. The sol-gel synthesis of TiO_2-SiO_2 materials usually involves the hydrolysis and condensation of titanium and silicon alkoxide precursors that lead to the formation of polymeric gels. By changing the experimental conditions, that include the amounts and types of precursors and solvents, water, pH, and temperature, the structural properties of the materials can be tailored. Furthermore, the porosities of the materials can be tuned by using an appropriate drying method. In a typical synthesis of xerogels materials, appropriate amounts of silica precursors and titania precursors are mixed with an alcoholic solvent, that include ethanol, methanol, or isopropanol, under vigorous stirring at ambient conditions. The sol is allowed to gel at ambient conditions and the solvent is allowed to evaporate. The dry powder obtained is then calcined. Generation of homogeneous gel is critical due to the unequal hydrolysis and condensation rates of the two different titanium and silicon alkoxide precursors. The unequal hydrolysis rates of these two alkoxide precursors can be explained by the differences in the partial charge of Si (+ 0.32) and Ti (+ 0.61). Due to their higher partial charge, titanium alkoxides undergo more rapid hydrolysis than silicon alkoxides, and this may lead to inhomogeneous distribution of titania in the mixed oxide materials. Thus, prehydrolysis of silicon alkoxides is necessary [246].

Preparation of TiO_2/SiO_2 nanomaterials was attained from the hydrolysis and polycondensation of tetrabutyl orthotitanate and tetraethyl orthosilicate via a sol-gel process by Cheng et al. [165]. Various amounts of silica doped with nanocrystalline titania powders were prepared and the influence of dopant concentration on the phase transition and grain growth was analyzed in their work. In addition, a constant dopant concentration of the sample was utilized to investigate the effect of calcination temperature on the photoactivity of titania. Spherical titania/silica particles with higher surface area, ranging from 400 to 700 m^2/g, and pore volume of 0.9–1.4 cm^3/g were prepared via the combination of emulsion and gelation of mixed sols [247]. The emulsion and gelation processes were carried out in the presence of dodecanol or hexane to the acid mixed sols prepared by mixing the prehydrolyzed silicon and the titanium alkoxides. The polar nature of dodecanol provides suitable equilibrium composition of the biphasic system and controls the hydrolysis rate, whereas direct emulsion formation took place in the presence of hexane.

Homogeneous hydrolysis and condensation can also be achieved as discussed thereafter. The silicon alkoxide is hydrolyzed in an alcohol solution in the presence of concentrated acid, for example, HNO_3, HCl, or H_2SO_4, and water with vigorous stirring to create silanol groups [248–251], or the silicon alkoxide can be refluxed at 80°C in the presence of HCl or acetic acid [252, 253]. Then, these silanol groups undergo condensation process with the titanium alkoxide in the presence of water and form the active Ti-O-Si heterolinkages. Furthermore, acetic acid (AcOH) is utilized as a modifying agent to decrease the hydrolysis of titanium alkoxide in aqueous solutions via bridging of the acetate ligand with the terminal isopropoxyl groups present on the titanium alkoxide precursor [254, 255]. Acetylacetone (acac) has also been utilized to modify titanium alkoxides in several studies. acac can form chelated titanate species and decreases the hydrolysis rate of titanium alkoxide by increasing the coordination of titania from four to five [256–260]. 2-Methoxyethanol, a polar protic alcoholic solvent, was used as solution medium by Pirson et al. and can serve as a stabilizer of the titanium alkoxide towards the hydrolysis and condensation reactions [261]. In another study, isoamyl alcohol was used as a stabilizer for tetraisopropyl orthotitanate to reduce its rate of hydrolysis. Even though enhanced homogeneity of the gel was achieved by prehydrolysis of silicon alkoxides, the hydrolysis and condensation reactions were found to be slow and incomplete under ambient conditions. In addition, the ambient procedure requires long processing time to form a gel (a week to a month period of time) [91, 262]. Hence, reaction conditions, such as temperature and pressure, have been modified to overcome these challenges.

The hydrothermal treatment has been utilized by several researchers to achieve complete hydrolysis and condensation of the silica and titania precursors in a short period of time [263]. In this method, the reaction mixture containing the silica and titania precursors is placed in an autoclave reactor and heated to temperatures typically in the range of 100 to 200°C for a period of up to 24 h. Even though the hydrothermal synthesis method has been found to be a facile synthetic method to prepare crystalline and relatively stable materials, additional steps of washing, filtering, and drying are unavoidable. These additional steps can be avoided by the use of a supercritical drying method. Supercritical drying has been attempted to produce aerogels materials with enhanced porosities and high surface areas [263, 264]. Although these hydrothermal and supercritical drying methods result in materials with high crystallinity of the titania phase and high surface area, these are energy-intensive methods that require either extra processing steps or the use of expensive high-pressure equipment.

Different synthetic recipes have been attempted for the preparation of TiO_2-SiO_2 materials in order to attain desirable structural properties that are responsible for enhanced photocatalytic activity. Use of appropriate solvents, acids, or bases, and effective metal precursors in the synthesis

procedure leads to the formation of materials with enhanced porosities and surface area. TiO_2-SiO_2 xerogel materials with different pore sizes and surface areas have been prepared with a constant 1 : 4 molar composition of Ti : Si by simply changing the amounts of water, acids, or bases and hydrolysis procedure [265]. Gels formed in basic conditions possessed larger mesopores and lower surface area in comparison to the gel prepared in acid conditions due to lower pore collapse during drying. The partial hydrolysis of the silicon alkoxide in basic medium followed by the mixing of titanium alkoxide produced microporous xerogels owing to the high collapse of pores. However, even after the treatment in air at 600°C, the titania phase was amorphous. Pirson and coworkers have reported the synthesis of SiO_2-TiO_2 xerogels by a sol-gel method in the presence of polar protic solvents [261]. It was noticed that the alcoholic solvents act as stabilizers for titania and control the reactivity of the titania precursor. The gels were found to be microporous, and calcination at temperatures above 350°C diminished the pores in these materials.

Avendaño and coworkers developed an experimental strategy to obtain mesoporous ZrO_2-SiO_2 and TiO_2-SiO_2 mixed oxides via the sol-gel process [174]. The surface acidity was examined by adsorbing pyridine. A simple acid-catalyzed sol-gel process without the addition of any chelating agents or prehydrolysis step was utilized to synthesize microporous titania-silica mixed oxides [266, 267]. The materials showed a narrow unimodal pore size distribution centred near 0.7 nm. A high dispersion of titania in the silica matrix was obtained by first mixing titanium alkoxide with TEOS in alcoholic solution and aqueous hydrochloric acid followed by calcination of the resulting solid material. However, the resulting materials were found to be amorphous. The surface area varied as a function of Si/Ti ratio. Budhi et al. synthesized a series of TiO_2-SiO_2 xerogels [268]. Addition of nonpolar cosolvents, such as toluene, *p*-xylene, and mesitylene, resulted in materials with enhanced gelation rates and enlarged pores. The resulting materials have been utilized for phenol degradation and the TiO_2-SiO_2 xerogels showed higher activity in comparison to a sample prepared by the hydrothermal method due to better adsorptive and highly reactive TiO_2 sites.

It has been postulated that, by improving the hydrophobic nature of titania-silica, one can enhance the adsorption of organic compounds on them compared to bare TiO_2. Larsen and coworkers tried to enhance the hydrophobicity of titania-silica materials using noncyclic silicon precursors [269]. These materials were prepared by acid prehydrolysis of TEOS and dimethyldimethoxysilane in ethanol medium, followed by the addition of $TiCl_4$ in isopropanol [270]. In another study, Mariscal et al. enhanced the hydrophobic nature of TiO_2-SiO_2 xerogels by mixing the titanium and silicon alkoxides with a hexane solution of trimethylchlorosilane (TMCS) in N_2 atmosphere [271]. Dagan and coworkers modified silica with methyl and phenyl moieties to control the polarity, hydrophobicity, ion-exchange capacity, and concentration of silanol groups on the surface of TiO_2-SiO_2 xerogels [272]. The resultant modified silica sols were mixed with ethanol and addition of titanium alkoxide formed mixed oxide gels. These methyl and phenyl moieties provide better adsorptive sites on the TiO_2-SiO_2 mixed oxide materials.

TiO_2/SiO_2 composite nanoparticles were prepared directly from the acidic precursor solutions of $TiOSO_4$ and TEOS by hydrolysis under hydrothermal conditions by Hirano et al. [273]. An increasing surface area with increasing silica content was attained with the materials prepared in their study. Enhanced photocatalytic activity was obtained with these materials in comparison to pure TiO_2 for the removal of NO gas. In another study, nanophase silica-titania particles were prepared by sol-gel and hydrothermal processing [250]. The textural properties of these materials such as surface area, particle size, crystallinity, and crystallographic phases were controlled by varying the calcination temperature and the molar ratio of Si and Ti. It was noticed that the crystallite sizes of SiO_2-TiO_2 decreased when the mole fraction of silica increased and this behaviour was explained by the fact that the silica suppresses the growth of titania [89, 274]. In a following study, a similar method has been utilized by the same group, for the preparation of silica embedded nanocrystalline TiO_2 powders [89]. The crystal phase of titania was found to be strongly dependent on the silica content and the solvent composition. In addition, the silica embedded titania materials exhibit a strong inhibition for the formation of rutile phase. Thus, these materials show efficient photocatalytic activity, about 1.2 times better than the commercially available Degussa P25. The role of crystallinity of the titania phase in TiO_2-SiO_2 prepared by a cosolvent induced gelation method was examined towards the degradation of phenol by our group [84]. It was found that addition of cosolvents enhanced the gelation process and the crystallinity of the titania phase, resulting in the formation of mesoporous TiO_2-SiO_2 with higher photocatalytic activities for the degradation of phenol.

Li and coworkers synthesized silica-modified TiO_2 by utilizing hydrothermal methods [275]. Formation of Ti-O-Si bond with strong interaction between SiO_2 and TiO_2 in the materials was proven by XPS and FT-IR analysis. The silica content in the materials affected the crystallinity and the nature of the titania phase. Furthermore, these mixed oxide materials showed better photocatalytic activity in comparison to pure TiO_2.

Another approach to significantly enhance the porosities and surface area is preparation of aerogels under supercritical conditions. In this method, the wet gel prepared by the same procedures explained above is slowly heated to critical temperature (Tc) and critical pressure (Pc) of the solvent employed. The solvent is then removed once the appropriate supercritical conditions of temperature and pressure are attained. Removal of solvent under such conditions prevents the formation of both the liquid-vapor meniscus and capillary pressure in the pores. Thus, pore collapse is prevented and the final materials possess relatively large pores.

Dutoit et al. synthesized mesoporous titania-silica aerogels with highly dispersed titania by a sol-gel process [276, 277]. An acidic hydrolysant (doubly distilled water and hydrochloric acid, 37 wt.%) was added to the solution of acetylacetonate modified tetraisopropyl orthotitanate and

tetramethyl orthosilicate in isopropanol solvent. The gel formed was subjected to different drying conditions including conventional drying, high-temperature supercritical drying, and supercritical CO_2 drying. It was noticed that the textural properties were affected by the drying conditions employed and the pH used for initiating the hydrolysis reactions [278]. A drop in mesoporosity and surface area was noticed in the materials, which contained low amounts of titania. In addition, it has been noted that the use of acidic conditions for sol-gel method leads to materials with substantial amounts of micropores [279].

Deng et al. synthesised TiO_2-SiO_2 aerogel materials with different TiO_2 contents [263]. Anatase microcrystallites were obtained after supercritical drying in ethanol. In addition, the photocatalytic degradation of phenol using these aerogels was examined and maximum activity was observed at molar ratio of $TiO_2/SiO_2 = 1$. Crack-free titania-silica aerogels with high titanium content, Ti/Si = 1, were successfully prepared by Cao and coworkers by simply adjusting the hydrolysis rate of the titanium and silicon alkoxide precursors [280]. Tailoring the interconnectivity of the pore network in the aerogel materials was found to improve the physicochemical characteristics of these materials. In their work, well-dispersed, nanometer-sized anatase crystal domains were crystallized by high-temperature supercritical drying in ethanol medium. In addition, the crystalline domains contained Ti-O-Si bonds.

Kim et al. synthesized titania-silica binary aerogel with 1 : 1 molar ratio of Ti to Si by first modifying tetrabutylorthotitanate (TBOT) with acetylacetone in methanol solution followed by the addition of TEOS [281]. In addition, a nonalkoxide sol-gel route for the synthesis of TiO_2-SiO_2 aerogel materials was also done by addition of $TiCl_4$ and $SiCl_4$ in a methanol medium. High surface area titania and titania-silica aerogels were obtained by the nonalkoxide sol-gel route and by a subsequent carbon dioxide supercritical drying step. However, the surface area of the resulting aerogel was found to be similar to that of the aerogel prepared by alkoxide sol-gel route.

The influence of the preparation method on the physicochemical properties of titania-silica aerogel materials was assessed by Brodzik and coworkers [222] using four different synthesis procedures: (i) modified titania precursor, (ii) fully hydrolyzed silica precursor, (iii) titanium and silicon precursors that were hydrolyzed and gelled without any modification, and (iv) impregnation of a preformed silica gel by a modified titania precursor. Anhydrous ethanol and methanol were used as solvents and the gel formation was induced by adjusting the pH of the system with ammonia. Finally, highly porous aerogels were obtained and the presence of anatase crystallites was inferred from XRD studies. In addition, the amount of water present in the reaction mixture was found to play a key role in formation of titania-silica lattice and strongly influenced the resulting photocatalytic activity. Furthermore, the impregnation and simultaneous hydrolysis methods resulted in highly active photocatalysts.

In summary, the synthetic routes for preparation of the binary aperiodic mixed oxide materials significantly influence the structural properties of the materials, which ultimately affect their photocatalytic activity. The following section will provide a brief discussion of several characterization techniques.

3.2.2. Characterization of Aperiodic TiO_2-SiO_2 Mixed Oxides

Powder X-Ray Diffraction. X-ray diffraction (XRD) is a nondestructive analytical technique that is routinely used for the structural characterization of titania-silica materials. A typical peak near $2\theta = 25^\circ$ in the wide range XRD profile indicates the presence of TiO_2 anatase phase in the mixed oxide materials due to d_{101} crystallographic plane. In addition, peaks at 2θ near 36°, 37°, 39°, 48°, 54°, 55°, 63°, 69°, 70°, 75°, and 76° that corresponded to d-spacings of d_{103}, d_{004}, d_{112}, d_{200}, d_{105}, d_{211}, d_{204}, d_{116}, d_{220}, d_{215}, and d_{301}, respectively, are due to anatase phase of TiO_2 and peaks at $2\theta = 27^\circ$, 37°, 39°, 41°, 54°, 55°, 63°, 68°, 70°, 75°, and 76° correspond to d-spacings of d_{110}, d_{101}, d_{200}, d_{111}, d_{211}, d_{220}, d_{002}, d_{301}, d_{112}, d_{320}, and d_{202}, respectively, for the rutile phase of TiO_2. However, addition of silica prevents the formation of rutile peaks [165].

In most of these TiO_2-SiO_2 mixed oxide materials the X-ray patterns show a broad amorphous peak due to the presence of silica. However, with an increase in the calcination temperature and/or use of cosolvents, the crystallinity can be modulated as depicted in Figure 13. It can be clearly seen that the crystallinity of the peaks is improved either by the addition of aromatic cosolvents or by the increase in the calcination temperature. Furthermore, different phases of TiO_2 may be obtained by adjusting the pH of system or by changing the ethanol (solvent) to water ratio [89].

Raman Spectroscopy. Raman spectroscopy is widely used to identify the phase of titania along with XRD. The Raman study of a TiO_2-SiO_2 mixed oxide showed peaks near 638, 519, 399, 197, and 144 cm^{-1} corresponding to E_{1g}, B_{1g}, B_{1g}, E_{1g}, and E_g symmetry modes, respectively [282]. A_{1g}, B_{1g}, and E_g modes are the active modes for anatase crystals [267].

Fourier Transform-Infrared (FT-IR) Spectroscopy. FT-IR technique is utilized for analyzing the stretching and bending vibration frequencies in the mixed oxide materials. In addition, this technique provides information regarding the presence of surface hydroxyl groups. The FT-IR spectrum of the titania-silica composites shows mainly four peaks with the wavenumbers of 780, 970, 1090, and 1200 cm^{-1} as depicted in Figure 14 [85]. The peaks at the wavenumbers of 1090 and 780 cm^{-1} are assigned to the symmetric and asymmetric stretching vibration of Si-O-Si in silica, respectively. The peak in the range of 920–970 cm^{-1} is commonly attributed to Ti-O-Si vibrations [257]. However, these bands also overlap with vibration involving Si-O-H bonds. Thus, FT-IR cannot be used to infer the presence of Ti-O-Si linkages and other techniques such as XPS spectroscopy need to be performed for the quantitative calculation of Ti-O-Si linkages. The peak near 400 cm^{-1} is commonly assigned for Ti-O-Ti bending.

N_2 Physisorption. Textural properties that include surface area, pore volume, and pore diameter of the mixed oxide materials are commonly investigated using nitrogen

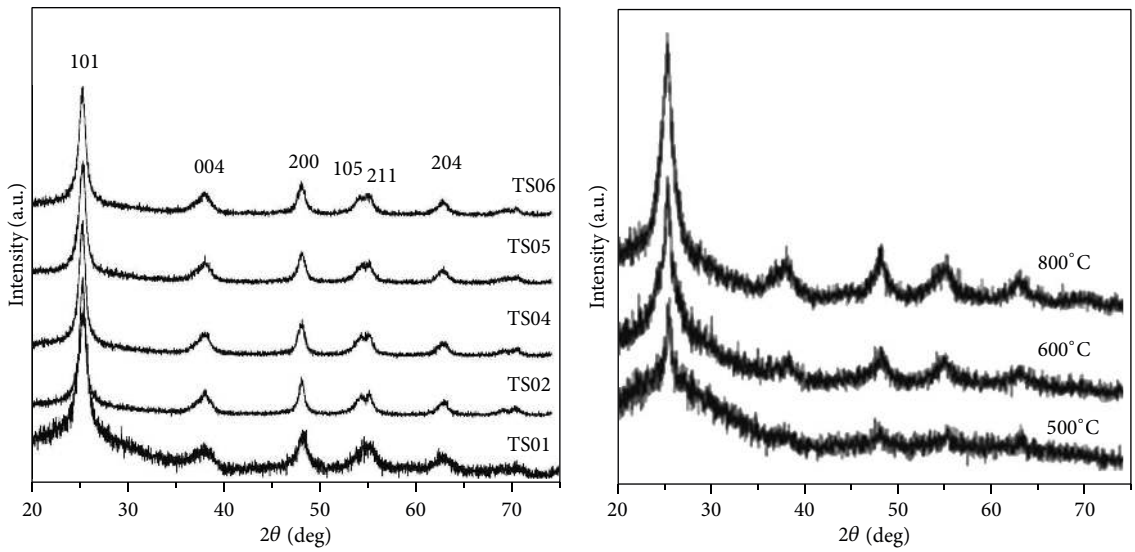

FIGURE 13: The wide-angle XRD patterns of TiO_2-SiO_2 materials: (a) prepared in the ratio of solvent: cosolvent = 1 : 1, in which the cosolvents for TS01, TS02, TS03, TS04, TS05, and TS06 are ethanol, hexane, toluene, *p*-xylene, and mesitylene, respectively, and (b) prepared under the same condition with the same catalyst composition, but calcined at 500°C, 600°C, and 800°C (reprinted with permission from [84]).

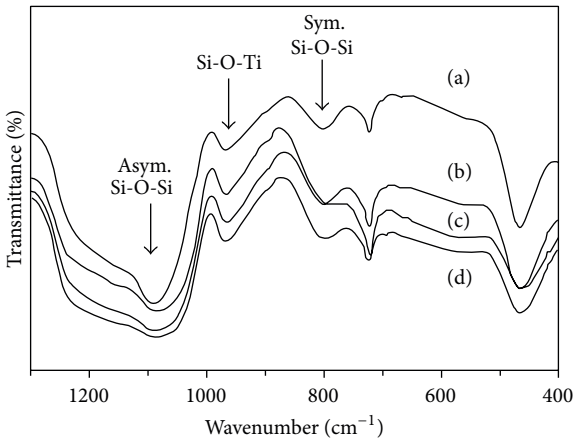

FIGURE 14: The FT-IR spectra of (a) calcined mesoporous silica, (b) titania modified silica with Ti/Si = 10, (c) Ti/Si = 2.5, and (d) Ti/Si = 5 (reprinted with permission from [85]).

physisorption studies. The typical isotherms show a slow increase with the amount of N_2 adsorbed at low relative pressure values due to monolayer adsorption. As the relative pressure value increases, multilayer adsorption occurs and this is followed by capillary condensation. The mesoporous materials show type IV isotherms as evidenced by a hysteresis loop [283].

The nitrogen physisorption patterns of a series of materials with different Ti/Si amount are illustrated in Figure 15 and are compared with the isotherms of pure titania and silica synthesized under similar conditions. The materials labelled as X-Ti-01 and X-Si-06 contain only titania or silica, respectively, and show H2 type hysteresis loops, which are usually found in materials with a cross-linked porous system. The isotherm of the titania-silica mixed oxide material with Ti/Si ratio of 1 (X-Ti-02) also shows H2 type of hysteresis with a relatively low surface area and pore volume in comparison with the rest of the mixed metal oxides.

On the other hand, the mixed oxide xerogels with higher silica contents, such as 1 : 2, 1 : 3, and 1 : 4 ratios of Ti : Si (X-TiSi-03, X-TiSi-04, and X-TiSi-05), exhibit H3 type loops that are not leveled off at relative pressure that are very close to that of saturation vapor pressure. The pore size distribution plots for the corresponding mixed oxide materials are shown in Figure 16. The pure silica material shows a broader pore size distribution than pure titania. In addition, a narrow unimodal distribution of pore sizes is observed with the mixed oxide materials that contain lower amounts of silica.

UV-Vis Diffuse Reflectance Spectroscopy (DRS). DRS has been widely employed in the characterization of aperiodic titania-silica mixed oxide materials. Bandgap estimates of the mixed oxides are derived from DRS studies. The electron transition from valence band to conduction band is mainly attributed to the absorption of the materials below the wavelength of 400 nm and it is well documented that the absorption near the band edge follows the expression of $\alpha h\vartheta = A(h\vartheta - E_g)^{n/2}$, where α, h, ϑ, A, E_g, and n are the absorption coefficient, Planck's constant, light frequency, constant, bandgap energy, and integer, respectively [284]. The bandgap values reported for TiO_2 anatase in TiO_2-SiO_2 mixed oxide materials differ due to use of different preparation methods, the presence of trace amounts of impurities or dopants in the crystalline network, or the particle size of TiO_2. The bandgap energies are commonly calculated from the plot of Kubelka-Munk function versus the energy as illustrated in Figure 17. However, some reports also determine the bandgap energies from the Tauc plot, which is the derivation of the Kubelka-Munk

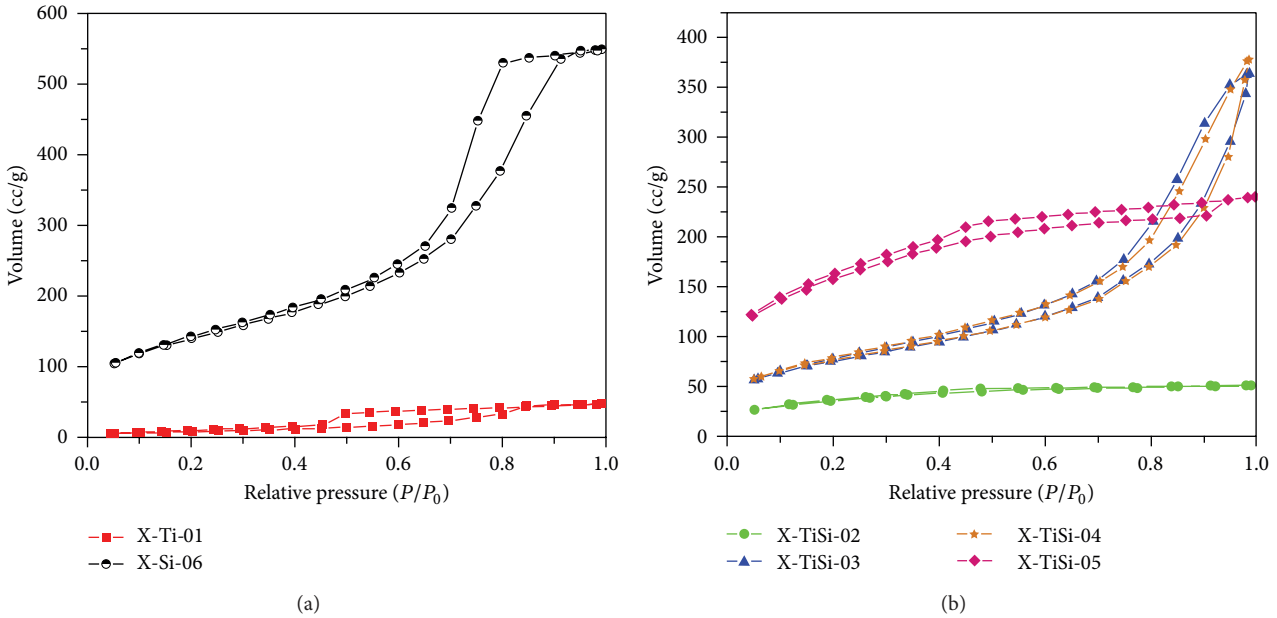

FIGURE 15: Nitrogen physisorption properties of TiO_2-SiO_2 xerogel materials: (a) pure titania (X-Ti-01) and pure silica (X-Si-06) and (b) TiO_2-SiO_2 mixed oxides with Ti/Si ratio of 1 : 1 (X-Ti-02), 1 : 2 (X-Ti-03), 1 : 3 (X-Ti-04), and 1 : 4 (X-Ti-05) prepared in ethanol-toluene solvent system (reprinted with permission from [86]).

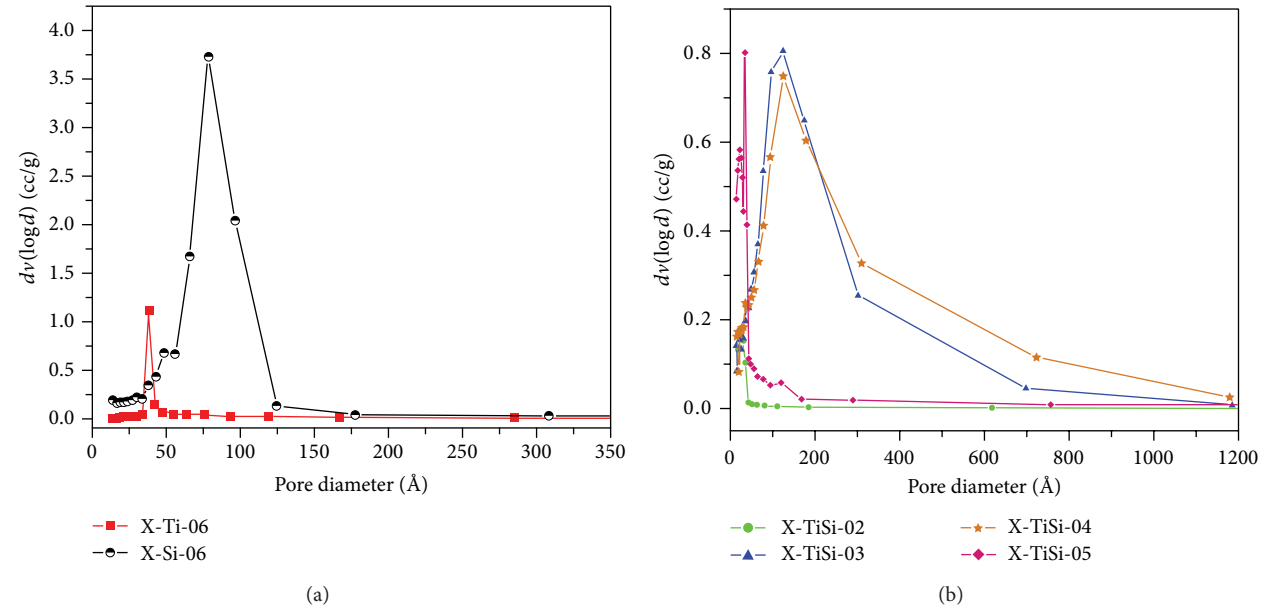

FIGURE 16: Pore size distribution of TiO_2-SiO_2 xerogel materials: (a) pure titania (X-Ti-01) and pure silica (X-Si-06) and (b) TiO_2-SiO_2 mixed oxides with Ti/Si ratio of 1 : 1 (X-Ti-02), 1 : 2 (X-Ti-03), 1 : 3 (X-Ti-04), and 1 : 4 (X-Ti-05) prepared in ethanol-toluene solvent system (reprinted with permission from [86]).

function. Aguado et al. used the Kubelka-Munk function (Figure 17) to calculate the bandgap energy of titania in their mixed oxide materials [87].

As the content of Si in the mixed oxides increases, the UV absorption edge shifts to higher energies. Furthermore, a blue shift was observed in the titania-silica mixed oxides prepared using different cosolvents and this shift was explained by changes in the crystallite size of the anatase TiO_2 [84]. In addition to the bandgap the particle size of TiO_2 can also be determined by DRS studies using the Brus equation.

Scanning Electron Microscopy (SEM). The information regarding the morphology of the materials can be obtained from SEM studies. Due to the irregular arrangements of

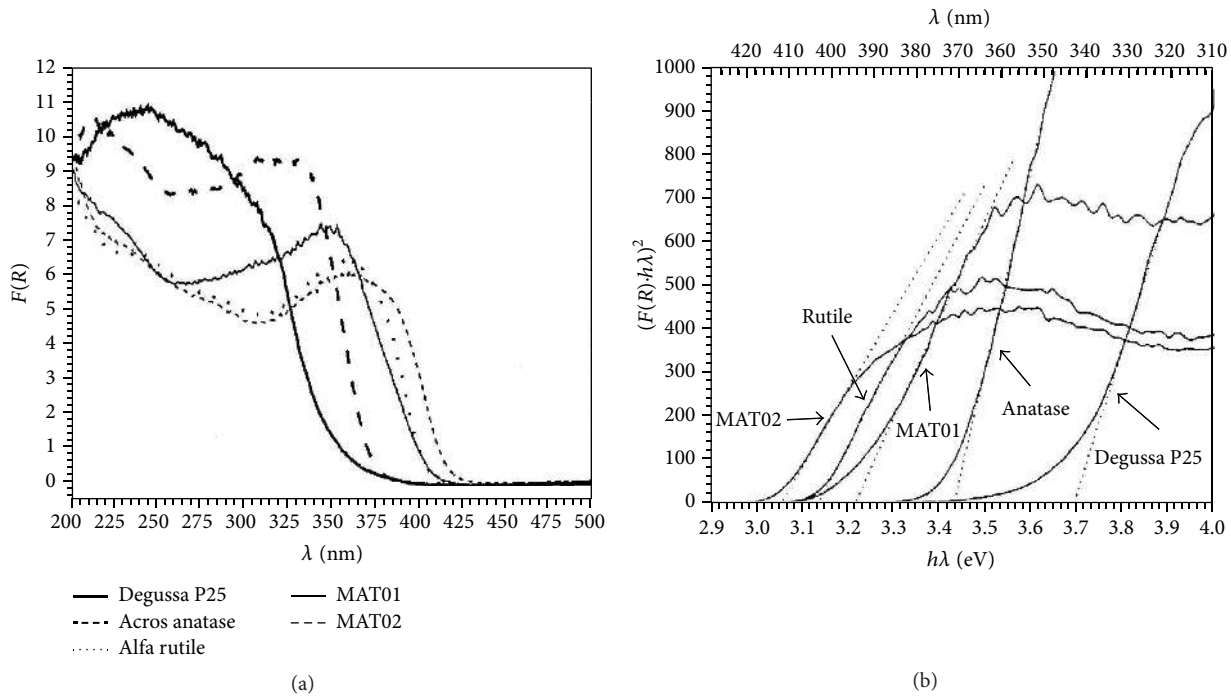

FIGURE 17: (a) UV-Vis DRS spectra of the mixed oxide materials MAT01, MAT02 along with Degussa P25, Acros anatase, and Alfa rutile materials and (b) the corresponding Kubelka-Munk function plot (reprinted with permission from [87]).

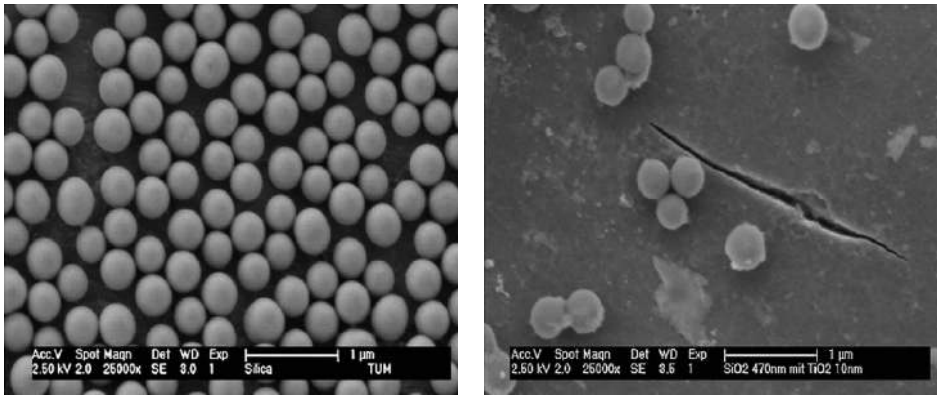

FIGURE 18: Typical scanning electron micrographs of (a) silica particles and (b) titania coated silica particles (reprinted with permission from [88]).

the pores in the aperiodic mixed oxide materials, the differences in the size and the morphologies are best obtained from SEM studies rather than TEM. Alaoui et al. and Cetinkaya et al. prepared TiO_2-SiO_2 particles with different sizes respectively [285, 286]. SEM studies indicate that TiO_2 powder is randomly distributed in the silica matrix. Wilhelm and Stephan utilized SEM technique to characterize silica spheres that were coated with titania as illustrated in Figure 18 [88].

The SEM image illustrates that the silica particles have spherical shape and smooth surface. The coating was carried out by the gradual addition of titania sol into the aqueous dispersion of silica which resulted in the attachment of small titania particles on the silica surface. The SEM image illustrates that, after coating, there is a loss in the smoothness of the silica surface.

Transmission Electron Microscopy (TEM). TEM is a powerful technique for structural characterization. The TEM image of TiO_2-SiO_2 mixed oxide materials prepared with 20 mole% silica embedded with TiO_2 is illustrated in Figure 19. The size of the silica embedded TiO_2 particle prepared in the ethanol-rich solvent was found to be 7 nm and the high resolution TEM image shows the lattice fringes of TiO_2 [89]. The high

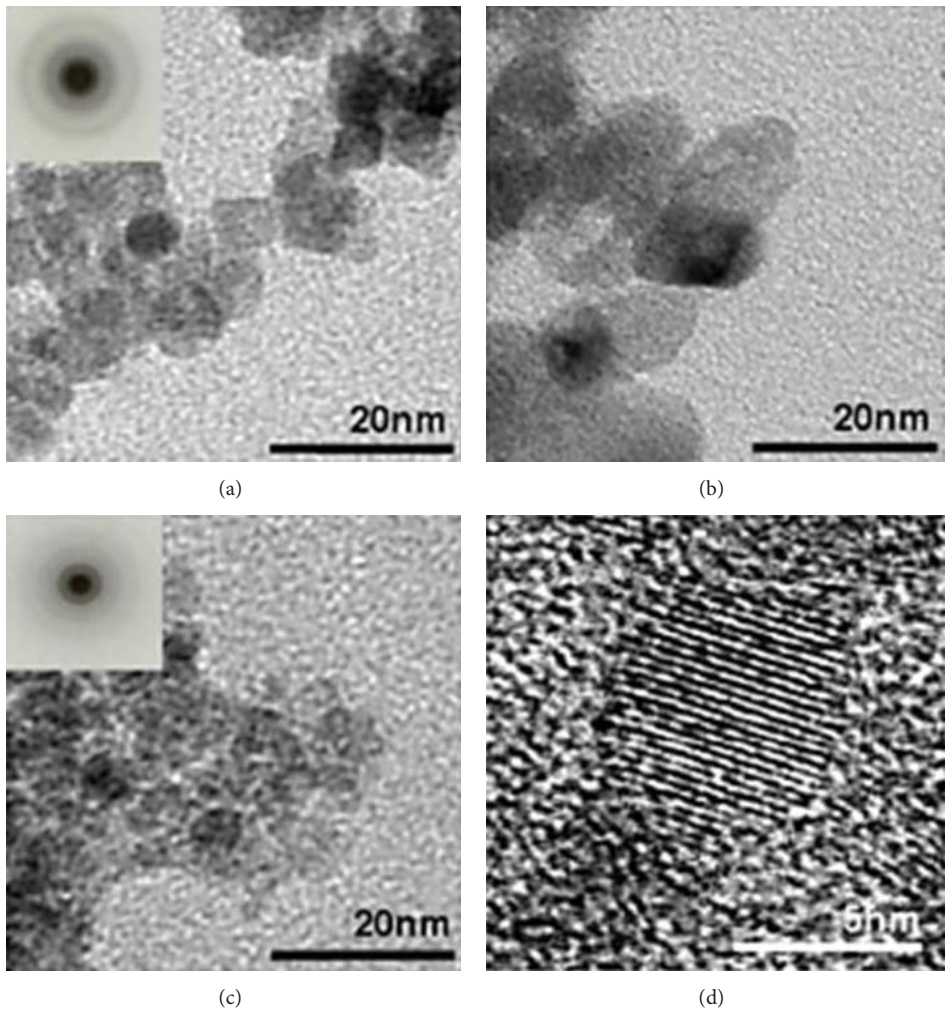

Figure 19: TEM images of TiO_2 nanoparticles prepared with different silica content and solvent composition: (a) pure TiO_2 (ethanol to water = 4 : 1), (b) pure TiO_2 (ethanol to water = 1 : 8), (c) 0.2 SiO_2-0.8 TiO_2 (ethanol to water = 4 : 1), and (d) high resolution TEM (HRTEM) image of (c) (reprinted with permission from [89]).

resolution TEM analysis offers information regarding the phase of titania via providing the *d*-spacing values from the presence of lattice fringes in the mixed oxide materials. However, it was noted that it is very challenging to obtain the TiO_2 lattice fringes in the materials with higher silica loadings.

X-Ray Photoelectron Spectroscopy (XPS). XPS studies provide information on the binding energies of the titania and silica species in the mixed oxide materials. In addition, the interaction between SiO_2 and TiO_2 species can also be understood by comparing the peak positions of Si and Ti in the TiO_2-SiO_2 mixed oxide with pure titania and silica. The XPS spectra obtained for the mixed oxides prepared with different Ti : Si ratios show a peak at the binding energy of 459.2 eV due to Ti (2p3/2), which is slightly higher than that observed in TiO_2 anatase (458.8 eV). In addition, a shift in the Ti (2p3/2) peak positions towards lower binding energies was observed, when the silica amount increases in the mixed oxide (Figure 20) [90].

In a different study, the O 1s peak was found to be shifted to the lower binding energy with an increase in the TiO_2 content (Figure 21) in a TiO_2-SiO_2 material. At higher TiO_2 contents, two O 1s bands were observed at around 530.5 and 532.5 eV indicating phase separation with titania-rich regions (Ti-O-Ti) and silica-rich regions (Si-O-Si) [91]. A further study evaluated the effect of calcination temperature to better understand the interaction between silica and titania species in the mixed oxide materials [287]. Li et al. experimentally found that the binding energies of Ti (2p1/2), Ti (2p3/2), and O 1s of titania-silica mixed oxide were shifted to higher values in the mixed oxide materials in comparison to pure TiO_2 [275]. This behavior was attributed to a decrease in the coordination number of Ti and a shortening of the Ti-O bond. The bond shortening resulted in the insertion of Ti^{4+} cations into the tetrahedral sites of the silica network to form Ti-O-Si linkages.

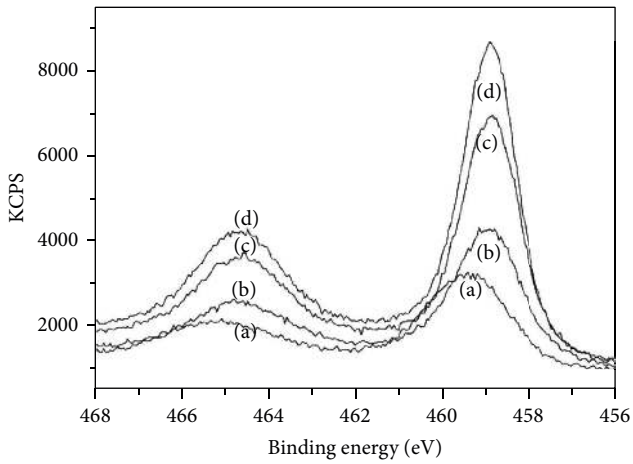

FIGURE 20: Ti (2p) peaks of TiO_2-SiO_2 mixed oxides prepared with different Ti : Si ratios: (a) Ti : Si = 1 : 10, (b) Ti : Si = 3 : 7, (c) Ti : Si = 7 : 5, and (d) Ti : Si = 7 : 3 (reprinted with permission from [90]).

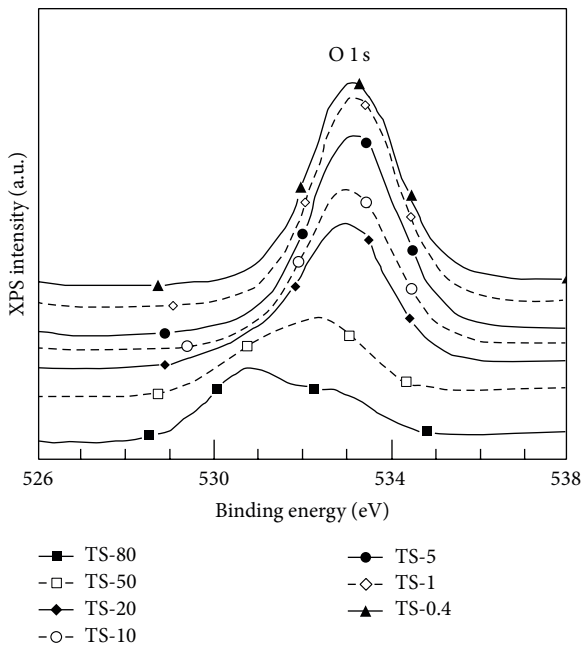

FIGURE 21: X-Ray photoelectron spectra of the O 1s level for Ti-Si binary oxides. The Ti weight % was in the range of 0.4–80 in the mixed oxide (reprinted with permission from [91]).

3.2.3. Photocatalysis. Semiconductor binary mixed oxides have emerged as promising materials for photocatalytic degradation of pollutants and photosplitting of water and, among them, TiO_2-SiO_2 has been quite well studied.

Various types of aquatic pollutants that include inorganic ions, aliphatic hydrocarbons, such as alkanes and alkenes and their substituted derivatives, benzyl compounds, dyes, phenolic compounds, and pesticides were experimented using advanced oxidation process. This section will review the various photocatalytic reactions that have utilized aperiodic TiO_2-SiO_2 materials.

Photocatalytic Degradation of Inorganics. A comparative study using titania-silica xerogels and aerogels was carried out for the photocatalytic degradation of cyanides from the wastewater by Ibrahim and coworkers [288]. A decrease in the cyanide removal efficiency from 80% to 70% was obtained with an increase in the calcination temperature from 100 to 400°C. A removal of 82% was achieved at the calcination temperature of 500°C. Further increase in the calcination temperature reduced the removal efficiency. The decrease in activity was explained by the formation of greater amounts of rutile phase. In contrast, higher removal efficiency (~98%) was attained with the aerogel materials and the efficiency has been credited to the larger surface area of aerogel materials. In addition, the supercritical drying time was not found to be a major factor in the photocatalytic performance of the aerogel materials since all the materials showed similar activity when subjected to different drying times. However, the heating time in the drying process was found to affect the photoactivity, since the crystallinity of the titania phase in the aerogel materials was found to vary.

Removal of cyanide ions using TiO_2-SiO_2 aerogel as photocatalysts has been examined in a separate study by Ismail et al. [289]. The molar ratio of Ti : Si was varied to find the optimum removal efficiency and the best degradation efficiency of 98% was achieved for the catalyst with the molar ratio of Ti : Si equivalent to 6 : 1. The higher efficiency of this material was explained by the larger specific surface area value of 850 m^2/g that allowed for effective dispersion of the photoactive titania species. Even though the cyanide removal in the wastewater has been carried out for water treatment, a survey of the literature indicates no reports for removal of other inorganic ions using TiO_2-SiO_2 aerogels.

Photocatalytic Degradation of Aliphatic Compounds. Photocatalytic reactions of alkenes and alkynes in water were investigated by Anpo et al. over titania-silica oxides photocatalysts. The photocatalytic activity in the mixed oxide system was found to be higher at low TiO_2 content due to a decrease in the radiationless energy transfer between titania and silica [290]. In a different study, the photocatalytic decomposition of dichlorodifluoromethane was carried out on various metal oxides that include CaO, zeolite, silica-alumina, and titania-silica [252]. Among these, titania-silica exhibited the best performance due to the presence of strong acid sites which enhanced the decomposition of dichlorodifluoromethane. It was found that deactivation of the catalyst occurred rapidly due to the attack of fluorine on silicon in titania-silica. In addition, a combined mixture of titania-silica and CaO reacted with fluorine more readily in comparison to silica and protected the titania-silica catalyst from corrosion by fluorine, and it was found that the lifetime of this catalyst was longer than that of the bare titania-silica. The presence of acidic sites on titania-silica mixed oxide was found to be favorable for the decomposition of 1,2-dichloroethane [291]. Titania coatings have been deposited on silica by hydrolysis of titanium alkoxide precursors and examined as photocatalysts

for the dehydration of 2-propanol [292]. Preformed silica was used as the support for titania and the nature of titania coating was controlled by the ratio of titanium alkoxide to water. 2-Propanol dehydration was used as a probe reaction. Propene formation was found to be directly correlated with the anatase surface area. However, when the titania-silica samples were heated to temperatures less than 400°C, no correlation was obtained between the surface area and propene formation. This may be due to the presence of amorphous titania.

Photocatalytic degradation of tetramethylammonium (TMA) ions in water was studied with pure TiO_2 and silica-loaded TiO_2 [293]. An improved activity was attained with the catalyst of Si/Ti atomic ratio of 18%. In addition, the calcination temperature was noted as one of the factors affecting the degradation. The increased thermal stability of TiO_2 in the mixed oxide prevents the formation of the less active rutile phase, and this may be the reason for the higher photoactivity of silica-loaded TiO_2. Loading silica onto titania created a highly negative surface and this enhanced the adsorption of cations such as TMA and, as a result, its degradation was enhanced.

Catalytic reactions that include epoxidation of olefins and selective oxidation of saturated hydrocarbons have been carried out by utilizing amorphous microporous titania-silica mixed oxide materials by Klein and coworkers [266]. The materials show catalytic activity for selective oxidation reactions and also for selective epoxidation of olefins due to their distinct microporosity. A decrease in epoxidation activity was observed with an increase of TiO_2 in the materials. However, the hydrophilicity of these amorphous binary oxides was found to be different in comparison to their zeolitic analogues. This was proven by adsorption experiments of water and octane.

Photocatalytic Degradation of Benzyl Compounds. Photocatalytic decomposition of 1,4-dichlorobenzene was monitored using TiO_2/SiO_2 nanoparticles [89, 250]. The rate constant for the degradation reaction was found to be higher for TiO_2/SiO_2 than that of Degussa P25. However, it was found that 20 mol% of silica was the optimum loading. Various adsorbent supports were evaluated for the mineralization of 3,5-dichloro-N-(3-methyl-1-butyn-3-yl)benzamide (propyzamide) in aqueous solution [294]. Zeolite, silica, and activated carbon were used as adsorbent supports for dispersing TiO_2. It was found that the TiO_2/SiO_2 system showed better adsorptive properties and increased the mineralization of propyzamide in comparison with bare TiO_2.

Decomposition of benzyl trimethyl ammonium chloride (BTMA) and propionic acid was carried out over SiO_2 loaded TiO_2 under UV irradiation. Propionic acid showed lower degradation rate due to the presence of more negative charge on the surface of TiO_2-SiO_2 at pH 6 [295]. The influence of pH on the surface charge of silica-loaded TiO_2 materials was studied by Vohra and Tanaka for the photocatalytic activity of cationic, neutral, and anionic pollutants [296]. An enhanced photocatalytic activity was achieved with the cationic pollutants due to the presence of silica that increased the surface area and introduced $Si–O^-$ groups, which facilitated the adsorption of the cationic pollutant species on the surface of the catalyst. However, due to the occlusion of the active sites, the efficiency of the supported catalysts was found to decrease with an increase in the substrate concentration. Furthermore, it was interesting to note that anionic and nonionic compounds such as acetate and phenol remained unaffected during the degradation process.

Photocatalytic Degradation of Phenols. Phenols and phenolic compounds are released into the aquatic environment along with several industrial wastes and have gained attention from researchers for their removal from water bodies. Photocatalytic degradation of phenol over silica supported titania catalysts was carried out by Alemany et al. and the intermediates and products formed during the process were also identified in their study [297]. Hydroquinone and maleic acid were found to be the two major intermediates that were later oxidized to acetic acid and formic acid on prolonged irradiation. A high selectivity to the partial oxidation products was observed for the catalysts containing 0.5 and 1.0 monolayers of titania which were formed by the homogeneous precipitation of titania on the silica support. CO_2 was found to be the dominant final product for all the catalysts. The study also focused on finding the optimal titanium content, and it was found that there should be an optimal particle size for the effective photodegradation of phenol. Higher loadings greater than 30% of titania on the silica materials limit the photoefficiency due to the presence of larger sized titania particles.

The utilization of TiO_2-SiO_2 aerogels for the photocatalytic degradation of phenol pollutant was investigated by Deng and coworkers and it was noticed that the aerogels contained anatase microcrystallites after supercritical drying in ethanol [263]. These binary aerogel materials showed more superior activity than the commercial TiO_2 and the pure TiO_2 aerogels. The aerogel with 1 : 1 molar ratio of TiO_2 and SiO_2 showed optimum photocatalytic performance. The photocatalytic activity of the aerogels increased with the SiO_2 content at first and came to a maximum at molar ratio = 1 : 1.

Malinowska and coworkers chose three different phenol *para*-derivatives, such as *p*-chlorophenol, *p*-nitrophenol, and 4-hydroxybenzoic acid, as model compounds for the photodegradation processes over TiO_2-SiO_2 aerogel materials synthesized by a sol-gel technique [298]. Even though the aerogels prepared in their studies showed reasonable photocatalytic activity, it was comparatively less than that of TiO_2 aerogels. This was explained by the segregation of titania and silica phases and their poor contact that hindered the photocatalytic activity. The photocatalytic degradation of phenol over a series of TiO_2-SiO_2 mixed oxide materials prepared by sol-gel hydrothermal treatment has been reported recently [299]. The higher photocatalytic activities of the binary mixed oxide materials prepared using nonpolar solvents were attributed to a combination of factors such as higher apparent surface coverage of Ti-O-Si heterolinkages, larger pore sizes, and higher crystallinities of the titania phase. In particular, high crystallinity of the titania phase seemed to be critical for the complete mineralization of phenol in this study. Larger pore sizes permitted better transport of phenol and photodegradation products that were

formed during the mineralization to and from the active sites and higher crystallinity of TiO_2 enhanced the degradation efficiency by minimizing the electron-hole recombination in these photocatalysts.

Photocatalytic Degradation of Dyes. The runoffs from several industries such as textile, leather, and paper are a major contributor to this type of pollutants in the water body. In particular, removal of dyes from several colored effluents involves processes that produce compounds that are very toxic to the environment [285]. Thus, it is necessary to remove these colored pollutants from the environment. Anderson and Bard have studied the effect of incorporation of SiO_2 on TiO_2 photocatalyst prepared by a sol-gel technique [14]. It has been well documented that the efficiency of TiO_2 can be improved by preventing the recombination of the photogenerated electrons (e^-) and holes (h^+) pairs by the addition of charge-transfer catalysts on the TiO_2 surface. Alternately, one can increase the photocatalytic activity by incorporation of effective adsorption sites on the photocatalyst surface. The second approach has been espoused in their studies in the preparation of TiO_2/SiO_2 composites with different ratios of Ti/Si.

The application of photocatalysts with different Ti/Si ratios for the photodecomposition of R6G has been investigated and it has been noted that a Ti/Si ratio of 30/70 produces a catalyst about three times more active than commercially available Degussa P25 due to the enhanced adsorption of the dye. However, it has been noticed that the presence of larger amounts of SiO_2 decreases the activity. In a following study, Anderson and Bard have utilized two different binary mixed oxides TiO_2/SiO_2 and TiO_2/Al_2O_3 for the photodecomposition of salicylic acid and phenol [92]. It was observed that the TiO_2/Al_2O_3 system gave improved activity for the decomposition of salicylic acid relative to bare TiO_2. Moreover, TiO_2/SiO_2 materials show higher activity than TiO_2/Al_2O_3 and TiO_2 towards the photocatalytic decomposition of phenol. The schematic diagram in Figure 22 illustrates the photocatalysis mechanism of the two mixed oxide catalysts TiO_2/Al_2O_3 and TiO_2/SiO_2 that have been utilized in their study.

It was noticed by Cheng and coworkers that the addition of silica in the titania-silica mixed oxides increases the photoactivity by suppressing the phase transformation of titania from anatase to rutile, and this has been also reported by several other researchers [165, 300, 301]. Also, the addition of silica facilitates the formation of oxygen vacancies in titania [165]. Yang and coworkers investigated the effect of addition of silica to titania, on the crystalline growth and the transformation of anatase to rutile phase [300]. It has been observed that the suppression in the crystallite size enhanced the surface area and resulted in a blue shift in the onset of absorption edge in the mixed oxide materials compared to pure titania. The photocatalytic activity of these silica-modified materials was evaluated by decolorization of MO solutions under UV-visible light irradiation and it was found that the silica content, calcination temperature, H_2SO_4, and presence of oxidants such as KIO_4, $(NH_4)_2S_2O_8$, and H_2O_2 greatly influenced the decolorizing process.

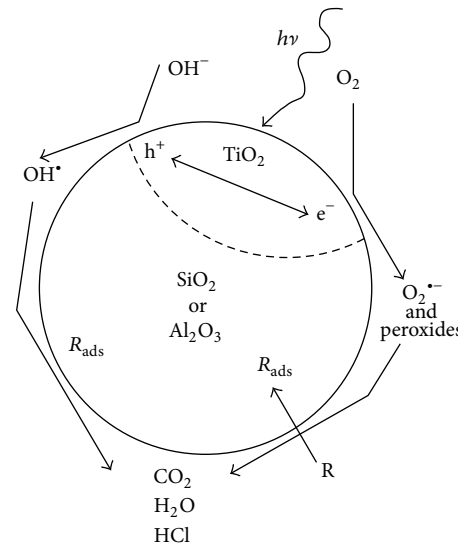

Figure 22: Schematic representation of the TiO_2/SiO_2 and TiO_2/Al_2O_3 photocatalysts with no interaction between the TiO_2 and SiO_2 or Al_2O_3 phases (reprinted with permission from [92]).

Photodegradation of two different dyes, reactive 15 (R15) and cationic blue X-GRL (CBX), was carried out over different surface bond conjugated TiO_2/SiO_2 materials prepared by impregnation method [302]. The material with 30 wt.% of TiO_2/SiO_2 shows higher activity due to the smaller particle size of TiO_2 on the sample. It was found that silica gel plays a key role in dispersion of TiO_2. In another study, photocatalysts were prepared by surface functionalization with thiol, cyano, and thiocyano groups on silica and silica-titania catalysts and these were investigated for the photocatalytic degradation of MB [81]. The adsorption of MB on these catalysts is significantly altered due to the surface modification and varies with the type of functional group bound to the surface. In addition, all these functional groups are very stable to UV and the surface bond TiO_2/SiO_2 materials provide good photocatalytic activity for the decomposition of MB.

The photocatalytic degradation of a RhB with TiO_2 [303] and TiO_2/SiO_2 in aqueous dispersion was investigated by several researchers under visible and UV irradiation [303–305]. Rasalingam et al. studied the deethylation of RhB dye molecule in the presence of both TiO_2 and TiO_2/SiO_2 under visible and UV irradiation. The detailed mechanism for the deethylation process of RhB was investigated by high performance liquid chromatograph (HPLC) and liquid chromatograph-mass spectrometry (LC-MS) techniques. It was reported that RhB adsorbs on the surface of TiO_2/SiO_2 particles by the positively charged diethylamino group, whereas adsorption was achieved through the negatively charged carboxyl group on TiO_2 at pH of 4.3. Similar adsorption behavior of RhB dye molecule over TiO_2-SiO_2 mixed oxide materials prepared under ambient conditions was recently studied by our group and it was concluded that, apart from the surface charge of the mixed oxide materials, the pore volume of the material also plays a key role in the adsorption of the dye molecule over the catalytic surface [86].

In addition, our group has investigated the influence of Ti-O-Si heterolinkages on the TiO_2-SiO_2 xerogel materials for the degradation of RhB dye [305]. The active heterolinkages (Ti-O-Si) were credited for the higher rate of degradation. The effect of cosolvent in increasing the surface area of these photocatalysts was reported by Budhi et al. [268]. Titania coated silica spheres prepared by heterocoagulation method were utilized as catalyst in the photodegradation of RhB dye in aqueous solution [88]. The experiments showed complete degradation of RhB without any photobleaching.

In another recent study, a series of aperiodic titania-silica photocatalysts was prepared in ethanolic solutions of polar aprotic cosolvents such as ethyl acetate (EtOAc), acetonitrile (ACN), acetone (ACT), and N,N-dimethylformamide (DMF) using sol-gel procedure by our group [304]. The use of polar aprotic solvents was found to be a feasible approach to modify the textural properties of the materials, such as surface areas and pore sizes, without the need to use expensive templates. Dark adsorption and degradation of RhB dye molecules on these titania-silica materials revealed that the pore volume of the mixed oxide mainly influenced the adsorption, while pore diameters enhanced the initial degradation rate. The larger pores permit the organics to diffuse in and out of the mesostructure to enhance their effective photocatalytic degradation under visible light irradiation.

Degradation of acid orange 7 (AO7) using TiO_2/SiO_2 composites, which were prepared by coating the SiO_2 surface with nano-TiO_2 by hydrolysis of $TiCl_4$, was examined by Cetinkaya and coworkers [286]. An improved adsorption of AO7 was attained with nano-TiO_2 on the surface of SiO_2 under UV light. Furthermore, the effect of calcination temperature on the photocatalytic degradation was also examined. A degradation efficiency of 40% was achieved with the sample calcined at 600°C. The high activity of this material was explained by the presence of a mixture of rutile and anatase phase in the structure that minimized electron-hole recombination.

Photocatalytic Degradation of Pesticides. Photocatalytic degradation of organophosphorous pesticides that include dichlorvos, monocrotophos, parathion, and phorate was investigated by using floating TiO_2/SiO_2 photocatalyst beads prepared by dip coating method [306]. Complete degradation was attained after 420 min. of sunlight irradiation. They have found that the addition of small amount of electron scavenger, Cu^{2+}, escalates the photodegradation efficiency of organophosphorus pesticides via reduced electron-hole recombination and increased formation of hydroxyl radicals. The formation of these hydroxyl radicals on the TiO_2 surface is favored in acidic and alkaline solutions. Furthermore, an effective conversion of phosphate ester into trimethyl phosphate ester, formic acid, and acetic acid was achieved in the presence of acids and bases. The trimethyl phosphate ester is then photocatalytically degraded into PO_4^{3-} and formic acid. Even though Cu^{2+} increases the degradation efficiency, higher concentrations of Cu^{2+} lead to the formation of $[Cu(H_2O)_4]^{2+}$ complex ions that absorb UV light and reduce the photoefficiency. Phanikrishna Sharma and coworkers utilized titania-silica composite materials prepared using a styrene-acrylic acid emulsion as a latex polymer template, for the degradation of isoproturon (*N*,*N*-dimethyl-*N*-[4-(1-methylethyl)phenyl]), identified as a hazardous class III herbicide. Effective degradation was obtained at an optimal loading of 5 wt.% TiO_2 under solar light. Furthermore, a similar approach was successfully used for the degradation of commercially available pesticides such as imidacloprid and phosphadium [307, 308]. In a recent study, remediation of dimethyl phthalate, which is used in pesticides, plastics, safety glasses, rubber coating agents, and insect repellants, using hollow glass microsphere (HGM) coated with photocatalytic TiO_2 has been carried out by Jiang and coworkers [309]. In their study, they have optimized the condition for the formation of hydroxyl radicals by using terephthalic acid as hydroxyl radical trapper. Three different variables, such as the loading of HGM-TiO_2, concentration of terephthalic acid, and irradiation time, were investigated on the photocatalysis. It is worth mentioning here that the HGM-TiO_2 catalyst is available in market for the removal of aqueous pollutants as well as gaseous pollutants.

4. Factors Influencing Photocatalytic Degradation Using TiO_2-SiO_2 Mixed Oxides

It is noted that the photocatalytic activity of TiO_2-SiO_2 mixed oxides is closely related to their structural properties, such as crystallinity and crystallite size of titania, crystal composition, surface area, particle size distribution, porosity, bandgap, surface hydroxyl density, dispersion of TiO_2, and Ti-O-Si linkages. The use of a high surface area silica support provides good dispersion of titania. Also, the silica support increases the hydrophobic nature of the mixed oxide. This helps to adsorb a wide variety of organic pollutants and concentrate them close to the reactive TiO_2 centre [272]. The crystallite or particle size of titania plays a key role in degradation. Silica support confines the TiO_2 particles in the nanosize range due to quantum size effect, and the smaller titania particles in general show enhanced photocatalytic activity. This is explained by a decrease in the rate of volume charge carrier recombination of the electron-hole pairs in smaller sized titania particles. The photocatalytic activity is maximum at an optimal particle size at which the volume and surface charge carrier recombination of the electron-hole pairs is minimized. However, at very small particle sizes, surface charge carrier recombination is enhanced, and, thus, the resulting photocatalytic activity will decrease. In addition to the particle size, the photocatalytic activity also depends on the amount of titania. The photocatalytic activity is usually maximum at an optimal loading of titania. At higher loadings of titania, larger aggregates of titania are formed that occlude the pores and limit the diffusion of the reactant molecules, and, thus, the photocatalytic activity is lowered. Also, the crystallinity and the nature (phase) of titania are important factors that profoundly affect the photocatalytic activity. Mixed oxide materials that contain highly crystalline titania show enhanced activities. This is because amorphous materials in general contain larger number of defects that enhance electron-hole recombination. In the mixed oxide

material, the silica support prevents the phase transformation of the more active anatase phase to rutile on calcination. In addition to these factors, the chemical property of the TiO_2-SiO_2 binary oxide materials is modulated by the addition of SiO_2 into the TiO_2 network, and the formation of Ti-O-Si heterolinkages has been implicated to play an important role in the photocatalytic activity.

The porous properties such as pore volume and pore size of the mixed oxide materials influence the adsorption of the pollutant. In particular, larger pore sized materials provide better transport (molecular trafficking) of the pollutants and the product(s), in and out from the active sites, and contribute to enhanced degradation. It is generally observed that the rate of degradation increases with an increase in the pollutant concentration to a certain level. However, further increase in the pollutant concentration results in a decrease in the degradation rate. Among the various ROS, $^{\bullet}OH$ radical is an important species in the degradation processes and the rate of degradation depends on both the probability of the formation of $^{\bullet}OH$ radicals on the catalyst surface and the reactivity of $^{\bullet}OH$ radicals with the pollutants. Thus, the enhancement in activity will rely on the probability of the reaction between the pollutant and these oxidizing species. However, the degradation efficiency decreases beyond a particular level of pollutant concentration. This is due to the inhibition of $^{\bullet}OH$ radical generation via the coverage of active sites on the catalysts by the pollutant molecules/ions. In addition, another reason that was reported for the low activity particularly for dye pollutants was the UV-screening effect by the dyes. At high dye concentrations, a significant amount of UV light may be absorbed by the dye molecules rather than by the semiconductor particles and this reduces the efficiency of the catalytic reaction by reducing the generation of $^{\bullet}OH$ radical and superoxide radical ($O_2^{\bullet-}$).

The characteristic features of the pollutant in the wastewater differ with the variation in the solution pH [310]. The pH of the medium may lead to changes in solubility, stability, hydrophobicity, and also the color of the substance (applicable to dyes). In addition, the pH of the medium can also change the surface charge of the photocatalysts and degree of ionization of the organics. An organic compound remains in the neutral state at pH below its pKa value and is negatively charged when the pH exceeds the pKa value. Furthermore, electrostatic interactions between the semiconductor surface, solvent molecules, pollutant substrate, and the ROS formed during photocatalytic oxidation vary with solution pH. Thus, these variations in the pH play a vital role in the photocatalytic degradation efficiency.

A comparative table is provided in the supplementary section (in the Supplementary Material available online at http://dx.doi.org/10.1155/2014/617405) to indicate the various classes of compounds that have been examined for removal for contaminants.

5. Conclusions

This review has attempted to cover a wide range of wastewater effluent removal techniques for water treatment. The reader can get an idea about the various types of removal methods and the basic principles behind each technique. Heterogeneous photocatalytic oxidation (HPO) has garnered extensive attention due to its effective removal of toxic compounds from waste effluents. The HPO process employs several oxide and mixed oxide catalysts, mainly for water purification. Among these materials, TiO_2-SiO_2 mixed oxides have been found to be more active than the other mixed oxides for the degradation of organics. In this work, we have covered the degradation of organics by utilizing TiO_2-SiO_2 binary mixed oxide materials and the factors that influence the degradation have been discussed. Furthermore, this review briefly explains the synthetic procedures and the main characterization techniques of the two main types of TiO_2-SiO_2 binary mixed oxides, periodic and aperiodic oxides. Even though these binary mixed oxides show better activity than pure TiO_2 materials in most instances, the utilization of these TiO_2-SiO_2 mixed oxides is limited for the mineralization of selected pollutants.

Conflict of Interests

The authors declare no conflict of interests.

Acknowledgments

Thanks are due to the National Science Foundation Grants NSF-CHE-0722632 and NSF-EPS-0903804 and the Department of Energy Grant DE-EE0000270.

References

[1] L. G. da Silva, R. Ruggiero, P. D. M. Gontijo et al., "Adsorption of Brilliant Red 2BE dye from water solutions by a chemically modified sugarcane bagasse lignin," *Chemical Engineering Journal*, vol. 168, no. 2, pp. 620–628, 2011.

[2] A. Dąbrowski, P. Podkościelny, Z. Hubicki, and M. Barczak, "Adsorption of phenolic compounds by activated carbon: a critical review," *Chemosphere*, vol. 58, no. 8, pp. 1049–1070, 2005.

[3] Y. Fu and T. Viraraghavan, "Fungal decolorization of dye wastewaters: a review," *Bioresource Technology*, vol. 79, no. 3, pp. 251–262, 2001.

[4] A. K. Biń and S. Sobera-Madej, "Comparison of the advanced oxidation processes (UV, UV/H_2O_2 and O_3) for the removal of antibiotic substances during wastewater treatment," *Ozone: Science and Engineering*, vol. 34, no. 2, pp. 136–139, 2012.

[5] A. Srinivasan and T. Viraraghavan, "Decolorization of dye wastewaters by biosorbents: a review," *Journal of Environmental Management*, vol. 91, no. 10, pp. 1915–1929, 2010.

[6] M. Govindaraj, R. Rathinam, C. Sukumar, M. Uthayasankar, and S. Pattabhi, "Electrochemical oxidation of bisphenol-A from aqueous solution using graphite electrodes," *Environmental Technology*, vol. 34, no. 4, pp. 503–511, 2013.

[7] K. Pirkanniemi and M. Sillanpää, "Heterogeneous water phase catalysis as an environmental application: a review," *Chemosphere*, vol. 48, no. 10, pp. 1047–1060, 2002.

[8] P. V. Suraja, Z. Yaakob, N. N. Binitha, M. R. Resmi, and P. P. Silija, "Photocatalytic degradation of dye pollutant over Ti and Co doped SBA-15: comparison of activities under visible light," *Chemical Engineering Journal*, vol. 176-177, pp. 265–271, 2011.

[9] R. Andreozzi, V. Caprio, A. Insola, and R. Marotta, "Advanced oxidation processes (AOP) for water purification and recovery," *Catalysis Today*, vol. 53, no. 1, pp. 51–59, 1999.

[10] B. Ning, N. Graham, Y. Zhang, M. Nakonechny, and M. G. El-Din, "Degradation of endocrine disrupting chemicals by ozone/AOPs," *Ozone: Science and Engineering*, vol. 29, no. 3, pp. 153–176, 2007.

[11] R. Thapa, S. Maiti, T. H. Rana, U. N. Maiti, and K. K. Chattopadhyay, "Anatase TiO_2 nanoparticles synthesis via simple hydrothermal route: dgradation of orange II, methyl orange and rhodamine B," *Journal of Molecular Catalysis A: Chemical*, vol. 363, pp. 223–229, 2012.

[12] Z. Guo, R. Ma, and G. Li, "Degradation of phenol by nanomaterial TiO_2 in wastewater," *Chemical Engineering Journal*, vol. 119, no. 1, pp. 55–59, 2006.

[13] J. Yang, C. Chen, H. Ji, W. Ma, and J. Zhao, "Mechanism of TiO_2-assisted photocatalytic degradation of dyes under visible irradiation: photoelectrocatalytic study by TiO_2-film electrodes," *Journal of Physical Chemistry B*, vol. 109, no. 46, pp. 21900–21907, 2005.

[14] C. Anderson and A. J. Bard, "An improved photocatalyst of TiO_2/SiO_2 prepared by a sol-gel synthesis," *Journal of Physical Chemistry*, vol. 99, no. 24, pp. 9882–9885, 1995.

[15] A. S. Malik, D. Letson, and S. R. Crutchfield, "Point nonpoint-source trading of pollution-abatement: choosing the right trading ratio," *The American Journal of Agricultural Economics*, vol. 75, no. 4, pp. 959–967, 1993.

[16] Y. Yuhong, Y. Baixing, and S. Wanbin, "Assessment of point and nonpoint sources pollution in Songhua River Basin, Northeast China by using revised water quality model," *Chinese Geographical Science*, vol. 20, no. 1, pp. 30–36, 2010.

[17] S. R. Carpenter, N. F. Caraco, D. L. Correll, R. W. Howarth, A. N. Sharpley, and V. H. Smith, "Nonpoint pollution of surface waters with phosphorus and nitrogen," *Ecological Applications*, vol. 8, no. 3, pp. 559–568, 1998.

[18] C.-G. Tang and C.-Q. Liu, "Nonpoint source pollution assessment of wujiang river watershed in Guizhou Province, SW China," *Environmental Modeling and Assessment*, vol. 13, no. 1, pp. 155–167, 2008.

[19] N. Štambuk-Giljanoviç, "The pollution load by nitrogen and phosphorus in the Jadro River," *Environmental Monitoring and Assessment*, vol. 123, no. 1–3, pp. 13–30, 2006.

[20] W. Ouyang, H. B. Huang, F. H. Hao, Y. S. Shan, and B. B. Guo, "Evaluating spatial interaction of soil property with non-point source pollution at watershed scale: the phosphorus indicator in Northeast China," *Science of the Total Environment*, vol. 432, pp. 412–421, 2012.

[21] V. Kertész, G. Bakonyi, and B. Farkas, "Water pollution by Cu and Pb can adversely affect mallard embryonic development," *Ecotoxicology and Environmental Safety*, vol. 65, no. 1, pp. 67–73, 2006.

[22] I. Razo, L. Carrizales, J. Castro, F. Díaz-Barriga, and M. Monroy, "Arsenic and heavy metal pollution of soil, water and sediments in a semi-arid climate mining area in Mexico," *Water, Air, and Soil Pollution*, vol. 152, no. 1–4, pp. 129–152, 2004.

[23] J. Cheng, T. Yuan, W. Wang et al., "Mercury pollution in two typical areas in Guizhou province, China and its neurotoxic effects in the brains of rats fed with local polluted rice," *Environmental Geochemistry and Health*, vol. 28, no. 6, pp. 499–507, 2006.

[24] R. Mu, Z. Xu, L. Li, Y. Shao, H. Wan, and S. Zheng, "On the photocatalytic properties of elongated TiO_2 nanoparticles for phenol degradation and Cr(VI) reduction," *Journal of Hazardous Materials*, vol. 176, no. 1–3, pp. 495–502, 2010.

[25] B. Haidari, A. R. Bakhtiari, V. Yavari, A. Kazemi, and G. Shirneshan, "Biomonitoring of Ni and V contamination using oysters (*Saccostrea cucullata*) at Lengeh Port, Persian Gulf, Iran," *Clean: Soil, Air, Water*, vol. 41, no. 2, pp. 166–173, 2013.

[26] S. T. Ingvertsen, H. Marcussen, and P. E. Holm, "Pollution and potential mobility of Cd, Ni and Pb in the sediments of a wastewater-receiving river in Hanoi, Vietnam," *Environmental Monitoring and Assessment*, vol. 185, no. 11, pp. 9531–9548, 2013.

[27] M. Zeiner, T. Rezic, B. Santek, I. Rezic, S. Hann, and G. Stingeder, "Removal of Cr, Mn, and Co from textile wastewater by horizontal rotating tubular bioreactor," *Environmental Science and Technology*, vol. 46, no. 19, pp. 10690–10696, 2012.

[28] Š. Mechora, P. Cuderman, V. Stibilj, and M. Germ, "Distribution of Se and its species in Myriophyllum spicatum and Ceratophyllum demersum growing in water containing se (VI)," *Chemosphere*, vol. 84, no. 11, pp. 1636–1641, 2011.

[29] D. Purushotham, M. Rashid, M. A. Lone et al., "Environmental impact assessment of air and heavy metal concentration in groundwater of Maheshwaram watershed, Ranga Reddy district, Andhra Pradesh," *Journal of the Geological Society of India*, vol. 81, no. 3, pp. 385–396, 2013.

[30] R. Lohmann, K. Breivik, J. Dachs, and D. Muir, "Global fate of POPs: current and future research directions," *Environmental Pollution*, vol. 150, no. 1, pp. 150–165, 2007.

[31] K. Breivik, R. Alcock, Y.-F. Li, R. E. Bailey, H. Fiedler, and J. M. Pacyna, "Primary sources of selected POPs: regional and global scale emission inventories," *Environmental Pollution*, vol. 128, no. 1-2, pp. 3–16, 2004.

[32] M. S. El-Shahawi, A. Hamza, A. S. Bashammakh, and W. T. Al-Saggaf, "An overview on the accumulation, distribution, transformations, toxicity and analytical methods for the monitoring of persistent organic pollutants," *Talanta*, vol. 80, no. 5, pp. 1587–1597, 2010.

[33] H. W. Vallack, D. J. Bakker, I. Brandt et al., "Controlling persistent organic pollutants-what next?" *Environmental Toxicology and Pharmacology*, vol. 6, no. 3, pp. 143–175, 1998.

[34] K. C. Jones and P. De Voogt, "Persistent organic pollutants (POPs): state of the science," *Environmental Pollution*, vol. 100, no. 1–3, pp. 209–221, 1998.

[35] L. H. Keith and W. A. Telliard, "Priority pollutants. I. A perspective view," *Environmental Science and Technology*, vol. 13, no. 4, pp. 416–423, 1979.

[36] C. A. Basar, A. Karagunduz, A. Cakici, and B. Keskinler, "Removal of surfactants by powdered activated carbon and microfiltration," *Water Research*, vol. 38, no. 8, pp. 2117–2124, 2004.

[37] K. Hunger, *Industrial Dyes: Chemistry, Properties, Applications*, Wiley VCH, Weinheim, Germany, 2003.

[38] J. Michałowicz and W. Duda, "Phenols: sources and toxicity," *Polish Journal of Environmental Studies*, vol. 16, no. 3, pp. 347–362, 2007.

[39] M. Hayashi, Y. Nakamura, K. Higashi, H. Kato, F. Kishida, and H. Kaneko, "A quantitative structure-activity relationship study of the skin irritation potential of phenols," *Toxicology in Vitro*, vol. 13, no. 6, pp. 915–922, 1999.

[40] A. Dominguez-Ramos and A. Irabien, "Analysis and modeling of the continuous electro-oxidation process for organic matter removal in urban wastewater treatment," *Industrial and Engineering Chemistry Research*, vol. 52, no. 22, pp. 7534–7540, 2013.

[41] Y. M. Slokar and A. Majcen Le Marechal, "Methods of decoloration of textile wastewaters," *Dyes and Pigments*, vol. 37, no. 4, pp. 335–356, 1998.

[42] G. Odukkathil and N. Vasudevan, "Toxicity and bioremediation of pesticides in agricultural soil," *Reviews in Environmental Science and Bio/Technology*, vol. 12, no. 4, pp. 421–444, 2013.

[43] J. M. Prodanovic and V. M. Vasic, "Application of membrane processes for distillery wastewater purification: a review," *Desalination and Water Treatment*, vol. 51, no. 16–18, pp. 3325–3334, 2013.

[44] S. Papić, N. Koprivanac, A. Lončarić Božić, and A. Meteš, "Removal of some reactive dyes from synthetic wastewater by combined Al(III) coagulation/carbon adsorption process," *Dyes and Pigments*, vol. 62, no. 3, pp. 291–298, 2004.

[45] J.-W. Lee, S.-P. Choi, R. Thiruvenkatachari, W.-G. Shim, and H. Moon, "Evaluation of the performance of adsorption and coagulation processes for the maximum removal of reactive dyes," *Dyes and Pigments*, vol. 69, no. 3, pp. 196–203, 2006.

[46] I. Ilisz, A. Dombi, K. Mogyorósi, A. Farkas, and I. Dékány, "Removal of 2-chlorophenol from water by adsorption combined with TiO_2 photocatalysis," *Applied Catalysis B: Environmental*, vol. 39, no. 3, pp. 247–256, 2002.

[47] P. V. Messina and P. C. Schulz, "Adsorption of reactive dyes on titania-silica mesoporous materials," *Journal of Colloid and Interface Science*, vol. 299, no. 1, pp. 305–320, 2006.

[48] R. Jain, M. Mathur, S. Sikarwar, and A. Mittal, "Removal of the hazardous dye rhodamine B through photocatalytic and adsorption treatments," *Journal of Environmental Management*, vol. 85, no. 4, pp. 956–964, 2007.

[49] M. Rafatullah, O. Sulaiman, R. Hashim, and A. Ahmad, "Adsorption of methylene blue on low-cost adsorbents: a review," *Journal of Hazardous Materials*, vol. 177, no. 1–3, pp. 70–80, 2010.

[50] M.-X. Zhu, L. Lee, H.-H. Wang, and Z. Wang, "Removal of an anionic dye by adsorption/precipitation processes using alkaline white mud," *Journal of Hazardous Materials*, vol. 149, no. 3, pp. 735–741, 2007.

[51] C. D. Vecitis, Y. Wang, J. Cheng, H. Park, B. T. Mader, and M. R. Hoffmann, "Sonochemical degradation of perfluorooctanesulfonate in aqueous film-forming foams," *Environmental Science and Technology*, vol. 44, no. 1, pp. 432–438, 2010.

[52] N. L. Stock, J. Peller, K. Vinodgopal, and P. V. Kamat, "Combinative sonolysis and photocatalysis for textile dye degradation," *Environmental Science and Technology*, vol. 34, no. 9, pp. 1747–1750, 2000.

[53] C. A. Martínez-Huitle and S. Ferro, "Electrochemical oxidation of organic pollutants for the wastewater treatment: direct and indirect processes," *Chemical Society Reviews*, vol. 35, no. 12, pp. 1324–1340, 2006.

[54] S. Tanaka, Y. Nakata, T. Kimura, Y. Yustiawati, M. Kawasaki, and H. Kuramitz, "Electrochemical decomposition of bisphenol A using Pt/Ti and SnO_2/Ti anodes," *Journal of Applied Electrochemistry*, vol. 32, no. 2, pp. 197–201, 2002.

[55] J.-F. Zhi, H.-B. Wang, T. Nakashima, T. N. Rao, and A. Fujishima, "Electrochemical incineration of organic pollutants on boron-doped diamond electrode. Evidence for direct electrochemical oxidation pathway," *Journal of Physical Chemistry B*, vol. 107, no. 48, pp. 13389–13395, 2003.

[56] P. Cañizares, C. Sáez, J. Lobato, and M. A. Rodrigo, "Electrochemical oxidation of polyhydroxybenzenes on boron-doped diamond anodes," *Industrial and Engineering Chemistry Research*, vol. 43, no. 21, pp. 6629–6637, 2004.

[57] C. A. Martínez-Huitle, M. A. Quiroz, C. Comninellis, S. Ferro, and A. De Battisti, "Electrochemical incineration of chloranilic acid using Ti/IrO_2, Pb/PbO_2 and Si/BDD electrodes," *Electrochimica Acta*, vol. 50, no. 4, pp. 949–956, 2004.

[58] X. Zhu, S. Shi, J. Wei et al., "Electrochemical oxidation characteristics of p-substituted phenols using a boron-doped diamond electrode," *Environmental Science and Technology*, vol. 41, no. 18, pp. 6541–6546, 2007.

[59] J. Jiang, M. Chang, and P. Pan, "Simultaneous hydrogen production and electrochemical oxidation of organics using boron-doped diamond electrodes," *Environmental Science and Technology*, vol. 42, no. 8, pp. 3059–3063, 2008.

[60] M. Murugananthan, S. Yoshihara, T. Rakuma, and T. Shirakashi, "Mineralization of bisphenol A (BPA) by anodic oxidation with boron-doped diamond (BDD) electrode," *Journal of Hazardous Materials*, vol. 154, no. 1–3, pp. 213–220, 2008.

[61] N. Borràs, R. Oliver, C. Arias, and E. Brillas, "Degradation of atrazine by electrochemical advanced oxidation processes using a boron-doped diamond anode," *Journal of Physical Chemistry A*, vol. 114, no. 24, pp. 6613–6621, 2010.

[62] M. Govindaraj, M. Muthukumar, and G. Bhaskar Raju, "Electrochemical oxidation of tannic acid contaminated wastewater by RuO_2/IrO_2/TaO_2-coated titanium and graphite anodes," *Environmental Technology*, vol. 31, no. 14, pp. 1613–1622, 2010.

[63] M. Murugananthan, S. S. Latha, G. Bhaskar Raju, and S. Yoshihara, "Anodic oxidation of ketoprofen-An anti-inflammatory drug using boron doped diamond and platinum electrodes," *Journal of Hazardous Materials*, vol. 180, no. 1–3, pp. 753–758, 2010.

[64] S. Song, L. Zhan, Z. He et al., "Mechanism of the anodic oxidation of 4-chloro-3-methyl phenol in aqueous solution using Ti/SnO_2-Sb/PbO2 electrodes," *Journal of Hazardous Materials*, vol. 175, no. 1–3, pp. 614–621, 2010.

[65] N. Bensalah, B. Louhichi, and A. Abdel-Wahab, "Electrochemical oxidation of succinic acid in aqueous solutions using boron doped diamond anodes," *International Journal of Environmental Science and Technology*, vol. 9, no. 1, pp. 135–143, 2012.

[66] C. I. Brinzila, M. J. Pacheco, L. Ciríaco, R. C. Ciobanu, and A. Lopes, "Electrodegradation of tetracycline on BDD anode," *Chemical Engineering Journal*, vol. 209, pp. 54–61, 2012.

[67] J. M. Peralta-Hernandez, M. Mendez-Tovar, R. Guerra-Sanchez, C. A. Martinez-Huitle, and J. L. Nava, "A brief review on environmental application of boron doped diamond electrodes as a new way for electrochemical incineration of synthetic dyes," *International Journal of Electrochemistry*, vol. 2012, Article ID 154316, 18 pages, 2012.

[68] N. Rabaaoui and M. S. Allagui, "Anodic oxidation of salicylic acid on BDD electrode: variable effects and mechanisms of degradation," *Journal of Hazardous Materials*, vol. 243, pp. 187–192, 2012.

[69] M. G. Tavares, L. V. A. da Silva, A. M. Sales Solano, J. Tonholo, C. A. Martínez-Huitle, and C. L. P. S. Zanta, "Electrochemical oxidation of methyl red using Ti/$Ru_{0.3}Ti_{0.7}O_2$ and Ti/Pt anodes," *Chemical Engineering Journal*, vol. 204–206, pp. 141–150, 2012.

[70] R. B. Alencar de Souza and L. A. Martins Ruotolo, "Phenol electrooxidation in different supporting electrolytes using boron-doped diamond anodes," *International Journal of Electrochemical Science*, vol. 8, no. 1, pp. 643–657, 2013.

[71] M. Gaber, N. Abu Ghalwa, A. M. Khedr, and M. F. Salem, "Electrochemical degradation of reactive yellow 160 Dye in real wastewater using C/PbO_2, $Pb^+Sn/PbO_2^+SnO_2$, and Pb/PbO_2

modified electrodes," *Journal of Chemistry*, Article ID 691763, 9 pages, 2013.

[72] N. Rabaaoui, Y. Moussaoui, M. S. Allagui, B. Ahmed, and E. Elaloui, "Anodic oxidation of nitrobenzene on BDD electrode: variable effects and mechanisms of degradation," *Separation and Purification Technology*, vol. 107, pp. 318–323, 2013.

[73] N. Rabaaoui, M. E. K. Saad, Y. Moussaoui, M. S. Allagui, A. Bedoui, and E. Elaloui, "Anodic oxidation of o-nitrophenol on BDD electrode: variable effects and mechanisms of degradation," *Journal of Hazardous Materials*, vol. 250-251, pp. 447–453, 2013.

[74] W. K. Lafi and Z. Al-Qodah, "Combined advanced oxidation and biological treatment processes for the removal of pesticides from aqueous solutions," *Journal of Hazardous Materials*, vol. 137, no. 1, pp. 489–497, 2006.

[75] J.-M. Herrmann, "Heterogeneous photocatalysis: fundamentals and applications to the removal of various types of aqueous pollutants," *Catalysis Today*, vol. 53, no. 1, pp. 115–129, 1999.

[76] Z. Wang, F. Zhang, Y. Yang, B. Xue, J. Cui, and N. Guan, "Facile postsynthesis of visible-light-sensitive titanium dioxide/mesoporous SBA-15," *Chemistry of Materials*, vol. 19, no. 13, pp. 3286–3293, 2007.

[77] Y. J. Acosta-Silva, R. Nava, V. Hernández-Morales, S. A. Macías-Sánchez, M. L. Gómez-Herrera, and B. Pawelec, "Methylene blue photodegradation over titania-decorated SBA-15," *Applied Catalysis B: Environmental*, vol. 110, pp. 108–117, 2011.

[78] S. Artkla, "Photodecomposition of polyphenols in E. camaldulensis leaves in the presence of hybrid catalyst of titania and MCM-41 synthesized from rice husk silica," *Korean Journal of Chemical Engineering*, vol. 29, no. 5, pp. 555–562, 2012.

[79] S. Zhu, D. Zhang, X. Zhang et al., "Sonochemical incorporation of nanosized TiO_2 inside mesoporous silica with high photocatalytic performance," *Microporous and Mesoporous Materials*, vol. 126, no. 1-2, pp. 20–25, 2009.

[80] Y.-J. Do, J.-H. Kim, J.-H. Park et al., "Photocatalytic decomposition of 4-nitrophenol on Ti-containing MCM-41," *Catalysis Today*, vol. 101, no. 3-4, pp. 299–305, 2005.

[81] K. Gude, V. M. Gun'ko, and J. P. Blitz, "Adsorption and photocatalytic decomposition of methylene blue on surface modified silica and silica-titania," *Colloids and Surfaces A: Physicochemical and Engineering Aspects*, vol. 325, no. 1-2, pp. 17–20, 2008.

[82] E. A. El-Sharkawy, A. Y. Soliman, and K. M. Al-Amer, "Comparative study for the removal of methylene blue via adsorption and photocatalytic degradation," *Journal of Colloid and Interface Science*, vol. 310, no. 2, pp. 498–508, 2007.

[83] Y. Li, N. Li, J. Tu et al., "TiO_2 supported on rod-like mesoporous silica SBA-15: preparation, characterization and photocatalytic behaviour," *Materials Research Bulletin*, vol. 46, no. 12, pp. 2317–2322, 2011.

[84] H. S. Kibombo, D. Zhao, A. Gonshorowski, S. Budhi, M. D. Koppang, and R. T. Koodali, "Cosolvent-induced gelation and the hydrothermal enhancement of the crystallinity of titania-silica mixed oxides for the photocatalytic remediation of organic pollutants," *Journal of Physical Chemistry C*, vol. 115, no. 13, pp. 6126–6135, 2011.

[85] A. A. Belhekar, S. V. Awate, and R. Anand, "Photocatalytic activity of titania modified mesoporous silica for pollution control," *Catalysis Communications*, vol. 3, no. 10, pp. 453–458, 2002.

[86] S. Rasalingam, R. Peng, and R. T. Koodali, "An investigation into the effect of porosities on the adsorption of rhodamine B using titania-silica mixed oxide xerogels," *Journal of Environmental Management*, vol. 128, pp. 530–539, 2013.

[87] J. Aguado, R. van Grieken, M.-J. López-Muñoz, and J. Marugán, "A comprehensive study of the synthesis, characterization and activity of TiO_2 and mixed TiO_2/SiO_2 photocatalysts," *Applied Catalysis A: General*, vol. 312, no. 1-2, pp. 202–212, 2006.

[88] P. Wilhelm and D. Stephan, "Photodegradation of rhodamine B in aqueous solution via SiO_2@TiO_2 nano-spheres," *Journal of Photochemistry and Photobiology A: Chemistry*, vol. 185, no. 1, pp. 19–25, 2007.

[89] E. Y. Kim, C. M. Whang, W. I. Lee, and Y. H. Kim, "Photocatalytic property of SiO_2/TiO_2 nanoparticles prepared by sol-hydrothermal process," *Journal of Electroceramics*, vol. 17, no. 2–4, pp. 899–902, 2006.

[90] D. Sun, Y. Huang, B. Han, and G. Yang, "Ti-Si mixed oxides prepared by polymer in situ sol-gel chemistry with the aid of CO_2," *Langmuir*, vol. 22, no. 10, pp. 4793–4798, 2006.

[91] H. Yamashita, S. Kawasaki, Y. Ichihashi et al., "Characterization of titanium-silicon binary oxide catalysts prepared by the sol-gel method and their photocatalytic reactivity for the liquid-phase oxidation of 1-octanol," *Journal of Physical Chemistry B*, vol. 102, no. 30, pp. 5870–5875, 1998.

[92] C. Anderson and A. J. Bard, "Improved photocatalytic activity and characterization of mixed TiO_2/SiO_2 and TiO_2/Al_2O_3 materials," *Journal of Physical Chemistry B*, vol. 101, no. 14, pp. 2611–2616, 1997.

[93] H. Eccles, "Treatment of metal-contaminated wastes: why select a biological process?" *Trends in Biotechnology*, vol. 17, no. 12, pp. 462–465, 1999.

[94] N. Lu, J. Pei, Y. Zhao, R. Qi, and J. Liu, "Performance of a biological degradation method for indoor formaldehyde removal," *Building and Environment*, vol. 57, pp. 253–258, 2012.

[95] W. Chen, S. Z. Jianshun, and Z. Zhang, "Performance of air cleaners for removing multiple volatile organic compounds in indoor air," *SHRAE Transactions*, vol. 111, no. 1, p. 1101, 2005.

[96] T. N. Obee, "Photooxidation of sub-parts-per-million toluene and formaldehyde levels an titania using a glass-plate reactor," *Environmental Science and Technology*, vol. 30, no. 12, pp. 3578–3584, 1996.

[97] Z. Wang and J. S. Zhang, "Characterization and performance evaluation of a full-scale activated carbon-based dynamic botanical air filtration system for improving indoor air quality," *Building and Environment*, vol. 46, no. 3, pp. 758–768, 2011.

[98] C. Di Iaconi, R. Ramadori, and A. Lopez, "Combined biological and chemical degradation for treating a mature municipal landfill leachate," *Biochemical Engineering Journal*, vol. 31, no. 2, pp. 118–124, 2006.

[99] G. Sudarjanto, B. Keller-Lehmann, and J. Keller, "Optimization of integrated chemical-biological degradation of a reactive azo dye using response surface methodology," *Journal of Hazardous Materials*, vol. 138, no. 1, pp. 160–168, 2006.

[100] C. Y. Chen, J. T. Kuo, H. A. Yang, and Y. C. Chung, "A coupled biological and photocatalysis pretreatment system for the removal of crystal violet from wastewater," *Chemosphere*, vol. 92, no. 6, pp. 695–701, 2013.

[101] Y. Lester, H. Mamane, I. Zucker, and D. Avisar, "Treating wastewater from a pharmaceutical formulation facility by biological process and ozone," *Water Research*, vol. 47, no. 13, pp. 4349–4356, 2013.

[102] R. Rosal, A. Rodríguez, J. A. Perdigón-Melón et al., "Occurrence of emerging pollutants in urban wastewater and their removal

through biological treatment followed by ozonation," *Water Research*, vol. 44, no. 2, pp. 578–588, 2010.

[103] S. Malato, J. Blanco, A. R. Fernández-Alba, and A. Agüera, "Solar photocatalytic mineralization of commercial pesticides: acrinathrin," *Chemosphere*, vol. 40, no. 4, pp. 403–409, 2000.

[104] F. Javier Benitez, J. L. Acero, and F. J. Real, "Degradation of carbofuran by using ozone, UV radiation and advanced oxidation processes," *Journal of Hazardous Materials*, vol. 89, no. 1, pp. 51–65, 2002.

[105] E. Tamer, Z. Hamid, A. M. Aly, E. T. Ossama, M. Bo, and G. Benoit, "Sequential UV-biological degradation of chlorophenols," *Chemosphere*, vol. 63, no. 2, pp. 277–284, 2006.

[106] J. Benner, D. E. Helbling, H. P. E. Kohler et al., "Is biological treatment a viable alternative for micropollutant removal in drinking water treatment processes?" *Water Research*, vol. 47, no. 16, pp. 5955–5976, 2013.

[107] M. Kröger, M. E. Schumacher, H. Risse, and G. Fels, "Biological reduction of TNT as part of a combined biological-chemical procedure for mineralization," *Biodegradation*, vol. 15, no. 4, pp. 241–248, 2004.

[108] S. Le Borgne, D. Paniagua, and R. Vazquez-Duhalt, "Biodegradation of organic pollutants by halophilic bacteria and archaea," *Journal of Molecular Microbiology and Biotechnology*, vol. 15, no. 2-3, pp. 74–92, 2008.

[109] G. Lofrano, S. Meriç, G. E. Zengin, and D. Orhon, "Chemical and biological treatment technologies for leather tannery chemicals and wastewaters: a review," *Science of the Total Environment*, vol. 461–462, pp. 265–281, 2013.

[110] M. Desai, A. Dogra, S. Vora, P. Bahadur, and R. N. Ram, "Adsorption of some acid dyes from aqueous solutions onto neutral alumina," *Indian Journal of Chemistry A*, vol. 36, no. 11, pp. 938–944, 1997.

[111] T. A. Khan, V. V. Singh, and D. Kumar, "Removal of some basic dyes from artificial textile wastewater by adsorption on Akash Kinari coal," *Journal of Scientific and Industrial Research*, vol. 63, no. 4, pp. 355–364, 2004.

[112] J. X. Lin, S. L. Zhan, M. H. Fang, X. Q. Qian, and H. Yang, "Adsorption of basic dye from aqueous solution onto fly ash," *Journal of Environmental Management*, vol. 87, no. 1, pp. 193–200, 2008.

[113] K. Haarstad, H. J. Bavor, and T. Mæhlum, "Organic and metallic pollutants in water treatment and natural wetlands: a review," *Water Science and Technology*, vol. 65, no. 1, pp. 76–99, 2012.

[114] Ş. Kubilay, R. Gürkan, A. Savran, and T. Şahan, "Removal of Cu(II), Zn(II) and Co(II) ions from aqueous solutions by adsorption onto natural bentonite," *Adsorption*, vol. 13, no. 1, pp. 41–51, 2007.

[115] M. Rafatullah, O. Sulaiman, R. Hashim, and A. Ahmad, "Adsorption of copper (II), chromium (III), nickel (II) and lead (II) ions from aqueous solutions by meranti sawdust," *Journal of Hazardous Materials*, vol. 170, no. 2-3, pp. 969–977, 2009.

[116] J. K. Thomas, "Physical aspects of radiation-induced processes on SiO_2, γ-Al_2O_3, zeolites, and clays," *Chemical Reviews*, vol. 105, no. 5, pp. 1683–1734, 2005.

[117] G. Annadurai, R.-S. Juang, and D.-J. Lee, "Adsorption of rhodamine 6G from aqueous solutions on activated carbon," *Journal of Environmental Science and Health A: Toxic/Hazardous Substances and Environmental Engineering*, vol. 36, no. 5, pp. 715–725, 2001.

[118] D. Mohan, K. P. Singh, G. Singh, and K. Kumar, "Removal of dyes from wastewater using flyash, a low-cost adsorbent," *Industrial and Engineering Chemistry Research*, vol. 41, no. 15, pp. 3688–3695, 2002.

[119] M. Ahmaruzzaman, "Role of fly ash in the removal of organic pollutants from wastewater," *Energy and Fuels*, vol. 23, no. 3, pp. 1494–1511, 2009.

[120] G. Dursun, H. Çiçek, and A. Y. Dursun, "Adsorption of phenol from aqueous solution by using carbonised beet pulp," *Journal of Hazardous Materials*, vol. 125, no. 1–3, pp. 175–182, 2005.

[121] A. H. El-Sheikh, A. P. Newman, A. J. Said, A. M. Alzawahreh, and M. M. Abu-Helal, "Improving the adsorption efficiency of phenolic compounds into olive wood biosorbents by prewashing with organic solvents: equilibrium, kinetic and thermodynamic aspects," *Journal of Environmental Management*, vol. 118, pp. 1–10, 2013.

[122] L. N. Nguyen, F. I. Hai, S. Yang et al., "Removal of trace organic contaminants by an MBR comprising a mixed culture of bacteria and white-rot fungi," *Bioresource Technology*, vol. 148, pp. 234–241, 2013.

[123] H. Tada, M. Akazawa, Y. Kubo, and S. Ito, "Enhancing effect of SiO_x monolayer coverage of TiO_2 on the photoinduced oxidation of rhodamine 6G in aqueous media," *Journal of Physical Chemistry B*, vol. 102, pp. 6360–6366, 1998.

[124] R. M. Burton, *Oxidant concentation effects in the hydroxylation of phenol over titanium-based zeolites Al-free Ti-Beta and TS-1 [M.S. thesis]*, Stellenbosch University Chemical Engineering, 2006.

[125] M. Brigante and P. C. Schulz, "Adsorption of paraquat on mesoporous silica modified with titania: effects of pH, ionic strength and temperature," *Journal of Colloid and Interface Science*, vol. 363, no. 1, pp. 355–361, 2011.

[126] K. Cendrowski, X. Chen, B. Zielinska et al., "Synthesis, characterization, and photocatalytic properties of core/shell mesoporous silica nanospheres supporting nanocrystalline titania," *Journal of Nanoparticle Research*, vol. 13, no. 11, pp. 5899–5908, 2011.

[127] Y. Xu and C. H. Langford, "UV- or visible-light-induced degradation of X3B on TiO_2 nanoparticles: the influence of adsorption," *Langmuir*, vol. 17, no. 3, pp. 897–902, 2001.

[128] Y. S. Ho, C. T. Huang, and H. W. Huang, "Equilibrium sorption isotherm for metal ions on tree fern," *Process Biochemistry*, vol. 37, no. 12, pp. 1421–1430, 2002.

[129] Y. S. Ho, J. F. Porter, and G. McKay, "Equilibrium isotherm studies for the sorption of divalent metal ions onto peat: copper, nickel and lead single component systems," *Water, Air, and Soil Pollution*, vol. 141, no. 1–4, pp. 1–33, 2002.

[130] Y.-S. Ho, "Isotherms for the sorption of lead onto peat: comparison of linear and non-linear methods," *Polish Journal of Environmental Studies*, vol. 15, no. 1, pp. 81–86, 2006.

[131] S. Guiza, M. Bagane, A. H. Al-Soudani, and H. B. Amore, "Adsorption of basic dyes onto natural clay," *Adsorption Science and Technology*, vol. 22, no. 3, pp. 245–256, 2004.

[132] M. Bagane and S. Guiza, "Removal of a dye from textile effluents by adsorption," *Annales de Chimie: Science des Materiaux*, vol. 25, no. 8, pp. 615–626, 2000.

[133] A. Gürses, S. Karaca, Ç. Doğar, R. Bayrak, M. Açıkyıldız, and M. Yalçın, "Determination of adsorptive properties of clay/water system: methylene blue sorption," *Journal of Colloid and Interface Science*, vol. 269, no. 2, pp. 310–314, 2004.

[134] D. Ghosh and K. G. Bhattacharyya, "Adsorption of methylene blue on kaolinite," *Applied Clay Science*, vol. 20, no. 6, pp. 295–300, 2002.

[135] C. A. P. Almeida, N. A. Debacher, A. J. Downs, L. Cottet, and C. A. D. Mello, "Removal of methylene blue from colored effluents by adsorption on montmorillonite clay," *Journal of Colloid and Interface Science*, vol. 332, no. 1, pp. 46–53, 2009.

[136] G. Atun, G. Hisarli, W. S. Sheldrick, and M. Muhler, "Adsorptive removal of methylene blue from colored effluents on fuller's earth," *Journal of Colloid and Interface Science*, vol. 261, no. 1, pp. 32–39, 2003.

[137] S. Hong, C. Wen, J. He, F. Gan, and Y.-S. Ho, "Adsorption thermodynamics of Methylene Blue onto bentonite," *Journal of Hazardous Materials*, vol. 167, no. 1–3, pp. 630–633, 2009.

[138] R. A. Shawabkeh and M. F. Tutunji, "Experimental study and modeling of basic dye sorption by diatomaceous clay," *Applied Clay Science*, vol. 24, no. 1-2, pp. 111–120, 2003.

[139] S. Wang, Y. Boyjoo, A. Choueib, and Z. H. Zhu, "Removal of dyes from aqueous solution using fly ash and red mud," *Water Research*, vol. 39, no. 1, pp. 129–138, 2005.

[140] X. Querol, N. Moreno, J. C. Umaa et al., "Synthesis of zeolites from coal fly ash: an overview," *International Journal of Coal Geology*, vol. 50, no. 1–4, pp. 413–423, 2002.

[141] K. S. Hui and C. Y. H. Chao, "Synthesis of MCM-41 from coal fly ash by a green approach: influence of synthesis pH," *Journal of Hazardous Materials*, vol. 137, no. 2, pp. 1135–1148, 2006.

[142] P. Pavasant, R. Apiratikul, V. Sungkhum, P. Suthiparinyanont, S. Wattanachira, and T. F. Marhaba, "Biosorption of Cu^{2+}, Cd^{2+}, Pb^{2+}, and Zn^{2+} using dried marine green macroalga Caulerpa lentillifera," *Bioresource Technology*, vol. 97, no. 18, pp. 2321–2329, 2006.

[143] R. Apiratikul and P. Pavasant, "Batch and column studies of biosorption of heavy metals by Caulerpa lentillifera," *Bioresource Technology*, vol. 99, no. 8, pp. 2766–2777, 2008.

[144] K. Marungrueng and P. Pavasant, "High performance biosorbent (Caulerpa lentillifera) for basic dye removal," *Bioresource Technology*, vol. 98, no. 8, pp. 1567–1572, 2007.

[145] K. S. Low, C. K. Lee, and L. L. Heng, "Sorption of basic dyes by Hydrilla verticillata," *Environmental Technology*, vol. 15, no. 2, pp. 115–124, 1994.

[146] K. S. Low, C. K. Lee, and K. K. Tan, "Biosorption of basicdyes by water hyacinth roots," *Bioresource Technology*, vol. 52, no. 1, pp. 79–83, 1995.

[147] L. W. Low, T. T. Teng, M. Rafatullah, N. Morad, and B. Azahari, "Adsorption studies of methylene blue and malachite green from aqueous solutions by pretreated lignocellulosic materials," *Separation Science and Technology*, vol. 48, no. 11, pp. 1688–1698, 2013.

[148] N. F. Cardoso, E. C. Lima, I. S. Pinto et al., "Application of cupuassu shell as biosorbent for the removal of textile dyes from aqueous solution," *Journal of Environmental Management*, vol. 92, no. 4, pp. 1237–1247, 2011.

[149] T. Al-Khalid and M. H. El-Naas, "Aerobic biodegradation of phenols: a comprehensive review," *Critical Reviews in Environmental Science and Technology*, vol. 42, no. 16, pp. 1631–1690, 2012.

[150] B. F. Nabavi, M. Nikaeen, M. M. Amin, and H. Farrokhzadeh, "Biological treatment of polychlorinated biphenyls (PCBs) contaminated transformer oil by anaerobic-aerobic sequencing batch biofilm reactors," *International Biodeterioration and Biodegradation*, vol. 85, pp. 451–457, 2013.

[151] O. B. Yang, J. C. Kim, J. S. Lee, and Y. G. Kim, "Use of activated carbon fiber for direct removal of iodine from acetic acid solution," *Industrial and Engineering Chemistry Research*, vol. 32, no. 8, pp. 1692–1697, 1993.

[152] R. S. Juang and S. L. Swei, "Effect of dye nature on its adsorption from aqueous solutions onto activated carbon," *Separation Science and Technology*, vol. 31, no. 15, pp. 2143–2158, 1996.

[153] M. Streat, J. W. Patrick, and M. J. Camporro Perez, "Sorption of phenol and para-chlorophenol from water using conventional and novel activated carbons," *Water Research*, vol. 29, no. 2, pp. 467–472, 1995.

[154] G. M. Walker and L. R. Weatherley, "Adsorption of dyes from aqueous solution: the effect of adsorbent pore size distribution and dye aggregation," *Chemical Engineering Journal*, vol. 83, no. 3, pp. 201–206, 2001.

[155] L. D. T. Prola, F. M. Machado, C. P. Bergmann et al., "Adsorption of Direct Blue 53 dye from aqueous solutions by multi-walled carbon nanotubes and activated carbon," *Journal of Environmental Management*, vol. 130, pp. 166–175, 2013.

[156] D. D. Milenkovic, M. M. Milosavljevic, A. D. Marinkovic, V. R. Dokic, J. Z. Mitrovic, and A. L. Bojic, "Removal of copper(II) ion from aqueous solution by high-porosity activated carbon," *Water SA*, vol. 39, no. 4, pp. 515–522, 2013.

[157] X. X. Hou, Q. F. Deng, T. Z. Ren, and Z. Y. Yuan, "Adsorption of Cu^{2+} and methyl orange from aqueous solutions by activated carbons of corncob-derived char wastes," *Environmental Science and Pollution Research*, vol. 20, no. 12, pp. 8521–8534, 2013.

[158] V. K. Gupta, I. Ali, T. A. Saleh, M. N. Siddiqui, and S. Agarwal, "Chromium removal from water by activated carbon developed from waste rubber tires," *Environmental Science and Pollution Research*, vol. 20, no. 3, pp. 1261–1268, 2013.

[159] K. Ota, Y. Amano, M. Aikawa, and M. Machida, "Removal of nitrate ions from water by activated carbons (ACs)-Influence of surface chemistry of ACs and coexisting chloride and sulfate ions," *Applied Surface Science*, vol. 276, pp. 838–842, 2013.

[160] M. G. Krivova, D. D. Grinshpan, and N. Hedin, "Adsorption of C(n)TABr surfactants on activated carbons," *Colloids and Surfaces A: Physicochemical and Engineering Aspects*, vol. 436, pp. 62–70, 2013.

[161] C. Y. Yin, M. K. Aroua, and W. M. A. W. Daud, "Review of modifications of activated carbon for enhancing contaminant uptakes from aqueous solutions," *Separation and Purification Technology*, vol. 52, no. 3, pp. 403–415, 2007.

[162] A. Bhatnagar, W. Hogland, M. Marques, and M. Sillanpaa, "An overview of the modification methods of activated carbon for its water treatment applications," *Chemical Engineering Journal*, vol. 219, pp. 499–511, 2013.

[163] Y. Xu and C. H. Langford, "Photoactivity of titanium dioxide supported on MCM-41, zeolite X and zeolite Y," *Journal of Physical Chemistry B*, vol. 101, pp. 3115–3121, 1997.

[164] L. J. Alemany, M. A. Banares, E. Pardo, F. Martin, M. Galán-Fereres, and J. M. Blasco, "Photodegradation of phenol in water using silica-supported titania catalysts," *Applied Catalysis B*, vol. 13, no. 3-4, pp. 289–297, 1997.

[165] P. Cheng, M. Zheng, Y. Jin, Q. Huang, and M. Gu, "Preparation and characterization of silica-doped titania photocatalyst through sol-gel method," *Materials Letters*, vol. 57, no. 20, pp. 2989–2994, 2003.

[166] M. L. Fetterolf, H. V. Patel, and J. M. Jennings, "Adsorption of methylene blue and acid blue 40 on titania from aqueous solution," *Journal of Chemical and Engineering Data*, vol. 48, no. 4, pp. 831–835, 2003.

[167] K. Bourikas, M. Stylidi, D. I. Kondarides, and X. E. Verykios, "Adsorption of Acid Orange 7 on the surface of titanium dioxide," *Langmuir*, vol. 21, no. 20, pp. 9222–9230, 2005.

[168] V. Belessi, G. Romanos, N. Boukos, D. Lambropoulou, and C. Trapalis, "Removal of Reactive Red 195 from aqueous solutions by adsorption on the surface of TiO_2 nanoparticles," *Journal of Hazardous Materials*, vol. 170, no. 2-3, pp. 836–844, 2009.

[169] S. Jafari, S. Azizian, and B. Jaleh, "Adsorption kinetics of methyl violet onto TiO_2 nanoparticles with different phases," *Colloids and Surfaces A: Physicochemical and Engineering Aspects*, vol. 384, no. 1–3, pp. 618–623, 2011.

[170] C. R. Lee, H. S. Kim, I. H. Jang, J. H. Im, and N. G. Park, "Pseudo first-order adsorption kinetics of N719 dye on TiO_2 surface," *ACS Applied Materials and Interfaces*, vol. 3, no. 6, pp. 1953–1957, 2011.

[171] H. Ghobarkar, O. Schäf, and U. Guth, "Zeolites: from kitchen to space," *Progress in Solid State Chemistry*, vol. 27, no. 2, pp. 29–73, 1999.

[172] M. N. Ahmed, J. John, and R. N. Ram, "Kinetics of removal of Basic Violet 1 from aqueous solution using silica as an adsorbent," *Journal of Environmental Science and Health A: Environmental Science and Engineering*, vol. 28, no. 7, pp. 1581–1597, 1993.

[173] M. N. Ahmed and R. N. Ram, "Removal of basic dye from wastewater using silica as adsorbent," *Environmental Pollution*, vol. 77, no. 1, pp. 79–86, 1992.

[174] R. G. Avendaño, J. A. de los Reyes, J. A. Montoya, and T. Viveros, "Preparation and characterization of mesoporous titanium-silica and zirconia-silica mixed oxides," *Superficies Y Vacío*, vol. 19, no. 2, pp. 1–6, 2006.

[175] V. W. Atul, G. S. Gaikwad, M. G. Dhonde, N. T. Khaty, and S. R. Thakare, "Removal of organic pollutant from water by heterogenous photocatalysis: a review," *Research Journal of Chemistry and Environment*, vol. 17, no. 1, pp. 84–94, 2013.

[176] J. Wu, K. Rudy, and J. Spark, "Oxidation of aqueous phenol by ozone and peroxidase," *Advances in Environmental Research*, vol. 4, no. 4, pp. 339–346, 2000.

[177] P. Yogeswary, Y. Mohd, R. Mohd, A. Saidina, and A. Nor, "Degradation of phenol by catalytic ozonation," *Journal of Chemical and Natural Resources Engineering*, vol. 2, pp. 34–46, 2007.

[178] Y. Yamamoto, E. Niki, H. Shiokawa, and Y. Kamiya, "Ozonation of organic compounds. 2. Ozonation of phenol in water," *Journal of Organic Chemistry*, vol. 44, no. 13, pp. 2137–2142, 1979.

[179] K. Turhan and S. Uzman, "Removal of phenol from water using ozone," *Desalination*, vol. 229, no. 1–3, pp. 257–263, 2008.

[180] J. Staehelin, R. E. Bühler, and J. Hoigné, "Ozone decomposition in water studied by pulse radiolysis. 2. OH and HO_4 as chain intermediates," *Journal of Physical Chemistry*, vol. 88, no. 24, pp. 5999–6004, 1984.

[181] H. Einaga and S. Futamura, "Catalytic oxidation of benzene with ozone over Mn ion-exchanged zeolites," *Catalysis Communications*, vol. 8, no. 3, pp. 557–560, 2007.

[182] H. Einaga, Y. Teraoka, and A. Ogat, "Benzene oxidation with ozone over manganese oxide supported on zeolite catalysts," *Catalysis Today*, vol. 164, no. 1, pp. 571–574, 2011.

[183] H. Einaga, N. Maeda, and Y. Teraoka, "Effect of catalyst composition and preparation conditions on catalytic properties of unsupported manganese oxides for benzene oxidation with ozone," *Applied Catalysis B: Environmental*, vol. 142, pp. 406–413, 2013.

[184] J. Kanagaraj and A. B. Mandal, "Combined biodegradation and ozonation for removal of tannins and dyes for the reduction of pollution loads," *Environmental Science and Pollution Research*, vol. 19, no. 1, pp. 42–52, 2012.

[185] M. M. Huber, S. Canonica, G.-Y. Park, and U. Von Gunten, "Oxidation of pharmaceuticals during ozonation and advanced oxidation processes," *Environmental Science and Technology*, vol. 37, no. 5, pp. 1016–1024, 2003.

[186] O. Legrini, E. Oliveros, and A. M. Braun, "Photochemical processes for water treatment," *Chemical Reviews*, vol. 93, no. 2, pp. 671–698, 1993.

[187] S. R. Cater, M. I. Stefan, J. R. Bolton, and A. Safarzadeh-Amiri, "UV/H_2O_2 treatment of methyl tert-butyl ether in contaminated waters," *Environmental Science and Technology*, vol. 34, no. 4, pp. 659–662, 2000.

[188] J. M. Poyatos, M. M. Muñio, M. C. Almecija, J. C. Torres, E. Hontoria, and F. Osorio, "Advanced oxidation processes for wastewater treatment: state of the art," *Water, Air, and Soil Pollution*, vol. 205, no. 1–4, pp. 187–204, 2010.

[189] E. Felis, D. Marciocha, J. Surmacz-Gorska, and K. Miksch, "Photochemical degration of naproxen in the aquatic environment," *Water Science and Technology*, vol. 55, no. 12, pp. 281–286, 2007.

[190] J. J. Wu, M. Muruganandham, and S. H. Chen, "Degradation of DMSO by ozone-based advanced oxidation processes," *Journal of Hazardous Materials*, vol. 149, no. 1, pp. 218–225, 2007.

[191] H.-Y. Shu, "Degradation of dyehouse effluent containing C.I. Direct Blue 199 by processes of ozonation, UV/H_2O_2 and in sequence of ozonation with UV/H_2O_2," *Journal of Hazardous Materials*, vol. 133, no. 1–3, pp. 92–98, 2006.

[192] H.-Y. Shu and M.-C. Chang, "Pre-ozonation coupled with UV/H_2O_2 process for the decolorization and mineralization of cotton dyeing effluent and synthesized C.I. Direct Black 22 wastewater," *Journal of Hazardous Materials*, vol. 121, no. 1–3, pp. 127–133, 2005.

[193] T. Yonar, G. K. Yonar, K. Kestioglu, and N. Azbar, "Decolorisation of textile effluent using homogeneous photochemical oxidation processes," *Coloration Technology*, vol. 121, no. 5, pp. 258–264, 2005.

[194] A. Gutowska, J. Kałuzna-Czaplińska, and W. K. Jóźwiak, "Degradation mechanism of Reactive Orange 113 dye by H_2O_2/Fe^{2+} and ozone in aqueous solution," *Dyes and Pigments*, vol. 74, no. 1, pp. 41–46, 2007.

[195] E. S. Elmolla and M. Chaudhuri, "Degradation of the antibiotics amoxicillin, ampicillin and cloxacillin in aqueous solution by the photo-Fenton process," *Journal of Hazardous Materials*, vol. 172, no. 2-3, pp. 1476–1481, 2009.

[196] U. I. Gaya and A. H. Abdullah, "Heterogeneous photocatalytic degradation of organic contaminants over titanium dioxide: a review of fundamentals, progress and problems," *Journal of Photochemistry and Photobiology C: Photochemistry Reviews*, vol. 9, no. 1, pp. 1–12, 2008.

[197] Y. Chen, S. Yang, K. Wang, and L. Lou, "Role of primary active species and TiO_2 surface characteristic in UV-illuminated photodegradation of Acid Orange 7," *Journal of Photochemistry and Photobiology A: Chemistry*, vol. 172, no. 1, pp. 47–54, 2005.

[198] A. O. Ibhadon and P. Fitzpatrick, "Heterogeneous photocatalysis: recent advances and applications," *Catalysis*, vol. 3, pp. 189–218, 2013.

[199] D. Sud and P. Kaur, "Heterogeneous photocatalytic degradation of selected organophosphate pesticides: a review," *Critical Reviews in Environmental Science and Technology*, vol. 42, no. 22, pp. 2365–2407, 2011.

[200] T. Daimon, T. Hirakawa, M. Kitazawa, J. Suetake, and Y. Nosaka, "Formation of singlet molecular oxygen associated with the

formation of superoxide radicals in aqueous suspensions of TiO_2 photocatalysts," *Applied Catalysis A: General*, vol. 340, no. 2, pp. 169–175, 2008.

[201] A. Fujishima, X. Zhang, and D. A. Tryk, "TiO_2 photocatalysis and related surface phenomena," *Surface Science Reports*, vol. 63, no. 12, pp. 515–582, 2008.

[202] M. Stylidi, D. I. Kondarides, and X. E. Verykios, "Visible light-induced photocatalytic degradation of Acid Orange 7 in aqueous TiO_2 suspensions," *Applied Catalysis B: Environmental*, vol. 47, no. 3, pp. 189–201, 2004.

[203] M. Bizarro, "High photocatalytic activity of ZnO and ZnO:Al nanostructured films deposited by spray pyrolysis," *Applied Catalysis B: Environmental*, vol. 97, no. 1-2, pp. 198–203, 2010.

[204] S. N. Frank and A. J. Bard, "Heterogeneous photocatalytic oxidation of cyanide and sulfite in aqueous solutions at semiconductor powders," *Journal of Physical Chemistry*, vol. 81, no. 15, pp. 1484–1488, 1977.

[205] Y. K. Kho, A. Iwase, W. Y. Teoh, L. Mädler, A. Kudo, and R. Amal, "Photocatalytic H2 evolution over TiO_2 nanoparticles. The synergistic effect of anatase and rutile," *Journal of Physical Chemistry C*, vol. 114, no. 6, pp. 2821–2829, 2010.

[206] D. Y. C. Leung, X. Fu, C. Wang et al., "Hydrogen production over titania-based photocatalysts," *ChemSusChem*, vol. 3, no. 6, pp. 681–694, 2010.

[207] T. P. Chou, Q. Zhang, B. Russo, G. E. Fryxell, and G. Cao, "Titania particle size effect on the overall performance of dye-sensitized solar cells," *Journal of Physical Chemistry C*, vol. 111, no. 17, pp. 6296–6302, 2007.

[208] C. H. Pollema, J. L. Hendrix, E. B. Milosavljević, L. Solujić, and J. H. Nelson, "Photocatalytic oxidation of cyanide to nitrate at TiO_2 particles," *Journal of Photochemistry and Photobiology A: Chemistry*, vol. 66, no. 2, pp. 235–244, 1992.

[209] H. Hidaka, T. Nakamura, A. Ishizaka, M. Tsuchiya, and J. Zhao, "Heterogeneous photocatalytic degradation of cyanide on TiO_2 surfaces," *Journal of Photochemistry and Photobiology A: Chemistry*, vol. 66, no. 3, pp. 367–374, 1992.

[210] S. N. Frank and A. J. Bard, "Heterogeneous photocatalytic oxidation of cyanide ion in aqueous solutions at TiO_2 powder," *Journal of the American Chemical Society*, vol. 99, no. 1, pp. 303–304, 1977.

[211] A. Zafra, J. Garcia, A. Milis, and X. Domènech, "Kinetics of the catalytic oxidation of nitrite over illuminated aqueous suspensions of TiO_2," *Journal of Molecular Catalysis*, vol. 70, no. 3, pp. 343–349, 1991.

[212] F. Zhang, J. Zhao, T. Shen, H. Hidaka, E. Pelizzetti, and N. Serpone, "TiO_2-assisted photodegradation of dye pollutants II. Adsorption and degradation kinetics of eosin in TiO_2 dispersions under visible light irradiation," *Applied Catalysis B: Environmental*, vol. 15, no. 1-2, pp. 147–156, 1998.

[213] K. Vinodgopal, D. E. Wynkoop, and P. V. Kamat, "Environmental photochemistry on semiconductor surfaces: photosensitized degradation of a textile azo dye, acid orange 7, on TiO_2 particles using visible light," *Environmental Science and Technology*, vol. 30, no. 5, pp. 1660–1666, 1996.

[214] H. Lachheb, E. Puzenat, A. Houas et al., "Photocatalytic degradation of various types of dyes (Alizarin S, Crocein Orange G, Methyl Red, Congo Red, Methylene Blue) in water by UV-irradiated titania," *Applied Catalysis B: Environmental*, vol. 39, no. 1, pp. 75–90, 2002.

[215] J. Li, W. Ma, C. Chen, J. Zhao, H. Zhu, and X. Gao, "Photodegradation of dye pollutants on one-dimensional TiO_2 nanoparticles under UV and visible irradiation," *Journal of Molecular Catalysis A: Chemical*, vol. 261, no. 1, pp. 131–138, 2007.

[216] H. U. Lee, S. C. Lee, J. H. Seo et al., "Room temperature synthesis of nanoporous anatase and anatase/brookite TiO_2 photocatalysts with high photocatalytic performance," *Chemical Engineering Journal*, vol. 223, pp. 209–215, 2013.

[217] A. G. Agrios and P. Pichat, "Recombination rate of photogenerated charges versus surface area: opposing effects of TiO_2 sintering temperature on photocatalytic removal of phenol, anisole, and pyridine in water," *Journal of Photochemistry and Photobiology A: Chemistry*, vol. 180, no. 1-2, pp. 130–135, 2006.

[218] R. Vinu and G. Madras, "Kinetics of simultaneous photocatalytic degradation of phenolic compounds and reduction of metal ions with Nano-TiO_2," *Environmental Science and Technology*, vol. 42, no. 3, pp. 913–919, 2008.

[219] C. Su, B.-Y. Hong, and C.-M. Tseng, "Sol-gel preparation and photocatalysis of titanium dioxide," *Catalysis Today*, vol. 96, no. 3, pp. 119–126, 2004.

[220] W. Guo, X. Liu, P. Huo et al., "Hydrothermal synthesis spherical TiO_2 and its photo-degradation property on salicylic acid," *Applied Surface Science*, vol. 258, no. 18, pp. 6891–6896, 2012.

[221] R. J. Davis and Z. Liu, "Titania–Silica: a model binary oxide catalyst system," *Chemistry of Materials*, vol. 9, no. 11, pp. 2311–2324, 1997.

[222] K. Brodzik, J. Walendziewski, M. Stolarski, L. Van Ginneken, K. Elst, and V. Meynen, "The influence of preparation method on the physicochemical properties of titania-silica aerogels. Part II," *Journal of Porous Materials*, vol. 15, no. 5, pp. 541–549, 2008.

[223] A. Wold, "Photocatalytic properties of TiO_2," *Chemistry of Materials*, vol. 5, no. 3, pp. 280–283, 1993.

[224] I. K. Konstantinou and T. A. Albanis, "TiO_2-assisted photocatalytic degradation of azo dyes in aqueous solution: kinetic and mechanistic investigations: a review," *Applied Catalysis B: Environmental*, vol. 49, no. 1, pp. 1–14, 2004.

[225] D. Bahnemann, "Photocatalytic water treatment: solar energy applications," *Solar Energy*, vol. 77, no. 5, pp. 445–459, 2004.

[226] D. R. Sahu, L. Y. Hong, S.-C. Wang, and J.-L. Huang, "Synthesis, analysis and characterization of ordered mesoporous TiO_2/SBA-15 matrix: effect of calcination temperature," *Microporous and Mesoporous Materials*, vol. 117, no. 3, pp. 640–649, 2009.

[227] T. Kasahara, K. Inumaru, and S. Yamanaka, "Enhanced photocatalytic decomposition of nonylphenol polyethoxylate by alkyl-grafted TiO_2-MCM-41 organic-inorganic nanostructure," *Microporous and Mesoporous Materials*, vol. 76, no. 1–3, pp. 123–130, 2004.

[228] L. H. Tian, H. T. Liu, and Y. Gao, "Degradation and adsorption of rhodamine B and phenol on TiO_2/MCM-41," *Kinetics and Catalysis*, vol. 53, no. 5, pp. 554–559, 2012.

[229] J. Yang, J. Zhang, L. Zhu et al., "Synthesis of nano titania particles embedded in mesoporous SBA-15: characterization and photocatalytic activity," *Journal of Hazardous Materials*, vol. 137, no. 2, pp. 952–958, 2006.

[230] T.-H. Liou and B.-C. Lai, "Utilization of e-waste as a silica source for the synthesis of the catalyst support MCM-48 and highly enhanced photocatalytic activity of supported titania nanoparticles," *Applied Catalysis B: Environmental*, vol. 115-116, pp. 138–148, 2012.

[231] K. De Witte, V. Meynen, M. Mertens et al., "Multi-step loading of titania on mesoporous silica: influence of the morphology and the porosity on the catalytic degradation of aqueous

pollutants and VOCs," *Applied Catalysis B: Environmental*, vol. 84, no. 1-2, pp. 125–132, 2008.

[232] E. Beyers, E. Biermans, S. Ribbens et al., "Combined TiO_2/SiO_2 mesoporous photocatalysts with location and phase controllable TiO_2 nanoparticles," *Applied Catalysis B: Environmental*, vol. 88, no. 3-4, pp. 515–524, 2009.

[233] S. Anandan, "Photocatalytic effects of titania supported nanoporous MCM-41 on degradation of methyl orange in the presence of electron acceptors," *Dyes and Pigments*, vol. 76, no. 2, pp. 535–541, 2008.

[234] H. Ding, H. Sun, and Y. Shan, "Preparation and characterization of mesoporous SBA-15 supported dye-sensitized TiO_2 photocatalyst," *Journal of Photochemistry and Photobiology A: Chemistry*, vol. 169, no. 1, pp. 101–107, 2005.

[235] D. Jyothi, P. A. Deshpande, B. R. Venugopal, S. Chandrasekaran, and G. Madras, "Transition metal oxide loaded MCM catalysts for photocatalytic degradation of dyes," *Journal of Chemical Sciences*, vol. 124, no. 2, pp. 385–393, 2012.

[236] A. Bhattacharyya, S. Kawi, and M. B. Ray, "Photocatalytic degradation of orange II by TiO_2 catalysts supported on adsorbents," *Catalysis Today*, vol. 98, no. 3, pp. 431–439, 2004.

[237] H. H. Tseng, W. W. Lee, M. C. Wei, B. S. Huang, M. C. Hsieh, and P. Y. Cheng, "Synthesis of TiO_2/SBA-15 photocatalyst for the azo dye decolorization through the polyol method," *Chemical Engineering Journal*, vol. 210, pp. 529–538, 2012.

[238] M. Alvaro, C. Aprile, M. Benitez, E. Carbonell, and H. García, "Photocatalytic activity of structured mesoporous TiO_2 materials," *Journal of Physical Chemistry B*, vol. 110, no. 13, pp. 6661–6665, 2006.

[239] W. A. Adams, M. G. Bakker, T. MacIas, and I. A. Jefcoat, "Synthesis and characterization of mesoporous silica films encapsulating titanium dioxide particles: photodegradation of 2,4-dichlorophenol," *Journal of Hazardous Materials*, vol. 112, no. 3, pp. 253–259, 2004.

[240] A. Orlov, Q.-Z. Zhai, and J. Klinowski, "Photocatalytic properties of the SBA-15 mesoporous silica molecular sieve modified with titanium," *Journal of Materials Science*, vol. 41, no. 8, pp. 2187–2193, 2006.

[241] J. Aguado, R. Van Grieken, M. J. López-Muñoz, and J. Marugán, "Removal of cyanides in wastewater by supported TiO_2-based photocatalysts," *Catalysis Today*, vol. 75, no. 1–4, pp. 95–102, 2002.

[242] M.-J. López-Muñoz, R. V. Grieken, J. Aguado, and J. Marugán, "Role of the support on the activity of silica-supported TiO_2 photocatalysts: structure of the TiO_2/SBA-15 photocatalysts," *Catalysis Today*, vol. 101, no. 3-4, pp. 307–314, 2005.

[243] S. Artkla, W. Kim, W. Choi, and J. Wittayakun, "Highly enhanced photocatalytic degradation of tetramethylammonium on the hybrid catalyst of titania and MCM-41 obtained from rice husk silica," *Applied Catalysis B: Environmental*, vol. 91, no. 1-2, pp. 157–164, 2009.

[244] Y. M. Xu and C. H. Langford, "Photoactivity of titanium dioxide supported on MCM41, zeolite X, and zeolite Y," *Journal of Physical Chemistry B*, vol. 101, no. 16, pp. 3115–3121, 1997.

[245] H. S. Kibombo, R. Peng, S. Rasalingam, and R. T. Koodali, "Versatility of heterogeneous photocatalysis: synthetic methodologies epitomizing the role of silica support in TiO_2 based mixed oxides," *Catalysis Science and Technology*, vol. 2, no. 9, pp. 1737–1766, 2012.

[246] B. E. Yoldas, "Formation of titania-silica glasses by low temperature chemical polymerization," *Journal of Non-Crystalline Solids*, vol. 38-39, no. 1, pp. 81–86, 1980.

[247] F. Garbassi and L. Balducci, "Preparation and characterization of spherical TiO_2-SiO_2 particles," *Microporous and Mesoporous Materials*, vol. 47, no. 1, pp. 51–59, 2001.

[248] C. Murata, H. Yoshida, J. Kumagai, and T. Hattori, "Active sites and active oxygen species for photocatalytic epoxidation of propene by molecular oxygen over TiO_2-SiO_2 binary oxides," *Journal of Physical Chemistry B*, vol. 107, no. 18, pp. 4364–4373, 2003.

[249] A. S. Soult, D. F. Carter, H. D. Schreiber, L. J. van de Burgt, and A. E. Stiegman, "Spectroscopy of amorphous and crystalline titania-silica materials," *Journal of Physical Chemistry B*, vol. 106, no. 36, pp. 9266–9273, 2002.

[250] Y. K. Kim, E. Y. Kim, C. M. Whang, Y. H. Kim, and W. I. Lee, "Microstructure and photocatalytic property of SiO_2-TiO 2 under various process condition," *Journal of Sol-Gel Science and Technology*, vol. 33, no. 1, pp. 87–91, 2005.

[251] S. Lisinski, J. Krause, D. Schaniel, L. Ratke, and T. Woike, "Variable refractive indices in mixed oxide xerogels," *Scripta Materialia*, vol. 58, no. 7, pp. 553–555, 2008.

[252] S. Imamura, T. Shiomi, S. Ishida, K. Utani, and H. Jindai, "Decomposition of dichlorodifluoromethane on TiO_2/SiO_2," *Industrial and Engineering Chemistry Research*, vol. 29, no. 9, pp. 1758–1761, 1990.

[253] T.-V. Nguyen and O.-B. Yang, "Photoresponse and AC impedance characterization of TiO_2-SiO_2 mixed oxide for photocatalytic water decomposition," *Catalysis Today*, vol. 87, no. 1–4, pp. 69–75, 2003.

[254] S. Vives and C. Meunier, "Influence of the synthesis route on sol-gel SiO_2-TiO_2 (1:1) xerogels and powders," *Ceramics International*, vol. 34, no. 1, pp. 37–44, 2008.

[255] J. Ren, Z. Li, S. Liu, Y. Xing, and K. Xie, "Silica-titania mixed oxides: Si-O-Ti connectivity, coordination of titanium, and surface acidic properties," *Catalysis Letters*, vol. 124, no. 3-4, pp. 185–194, 2008.

[256] J. M. Miller and L. J. Lakshmi, "Spectroscopic characterization of sol-gel-derived mixed oxides," *Journal of Physical Chemistry B*, vol. 102, no. 34, pp. 6465–6470, 1998.

[257] M. P. Coles, C. G. Lugmair, K. W. Terry, and T. D. Tilley, "Titania-silica materials from the molecular precursor $Ti[OSi(O(t)Bu)_3]_4$: selective epoxidation catalysts," *Chemistry of Materials*, vol. 12, no. 1, pp. 122–131, 2000.

[258] R. Hutter, T. Mallat, A. Peterhans, and A. Baiker, "Control of acidity and selectivity of titania-silica aerogel for the epoxidation of β-isophorone," *Journal of Molecular Catalysis A: Chemical*, vol. 138, no. 2-3, pp. 241–247, 1999.

[259] G. Mountjoy, D. M. Pickup, G. W. Wallidge, J. M. Cole, R. J. Newport, and M. E. Smith, "In-situ high-temperature XANES observations of rapid and reversible changes in Ti coordination in titania-silica xerogels," *Chemical Physics Letters*, vol. 304, no. 3-4, pp. 150–154, 1999.

[260] D. M. Pickup, G. Mountjoy, G. W. Wallidge et al., "A structural study of $(TiO_2)(x)(SiO_2)(1-x)$ (x = 0.18, 0.30 and 0.41) xerogels prepared using acetylacetone," *Journal of Materials Chemistry*, vol. 9, no. 6, pp. 1299–1305, 1999.

[261] A. Pirson, A. Mohsine, P. Marchot et al., "Synthesis of SiO_2-TiO_2 xerogels by sol-gel process," *Journal of Sol-Gel Science and Technology*, vol. 4, no. 3, pp. 179–185, 1995.

[262] T. Fernandez, G. Jose, S. Mathew, R. Pr, and U. Nv, "An ultra-low hydrolysis sol-gel route for titanosilicate xerogels and their characterization," *Journal of Sol-Gel Science and Technology*, vol. 41, no. 2, pp. 163–168, 2007.

[263] Z. Deng, J. Wang, Y. Zhang et al., "Preparation and photocatalytic activity of TiO_2-SiO_2 binary aerogels," *Nanostructured Materials*, vol. 11, no. 8, pp. 1313–1318, 1999.

[264] A. C. Pierre and G. M. Pajonk, "Chemistry of aerogels and their applications," *Chemical Reviews*, vol. 102, no. 11, pp. 4243–4265, 2002.

[265] B. E. Handy, M. Maciejewski, A. Baiker, and A. Wokaun, "Genesis and structural properties of alkoxide-prepared titania-silica xerogels," *Journal of Materials Chemistry*, vol. 2, no. 8, pp. 833–840, 1992.

[266] S. Klein, S. Thorimbert, and W. F. Maier, "Amorphous microporous titania-silica mixed oxides: preparation, characterization, and catalytic redox properties," *Journal of Catalysis*, vol. 163, no. 2, pp. 476–488, 1996.

[267] X. Gao and I. E. Wachs, "Titania-silica as catalysts: molecular structural characteristics and physico-chemical properties," *Catalysis Today*, vol. 51, no. 2, pp. 233–254, 1999.

[268] S. Budhi, H. S. Kibombo, D. Zhao, A. Gonshorowski, and R. T. Koodali, "Synthesis of titania-silica xerogels by co-solvent induced gelation at ambient temperature," *Materials Letters*, vol. 65, no. 14, pp. 2136–2138, 2011.

[269] G. Larsen, H. S. Silva, and R. Venturini De Silva, "Structure of hybrid (organic/inorganic) TiO_2-SiO_2 xerogels as studied by neopentane adsorption at 273 K and Ti K-edge X-ray absorption spectroscopy," *Journal of Non-Crystalline Solids*, vol. 271, no. 1, pp. 1–11, 2000.

[270] G. Larsen, M. Buechler-Skoda, C. Nguyen, D. Vu, and E. Lotero, "Structure of hybrid (organic/inorganic) TiO_2-SiO_2 xerogels II: thermal behavior as monitored by temperature-programmed techniques and spectroscopy," *Journal of Non-Crystalline Solids*, vol. 279, no. 2-3, pp. 161–168, 2001.

[271] R. Mariscal, M. López-Granados, J. L. G. Fierro, J. L. Sotelo, C. Martos, and R. van Grieken, "Morphology and surface properties of titania-silica hydrophobic xerogels," *Langmuir*, vol. 16, no. 24, pp. 9460–9467, 2000.

[272] G. Dagan, S. Sampath, and O. Lev, "Preparation and utilization of organically modified silica-titania photocatalysts for decontamination of aquatic environments," *Chemistry of Materials*, vol. 7, no. 3, pp. 446–453, 1995.

[273] M. Hirano, K. Ota, M. Inagaki, and H. Iwata, "Hydrothermal synthesis of TiO_2/SiO_2 composite nanoparticles and their photocatalytic performances," *Journal of the Ceramic Society of Japan*, vol. 112, no. 1303, pp. 143–148, 2004.

[274] Z. Li, B. Hou, Y. Xu et al., "Comparative study of sol-gel-hydrothermal and sol-gel synthesis of titania-silica composite nanoparticles," *Journal of Solid State Chemistry*, vol. 178, no. 5, pp. 1395–1405, 2005.

[275] Z. Li, B. Hou, Y. Xu, D. Wu, and Y. Sun, "Hydrothermal synthesis, characterization, and photocatalytic performance of silica-modified titanium dioxide nanoparticles," *Journal of Colloid and Interface Science*, vol. 288, no. 1, pp. 149–154, 2005.

[276] D. C. M. Dutoit, M. Schneider, and A. Baiker, "Titania-silica mixed oxides. I. Influence of sol-gel and drying conditions on structural properties," *Journal of Catalysis*, vol. 153, no. 1, pp. 165–176, 1995.

[277] D. C. M. Dutoit, M. Schneider, and A. Baiker, "Titania-silica mixed oxides. I. Influence of sol-gel and drying conditions on structural properties," *Journal of Catalysis*, vol. 153, no. 1, pp. 165–176, 1995.

[278] R. Hutter, T. Mallat, and A. Baiker, "Titania silica mixed oxides. II. Catalytic behavior in olefin epoxidation," *Journal of Catalysis*, vol. 153, no. 1, pp. 177–189, 1995.

[279] B. E. Handy, M. Maciejewski, A. Baiker, and A. Wokaun, "Genesis and structural properties of alkoxide-prepared titania-silica xerogels," *Journal of Materials Chemistry*, vol. 2, no. 8, pp. 833–840, 1992.

[280] S. Cao, K. L. Yeung, and P.-L. Yue, "Preparation of freestanding and crack-free titania-silica aerogels and their performance for gas phase, photocatalytic oxidation of VOCs," *Applied Catalysis B: Environmental*, vol. 68, no. 3-4, pp. 99–108, 2006.

[281] W.-I. Kim, D. J. Suh, T.-J. Park, and I.-K. Hong, "Photocatalytic degradation of methanol on titania and titania-silica aerogels prepared by non-alkoxide sol-gel route," *Topics in Catalysis*, vol. 44, no. 4, pp. 499–505, 2007.

[282] Z. Y. Wu, Y. F. Tao, Z. Lin, L. Liu, X. X. Fan, and Y. Wang, "Hydrothermal synthesis and morphological evolution of mesoporous titania-silica," *Journal of Physical Chemistry C*, vol. 113, no. 47, pp. 20335–20348, 2009.

[283] M. Kruk and M. Jaroniec, "Gas adsorption characterization of ordered organic-inorganic nanocomposite materials," *Chemistry of Materials*, vol. 13, no. 10, pp. 3169–3183, 2001.

[284] W. Dong, C. W. Lee, X. Lu et al., "Synchronous role of coupled adsorption and photocatalytic oxidation on ordered mesoporous anatase TiO_2-SiO_2 nanocomposites generating excellent degradation activity of RhB dye," *Applied Catalysis B: Environmental*, vol. 95, no. 3-4, pp. 197–207, 2010.

[285] O. T. Alaoui, Q. T. Nguyen, and T. Rhlalou, "Preparation and characterization of a new TiO_2/SiO_2 composite catalyst for photocatalytic degradation of indigo carmin," *Environmental Chemistry Letters*, vol. 7, no. 2, pp. 175–181, 2009.

[286] T. Cetinkaya, L. Neuwirthová, K. M. Kutláková, V. Tomášek, and H. Akbulut, "Synthesis of nanostructured TiO_2/SiO_2 as an effective photocatalyst for degradation of acid orange," *Applied Surface Science*, vol. 279, pp. 384–390, 2013.

[287] Q. Yang, C. Xie, Z. Xu et al., "Effects of synthesis parameters on the physico-chemical and photoactivity properties of titania-silica mixed oxide prepared via basic hydrolyzation," *Journal of Molecular Catalysis A: Chemical*, vol. 239, no. 1-2, pp. 144–150, 2005.

[288] I. A. Ibrahim, A. A. Ismail, M. S. Ahmed, and A. K. Ismail, "Comparative study of titania silica aerogel and xerogel as photocatalysts for cyanide degradation from wastewaters," *Egyptian Journal of Chemistry*, vol. 45, no. 1, pp. 193–203, 2002.

[289] A. A. Ismail, I. A. Ibrahim, M. S. Ahmed, R. M. Mohamed, and H. El-Shall, "Sol-gel synthesis of titania-silica photocatalyst for cyanide photodegradation," *Journal of Photochemistry and Photobiology A: Chemistry*, vol. 163, no. 3, pp. 445–451, 2004.

[290] M. Anpo, H. Nakaya, S. Kodama, Y. Kubokawa, K. Domen, and T. Onishi, "Photocatalysis over binary metal oxides. Enhancement of the photocatalytic activity of TiO_2 in titanium-silicon oxides," *Journal of Physical Chemistry*, vol. 90, no. 8, pp. 1633–1636, 1986.

[291] S. Imamura, H. Tarumoto, and S. Ishida, "Decomposition of 1,2-dichloroethane on TiO_2/SiO_2," *Industrials and Engineering Chemistry Research*, vol. 28, no. 10, pp. 1449–1452, 1989.

[292] A. Hanprasopwattana, S. Srinivasan, A. G. Sault, and A. K. Datye, "Titania coatings on monodisperse silica spheres (characterization using 2-propanol dehydration and TEM)," *Langmuir*, vol. 12, no. 13, pp. 3173–3179, 1996.

[293] M. S. Vohra, J. Lee, and W. Choi, "Enhanced photocatalytic degradation of tetramethylammonium on silica-loaded titania," *Journal of Applied Electrochemistry*, vol. 35, no. 7-8, pp. 757–763, 2005.

[294] T. Torimoto, S. Ito, S. Kuwabata, and H. Yoneyama, "Effects of adsorbents used as supports for titanium dioxide loading on photocatalytic degradation of propyzamide," *Environmental Science and Technology*, vol. 30, no. 4, pp. 1275–1281, 1996.

[295] Y. Arai, K. Tanaka, and A. L. Khlaifat, "Photocatalysis of SiO_2-loaded TiO_2," *Journal of Molecular Catalysis A: Chemical*, vol. 243, no. 1, pp. 85–88, 2006.

[296] M. S. Vohra and K. Tanaka, "Photocatalytic degradation of aqueous pollutants using silica-modified TiO_2," *Water Research*, vol. 37, no. 16, pp. 3992–3996, 2003.

[297] L. J. Alemany, M. A. Banares, E. Pardo, F. Martin, M. Galán-Fereres, and J. Blasco, "Photodegradation of phenol in water using silica-supported titania catalysts," *Applied Catalysis B: Environmental*, vol. 13, no. 3-4, pp. 289–297, 1997.

[298] B. Malinowska, J. Walendziewski, D. Robert, J. V. Weber, and M. Stolarski, "The study of photocatalytic activities of titania and titania-silica aerogels," *Applied Catalysis B: Environmental*, vol. 46, no. 3, pp. 441–451, 2003.

[299] S. Rasalingam, H. S. Kibombo, C. M. Wu, R. Peng, J. Baltrusaitis, and R. T. Koodali, "Competitive role of structural properties of titania-silica mixed oxides and a mechanistic study of the photocatalytic degradation of phenol," *Applied Catalysis B: Environmental*, vol. 148-149, pp. 394–405, 2014.

[300] S. Yang, Y. Guo, X. Zhou, C. Lin, Y. Wang, and W. Zhang, "Enhanced photocatalytic activity for degradation of methyl orange over silica-titania," *Journal of Nanomaterials*, vol. 2011, Article ID 296953, 2011.

[301] A. Mahyar, M. A. Behnajady, and N. Modirshahla, "Enhanced photocatalytic degradation of C.I. Basic violet 2 using TiO_2-SiO_2 composite nanoparticles," *Photochemistry and Photobiology*, vol. 87, no. 4, pp. 795–801, 2011.

[302] H. Chun, W. Yizhong, and T. Hongxiao, "Preparation and characterization of surface bond-conjugated TiO_2/SiO_2 and photocatalysis for azo dyes," *Applied Catalysis B: Environmental*, vol. 30, no. 3-4, pp. 277–285, 2001.

[303] F. Chen, J. Zhao, and H. Hidaka, "Highly selective deethylation of Rhodamine B: adsorption and photooxidation pathways of the dye on the TiO_2/SiO_2 composite photocatalyst," *International Journal of Photoenergy*, vol. 5, no. 4, pp. 209–217, 2003.

[304] H. S. Kibombo, S. Rasalingam, and R. T. Koodali, "Facile template free method for textural property modulation that enhances adsorption and photocatalytic activity of aperiodic titania supported silica materials," *Applied Catalysis B: Environmental*, vol. 142, pp. 119–128, 2013.

[305] S. Rasalingam, H. S. Kibombo, C. M. Wu et al., "Influence of Ti–O–Si hetero-linkages in the photocatalytic degradation of Rhodamine B," *Catalysis Communications*, vol. 31, pp. 66–70, 2013.

[306] C. Shifu and C. Gengyu, "Photocatalytic degradation of organophosphorus pesticides using floating photocatalyst $TiO_2{\cdot}SiO_2$/beads by sunlight," *Solar Energy*, vol. 79, no. 1, pp. 1–9, 2005.

[307] M. V. Phanikrishna Sharma, G. Sadanandam, A. Ratnamala, V. Durga Kumari, and M. Subrahmanyam, "An efficient and novel porous nanosilica supported TiO_2 photocatalyst for pesticide degradation using solar light," *Journal of Hazardous Materials*, vol. 171, no. 1–3, pp. 626–633, 2009.

[308] M. V. Phanikrishna Sharma, V. Durga Kumari, and M. Subrahmanyam, "TiO_2 supported over SBA-15: an efficient photocatalyst for the pesticide degradation using solar light," *Chemosphere*, vol. 73, no. 9, pp. 1562–1569, 2008.

[309] W. Jiang, J. A. Joens, D. D. Dionysiou, and K. E. O'Shea, "Optimization of photocatalytic performance of TiO_2 coated glass microspheres using response surface methodology and the application for degradation of dimethyl phthalate," *Journal of Photochemistry and Photobiology A: Chemistry*, vol. 262, pp. 7–13, 2013.

[310] S. Ahmed, M. G. Rasul, R. Brown, and M. A. Hashib, "Influence of parameters on the heterogeneous photocatalytic degradation of pesticides and phenolic contaminants in wastewater: a short review," *Journal of Environmental Management*, vol. 92, no. 3, pp. 311–330, 2011.